



**CAST FILE
COPY**

**THE HYDROGEN PURIFICATION
OF SUBMICRON NICKEL POWDER**

by

A. David Douglas

prepared for

NATIONAL AERONAUTICS AND SPACE ADMINISTRATION

CONTRACT NAS 3-7274

SYLVANIA
A SUBSIDIARY OF
GENERAL TELEPHONE & ELECTRONICS

NOTICE

This report was prepared as an account of Government sponsored work. Neither the United States, nor the National Aeronautics and Space Administration (NASA), nor any person acting on behalf of NASA:

- A.) Makes any warranty or representation, expressed or implied, with respect to the accuracy, completeness, or usefulness of the information contained in this report, or that the use of any information, apparatus, method, or process disclosed in this report may not infringe privately owned rights; or
- B.) Assumes any liabilities with respect to the use of, or for damages resulting from the use of any information, apparatus, method or process disclosed in this report.

As used above, "person acting on behalf of NASA" includes any employee or contractor of NASA, or employee of such contractor, to the extent that such employee or contractor of NASA, or employee of such contractor prepares, disseminates, or provides access to, any information pursuant to his employment or contract with NASA, or his employment with such contractor.

Requests for copies of this report should be referred to

National Aeronautics and Space Administration
Office of Scientific and Technical Information
Attention: AFSS-A
Washington, D.C. 20546

Final Report

THE HYDROGEN PURIFICATION OF SUBMICRON NICKEL POWDER

by

A. David Douglas

prepared for

National Aeronautics and Space Administration

October 11, 1968

Contract NAS 3-7274

Technical Management
NASA Lewis Research Center
Cleveland, Ohio
Materials and Structures Division
Albert E. Anglin, Project Manager
Gustav Reinhardt, Research Advisor

Sylvania Electric Products Inc.
Chemical and Metallurgical Division
Towanda, Pennsylvania 18848

TABLE OF CONTENTS

	<u>Page No.</u>
ABSTRACT	1
SUMMARY	2
INTRODUCTION	3
CHARACTERIZATION OF THREE SUBMICRON POWDERS	5
DISPERSING TESTS	33a
POWDER PURIFICATION	75
CONCLUSIONS	103
REFERENCES	106
APPENDIX. ADDITIONAL STORAGE TESTS	107

LIST OF TABLES

	<u>Page No.</u>
TABLE 1 Chemical Analysis Results	7
TABLE 2 Spectrographic Analysis	8
TABLE 3 Summary of Physical Measurements	9
TABLE 4 Successive Analyses of Nickel Powder	30
TABLE 5 Impurity Metals and Their Oxygen Equivalents not Reduced by Hydrogen at 925°C	32
TABLE 6 Overnight Micromerograph Results	33
TABLE 7 Dispersing Tests I	47
TABLE 8 Dispersing Tests II	48
TABLE 9 Dispersing Tests III	57
TABLE 10 Dispersing Sherritt Gordon and NRC Submicron Nickel Powder	65
TABLE 11 Powders Examined by Electron Microscopy	67
TABLE 12 Gas-Temperature Measurements	82
TABLE 13 Gas Temperature Versus Tape Temperature	84
TABLE 14 Powder-Purification Tests	83
TABLE 15 Summary of Powder-Storage Tests	98
TABLE 16 Powder-Storage Tests	99
TABLE 17 Storage Tests in Stainless Steel Containers	108

LIST OF FIGURES

		<u>Page No.</u>
Figure 1	Particle-Size Distribution of NRC Ultra-fine Nickel Powder Agglomerates	10
Figure 2	Particle-Size Distribution of Sherritt Gordon GX-3 Nickel Powder Agglomerates	11
Figure 3	Particle-Size Distribution of Vitro Laboratories - Submicron Nickel Powder Agglomerates. .	12
Figure 4	Nickel Powders in Oil at 100X (a) NRC (b) Sherritt Gordon (c) Vitro Laboratories	16
Figure 5	Nickel Powders, as Dusted on Slide at 1000X . . . (a) NRC (b) Sherritt Gordon (c) Vitro Laboratories	17
Figure 6	Nickel Powders, Dusted and Smeared at 1000X . . . (a) NRC (b) Sherritt Gordon (c) Vitro Laboratories	18

Electron Micrographs

Figure 7	NRC Nickel Powder at 12,000X	20
Figure 8	NRC Nickel Powder at 50,000X	20
Figure 9	NRC Nickel Powder at 50,000X	21
Figure 10	NRC Nickel Powder at 50,000X	22
Figure 11	Sherritt Gordon Nickel Powder at 12,000X	23
Figure 12	Sherritt Gordon Nickel Powder at 50,000X	23
Figure 13	Sherritt Gordon Nickel Powder at 50,000X	24
Figure 14	Sherritt Gordon Nickel Powder at 50,000X	25
Figure 15	Vitro Laboratories Nickel Powder at 12,000X	26
Figure 16	Vitro Laboratories Nickel Powder at 50,000X	26
Figure 17	Vitro Laboratories Nickel Powder at 50,000X	27
Figure 18	Vitro Laboratories Nickel Powder at 50,000X	28
Figure 19	Feeding Apparatus	38
Figure 20	Apparatus I	40
Figure 21	Apparatus II	42

LIST OF FIGURES (Cont.)

	<u>Page No.</u>
Figure 22 Apparatus III	44
Figure 23 Apparatus III	45
Figure 24 Specific Surface Versus Argon Flow Rate (I)	49
Figure 25 Specific Surface Versus Disperser Potential (I) . .	50
Figure 26 Disperser Efficiency Versus Argon Concentration (II)	51
Figure 27 Specific Surface Versus Powder Concentration(II). .	52
Figure 28 SG Nickel Powder, Dispersed and Collected 12,200X	67
Figure 29 SG Nickel Powder, Dispersed and Collected 50,000X	68
Figure 30 SG Nickel Powder, Dispersed, Heated to 700°C., and Collected. 12,200X	69
Figure 31 SG Nickel Powder, Dispersed, Heated to 700°C., and Collected. 50,000X	70
Figure 32 NRC Nickel Powder, Dispersed and Collected 12,200X	71
Figure 33 NRC Nickel Powder, Dispersed and Collected 106,400X	72
Figure 34 NRC Nickel Powder, Dispersed, Heated to 700°C., and Collected. 12,200X	73
Figure 35 NRC Nickel Powder, Dispersed, Heated to 700°C., and Collected. 106,400X	74
Figure 36 Overall View of Apparatus	77
Figure 37 Feeder with Detachable Loading Assembly	78
Figure 38 Feeding Apparatus	80
Figure 39 Powder Collector	85
Figure 40 Glove-Box and Argon Schematic Diagram	87
Figure 41 Gas Temperature vs. Oxygen Content of Cleaned Nickel Powder	89
Figure 42 Gas Temperature vs. Specific Surface of Cleaned Nickel Powder	91

LIST OF FIGURES (Cont.)

	<u>Page No.</u>
Figure 43 Gas-Residence Time vs. Equivalent Particle Size of Cleaned Nickel Powder	93
Figure 44 Electron Micrograph Silhouette of Cleaned Nickel Particles at 12,000X	94
Figure 45 Electron Micrograph Silhouette of Cleaned Nickel Particles at 12,000X	95
Figure 46 Electron Micrograph Direct Replica of Cleaned Nickel Particles at 12,000X	96
Figure 47 Electron Micrograph Direct Replica of Cleaned Nickel Particles at 19,900X	97

THE HYDROGEN PURIFICATION OF SUBMICRON NICKEL POWDER

by

A. David Douglas

Sylvania Electric Products Inc.

ABSTRACT

A laboratory apparatus was designed, constructed, and operated to purify (to an oxygen content of less than 0.05%) 12.5 grams per hour of submicron nickel powder by hydrogen fluidization with transport through a zone which heated the suspension to 335°C for 22 seconds. Three nickel powders were characterized, one being used for dispersion, reduction, and storage tests. Although the treated powder retained a specific surface of at least three square meters per gram during processing, electron micrographs indicated a considerable degree of agglomeration of the ultimate particles. A glove box and argon purification system were assembled for handling feed, purified, and stored powder in argon containing less than 12 ppm oxygen and 8 ppm water.

SUMMARY

The purpose of this program was to develop equipment and a process for the handling, storage, and reduction purification of submicron nickel powder for use in dispersion-strengthened alloys. The equipment developed was to have a capacity for producing 100 grams per eight-hour day of nickel powder containing 0.05% by weight or less of oxygen and having a specific surface area equivalent to an average particle diameter of 0.15 micron or less.

Hydrogen, sometimes mixed with argon, was used to carry suspended, dispersed powder particles through a heated zone and to reduce chemically the nickel oxide contained. Gas temperatures in the hot zone between 150°C and 510°C were investigated for reduction using the hydrogen mixture at atmospheric pressure. The program goals were met using hydrogen without argon at a gas temperature of 335°C when passed concurrently with the nickel powder through a 15-inch-long hot zone at a flow rate which corresponded to a residence time in the hot zone of 22 seconds.

Procedures were developed for handling the nickel powder so that it was at no time exposed to air or oxygen either before processing or afterward. Storage tests were conducted using various types of containers and sealing methods to determine the best method of storing the cleaned powder to prevent oxygen pick-up. A stainless steel container which was thoroughly degassed prior to use, and

sealed with a rubber gasket under a cover which was tightly clamped to the container body, resulted in an oxygen increase at an average rate of only 4 ppm per day.

INTRODUCTION

Submicron metal powders are used to produce dispersion-strengthened alloys with fine interparticle spacing. However, these powders exhibit high specific surfaces which are readily contaminated, particularly with oxygen. Powders of chemically active metals such as nickel readily combine with adsorbed oxygen and thereby acquire a surface layer of metal oxide⁽¹⁾. This interferes with the proper sintering during processing to alloys, and may degrade the alloy properties. No method is known to exist by which submicron nickel powder may be purified of the last traces of oxide without the simultaneous growth of particles as indicated by a decrease in the powder's specific surface.

The purpose of this investigation was to develop a process by which a purchased submicron nickel powder (in the size range of about 0.02 to 0.1 micron) may be purified to an oxygen content of 0.05% by weight, or less, while maintaining a specific surface of 3.00 square meters per gram, or greater. That specific surface was considered to be equivalent to an average particle diameter of 0.15 micron according to the relationship⁽²⁾ which was established for this program:

$$\text{Particle Size (microns)} = \frac{4}{d \times S}$$

where S is the specific surface area (m^2/g) and d is the absolute density of the powder (8.9g/cc). The equipment designed and constructed to accomplish this is to have a capacity of 100 grams of purified powder per eight-hour day.

The investigation covered development of a process and the apparatus to reduce with hydrogen the oxide content of submicron nickel powder making use of the principle of fluidization with transport. Argon in various concentrations was sometimes mixed with the hydrogen to form the carrier gas. Also investigated were methods of storing the powder to eliminate or minimize any increase in the oxygen content, methods of dispersing the powder in the carrier gas, and characterization of three purchased submicron nickel powders.

CHARACTERIZATION OF THREE SUBMICRON NICKEL POWDERS

TABLE OF CONTENTS

	<u>Page No.</u>
Sampling Procedure	6
Analyses	7
Microscopic Examination	15
Electron Microscopy	15
Nature of the Oxygen Content	28
Micromerograph Measurements	30
Recommendation	32

NICKEL POWDER CHARACTERIZATION

Nickel powder in the submicron particle size range was found to be available from three sources, as listed:

1. National Research Corporation (NRC): 1 pound
2. Sherritt Gordon Mines Limited (SG): 2 pounds
3. Vitro Laboratories: 1 pound

The amounts listed above were purchased from each source for analysis and evaluation.

Sampling Procedure

The powder containers were placed in a glove box along with opening tools and sample containers such as glass bottles and collapsible tin capsules. Inside the glove box the samples for analysis were placed in weighed tin capsules in an argon atmosphere. These were folded shut and were crimped to provide a fairly good seal. They were then placed in a small glass bottle which was then sealed tightly. When the glass bottles were removed from the glove box, they were placed in a vacuum-type desiccator which was continuously flushed with pure cylinder argon. The samples were stored in this manner until the scheduled time for analysis. The glass bottles were then removed from the desiccator, and the tin capsules were removed and weighed on an analytical balance. They were put into the analyzing equipment as soon as possible, thus minimizing the exposure of the sample containers to air.

Analyses

Table 1 lists the analyses obtained in our Chemical Analytical Laboratory for oxygen, carbon, and sulfur.

TABLE 1
Chemical Analytical Results

<u>Powder</u>	<u>NRC</u>	<u>SG</u>	<u>VIT</u>
Sulfur, %	0.008	0.005	0.016
Carbon, %	0.19	0.17	0.032
Oxygen, %	8.1	5.4	1.2

It should be noted that, of the three powders, the Sherriitt-Gordon powder contains the least sulfur, while the Vitro powder contains the most. The carbon contents are considered to be of lesser importance because of the likelihood of carbon being removed from the powder during reduction. The oxygen content is tentatively also of lesser importance at this point, because of the unknowns of the reduction kinetics and problems that may be encountered. It would be desirable to be able to purify satisfactorily the powder having the highest oxygen content, assuming that those having lower contents would be purified more easily.

Table 2 lists the analyses obtained in our Spectrographic Laboratory, both qualitative and quantitative, for those detectable metallic impurities which are normally sought.

TABLE 2Spectrographic Analyses (Results in %)

<u>Powder</u>	<u>NRC</u>	<u>SG</u>	<u>VIT</u>
Al	0.16	0.006	0.005
Co	0.077	0.059	0.063
Cr	0.01	<0.004	<0.004
Cu	>0.01	0.002	0.003
Fe	0.23	0.012	0.026
Mg	0.003	<0.001	<0.001
Mn	0.004	<0.001	<0.001
Pb	>0.01	<0.0005	<0.0005
Si	0.019	0.005	>0.1
Ti	0.004	<0.003	<0.003
Zn	0.12	<0.01	<0.01
Ag	<0.0001	>0.01	N.D.
B	>0.001	N.D.	N.D.
Ca	>0.0001	>0.0001	>0.0001
Mo	>0.0001	N.D.	>0.001
Sn	>0.01	N.D.	N.D.
W	N.D.	N.D.	>0.001

N.D. = Not Detected.

Elements sought but not detected in any of the three powders: As, Ba, Be, Cd, Ge, Sb, Sr, Ta, Th, Bi.

The NRC powder has the highest content of metallic impurities, both in number detected and their quantity. The Vitro and Sherritt-Gordon powders are both purer, the latter being slightly better.

Table 3 summarizes the results of the physical measurements of surface area (Brunauer-Emmett-Teller)⁽³⁾ and particle size distribution (Micromerograph).

TABLE 3
Summary of Physical Measurements

<u>Powder</u>	<u>NRC</u>	<u>SG</u>	<u>VIT</u>	<u>TiO₂</u>
Surface Area (BET), m ² /g	39.6	25.3	10.7	13.5
Equivalent Particle Size, Micron	0.012	0.018	0.042	
Micromerograph at 50 psi				
Milligrams Charged	70	50	82	
Milligrams Collected	8.5	17	13.1	
Particles >5 Microns, %	22.3	50	95.3	
Maximum Particle Size, Microns	40	30	90	
Micromerograph at 400 psi				
Milligrams Charged	72	50	80	
Milligrams Collected	8.5	13	14	
Particles >5 Microns, %	20	4.8	89.3	
Maximum Particle Size, Microns	25	8	50	
X-Ray Crystallite Size, Microns	0.020	0.020	0.035	

Figures 1, 2, and 3 graphically illustrate the complete Micromerograph results of agglomerated powders. The flask used to hold the powder while measuring the surface area (B.E.T. method)

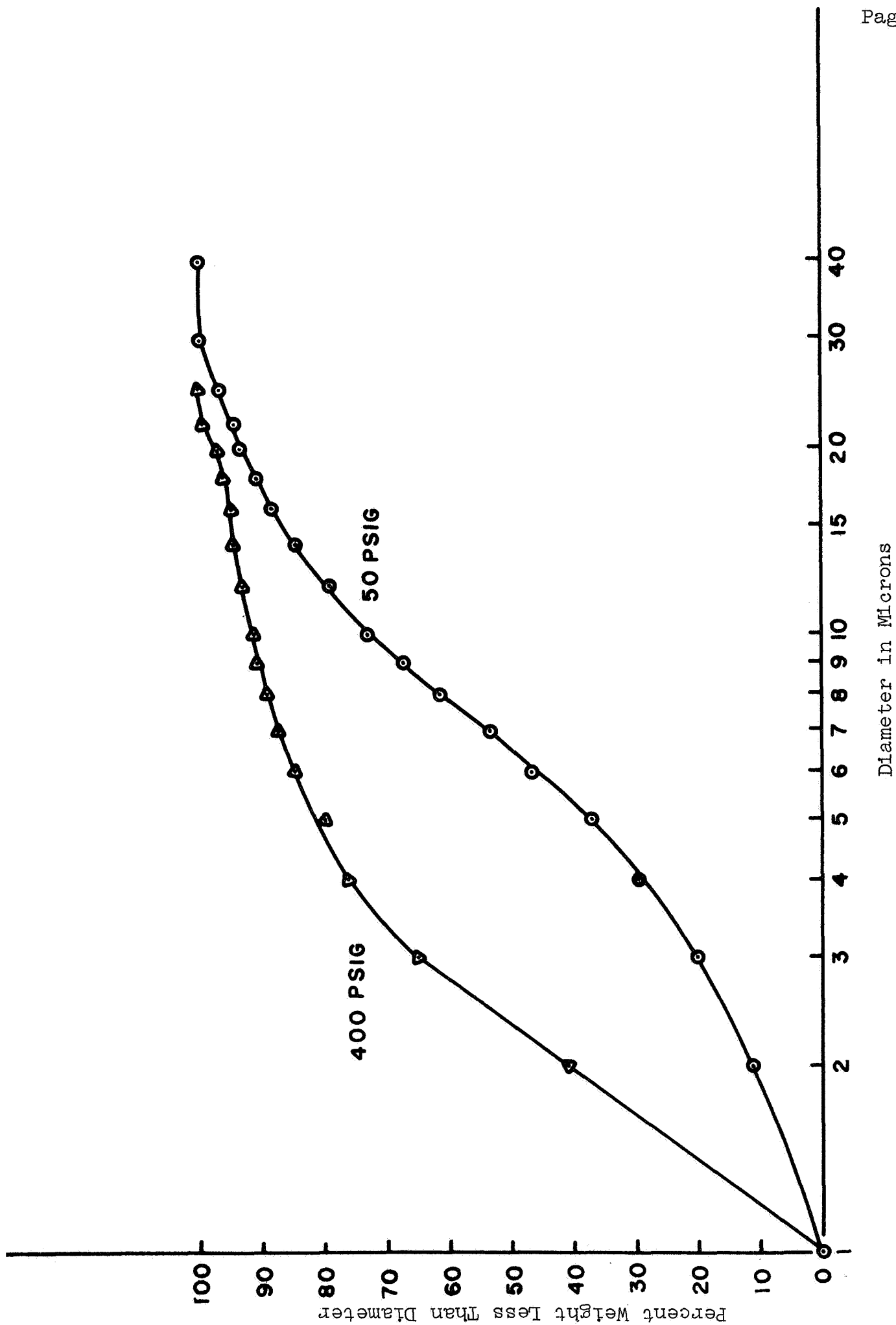


Figure 1 Particle Size Distribution of NRC Ultra-Fine Nickel Powder

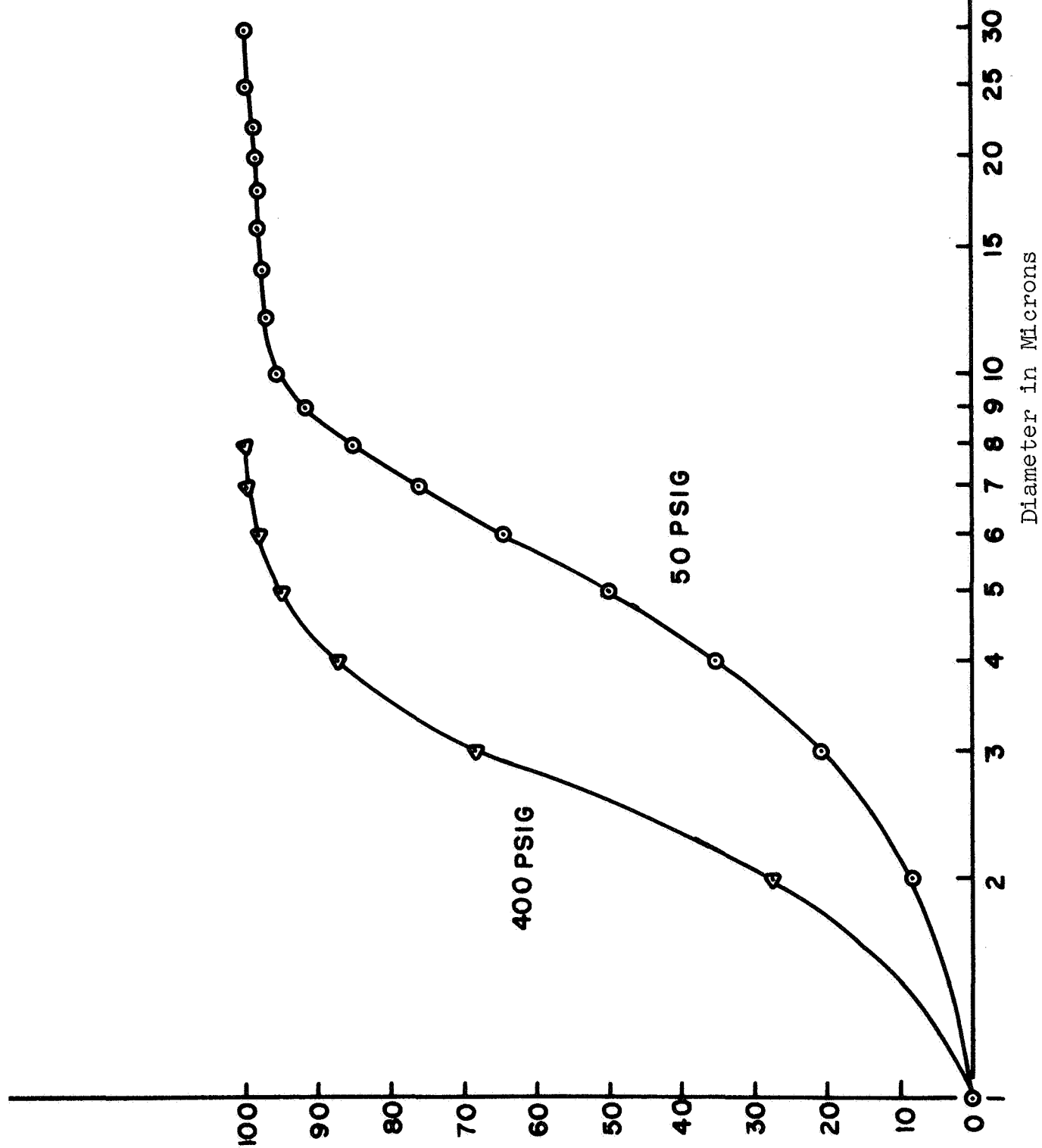


Figure 2 Particle Size Distribution of Sherritt Gordon GX-3 Nickel Powder

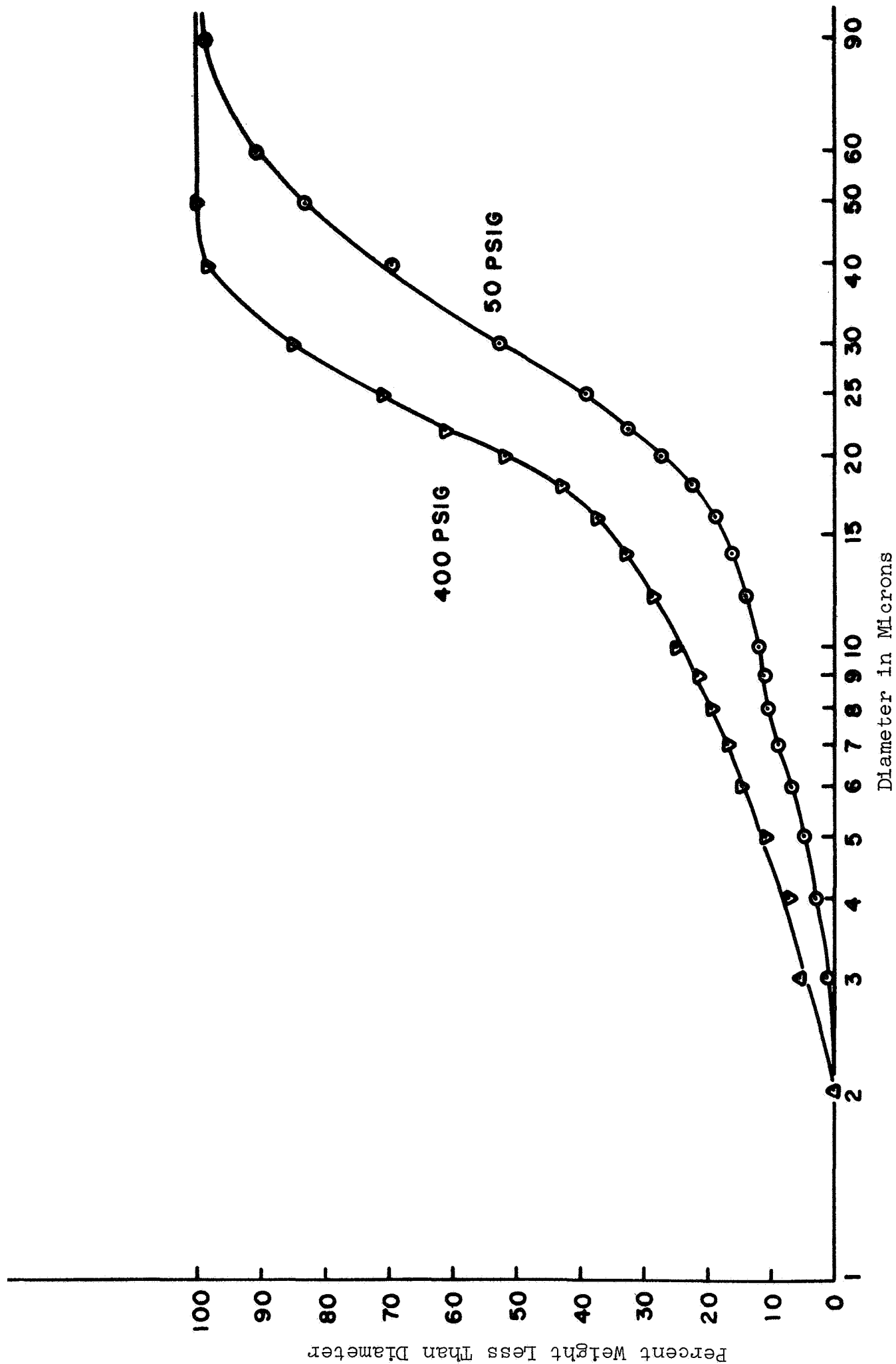


Figure 3 Particle Size Distribution of Vitro Laboratories Submicron Nickel Powder

was charged inside the glove box and was sealed with a rubber stopper. The long neck of the flask was then momentarily exposed to air while the stopper was removed, and the flask was quickly connected to the glass apparatus. The flask and glass apparatus were quickly evacuated with the vacuum pump, thus minimizing the exposure of the powder to any oxygen. As Table 3 indicates, all three powders have surface areas significantly greater than the minimum of 3.00 square meters per gram required for the finished powder and also greater than that required for the purchased powder to be used as raw material for the purification process. This minimum area is 4.5 square meters per gram, based on an equivalent average particle diameter of 0.10 microns. This table also lists the value of surface area (13.5 square meters per gram) as determined by the same technique and equipment for a titanium dioxide sample provided by Lewis Research Center. The Lewis result for this powder is 10.3 ± 0.2 square meters per gram.

The powder samples used for the Micromerograph measurements were stored in a small plastic vial in the argon-filled desiccator and were exposed to air a short time for weighing and charging to the Micromerograph apparatus. The atmosphere used in the Micromerograph for settling was nitrogen. The amount of powder charged and the amount of powder collected on the pan after it settled are recorded in the table. However, part of the powder normally collects on the walls of the apparatus and cannot settle onto the pan. This is reported to be approximately half of the powder charged in

the case of most powders tested. Particles smaller than about one micron in diameter fall too slowly to be collected on the pan during a normal length of time. However, it is assumed that a high fraction of the powder in each case consists of agglomerates which are incompletely broken up and therefore settle as relatively large particles. In order to observe differences in the measured particle-size distribution caused by dispersion techniques of differing severities, the Micromerograph was operated at different pressures in the deagglomerator. Data shown in Table 3 were obtained at 50 psi and at 400 psi. The differences in particle-size distribution obtained are seen more clearly in Figures 1, 2, and 3. In the case of all three powders, the use of higher pressure caused less of the larger particles (agglomerates) to be seen, a comparative indication of the relative forces required to cause the agglomerates to be broken up in the three powders. Judging by the results at 400 psig, the Sheritt-Gordon powder has the greater number of small particles (agglomerates) present after the deagglomerator treatment. Therefore, it would appear that this powder would require a dispersing treatment of lowest severity. This conclusion may not be entirely justified, however, after consideration is given to the electron micrographs of the powders discussed below.

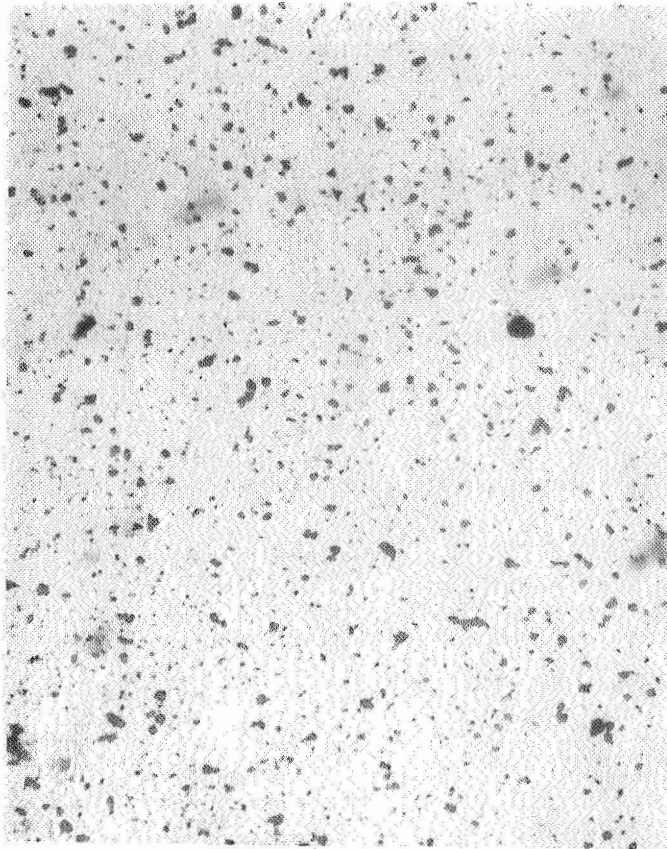
Microscopic Examination

As a preliminary evaluation technique, the three powders were examined with a metallograph at both 100X and 1000X. Photomicrographs of the powders are illustrated in Figures 4, 5, and 6. Figure 4 shows the powders as dispersed in microscope-slide oil at 100X. Figure 5 shows the result at 1000X when the powder is collected from a suspension in air falling from the vibratory screen onto a glass slide. Figure 6 shows the powders at 1000X on a metal slide after being smeared while wet with methanol and then dried. These examinations reveal the presence of many agglomerates, particularly before any shear forces are applied.

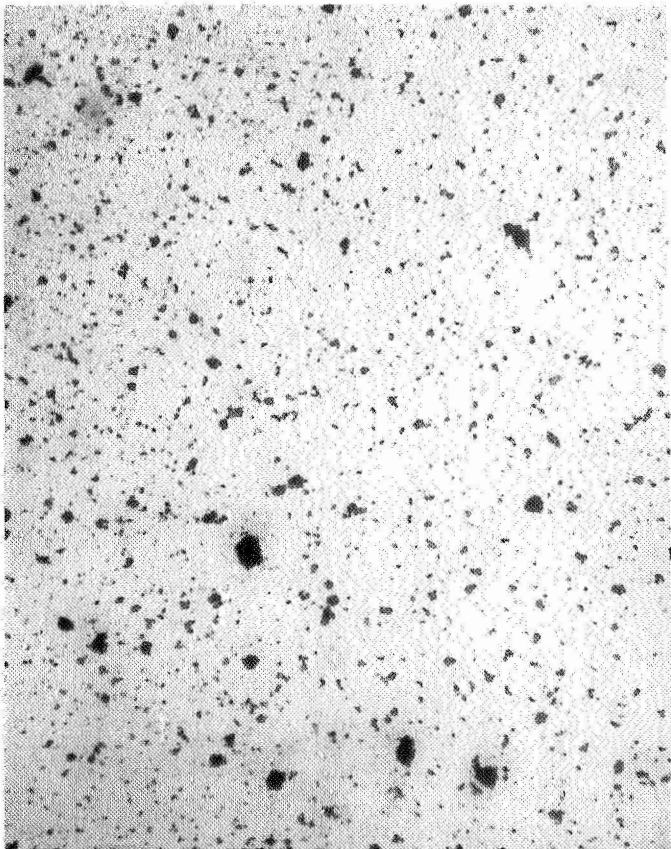
Even after being smeared, agglomerates several microns in diameter are still present. Particles smaller than about one-half micron in diameter probably do not appear in these photomicrographs. However, it is apparent that the Vitro powder contains more of the very large particles or agglomerates and that these particles or agglomerates require a greater shear force to be broken apart than those of the NRC or Sherritt-Gordon powders.

Electron Microscopy

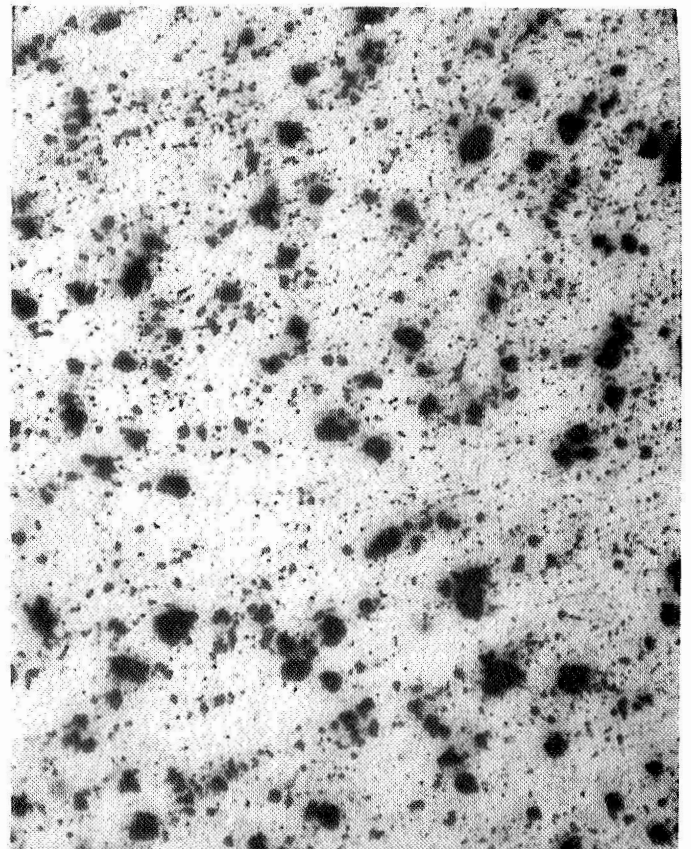
Examination with the electron microscope to provide micrographs at magnifications of 12,000X and 50,000X was subcontracted to the General Telephone and Electronics Laboratories at Bayside, New York. Both Sylvania Electric Products and General Telephone and Electronics Laboratories are subsidiaries of General Telephone and Electronics Corporation.



a) NRC

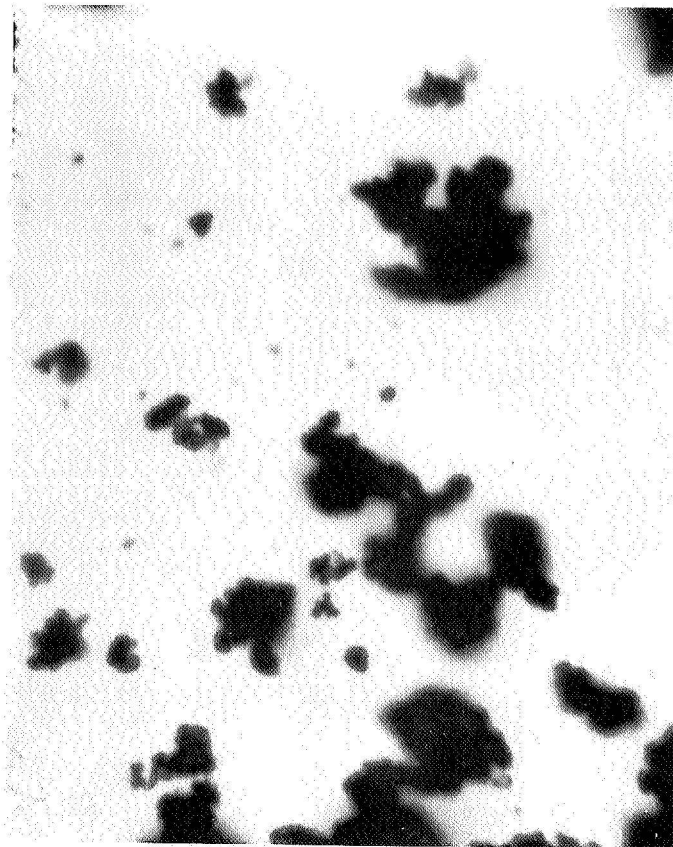


b) Sherriitt Gordon

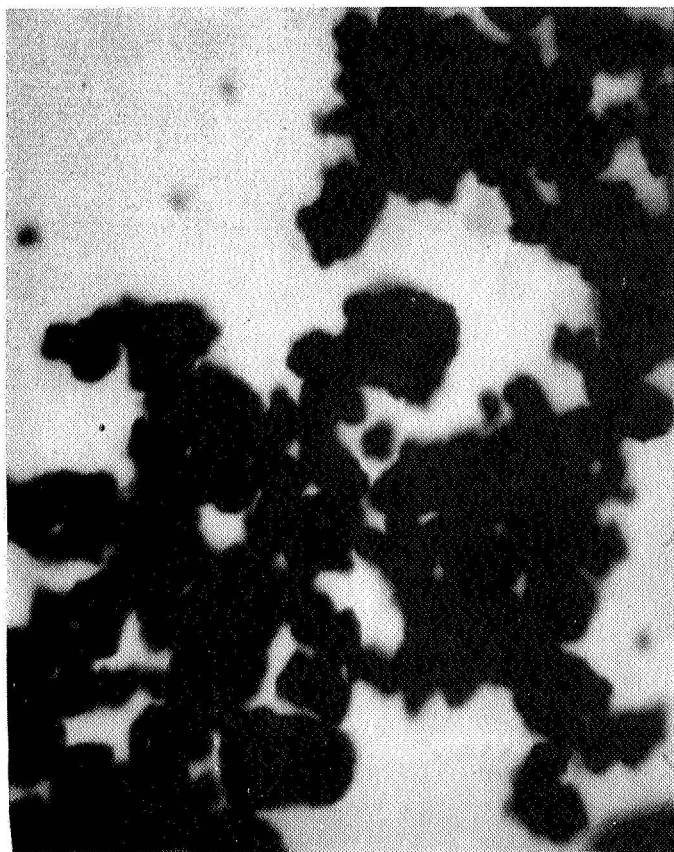


c) Vitro Laboratories

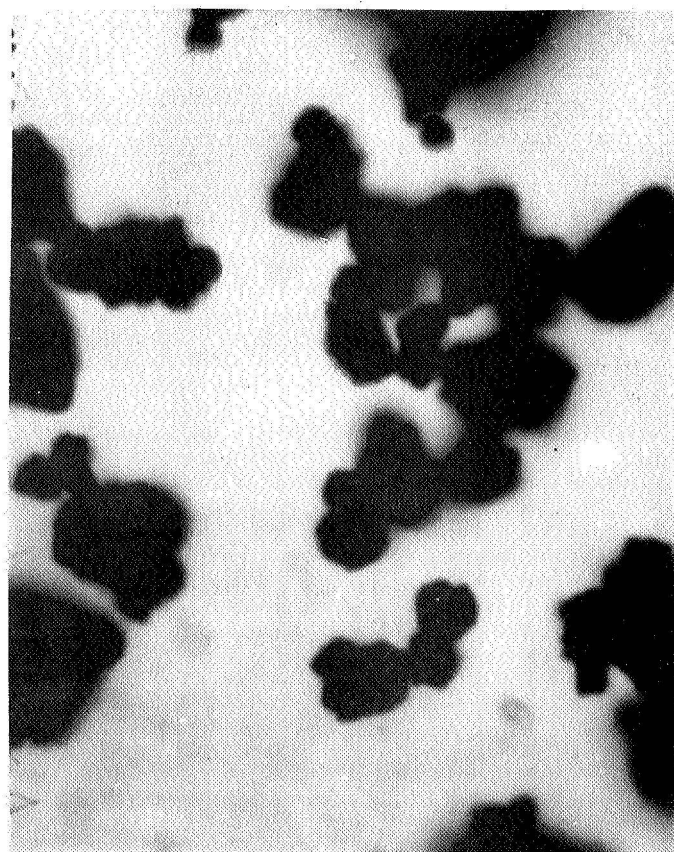
Figure 4 Nickel Powders in Oil at 100X



a) NRC

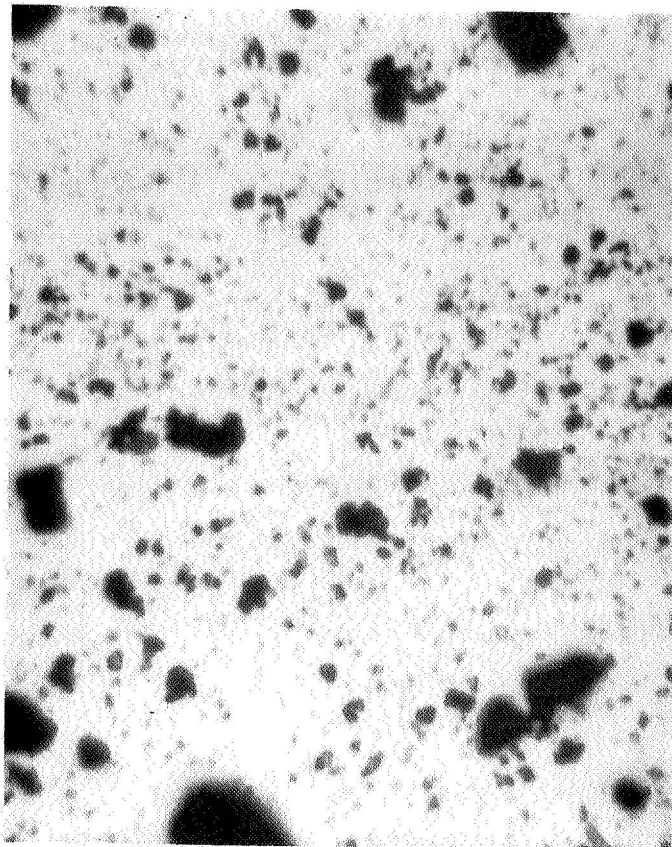


b) Sherritt Gordon

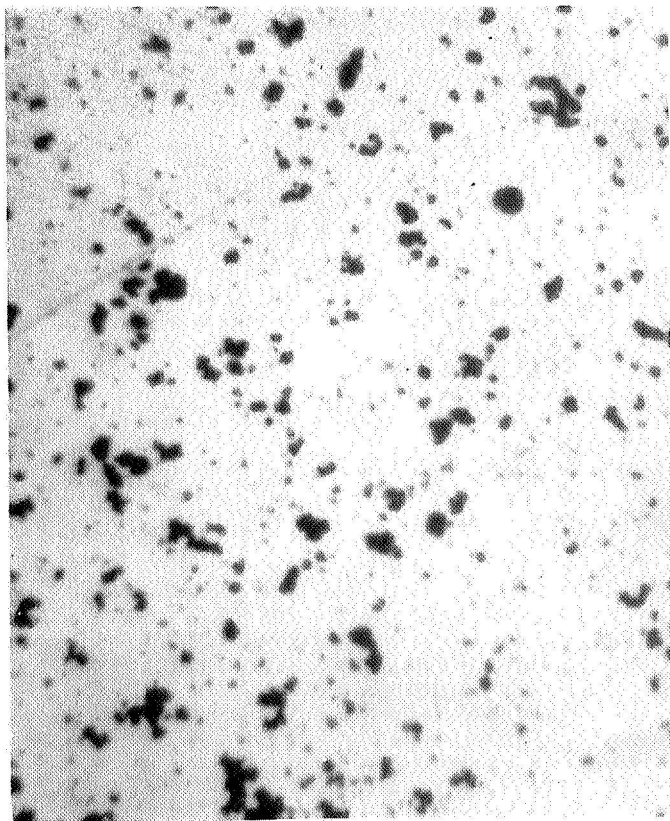


c) Vitro Laboratories

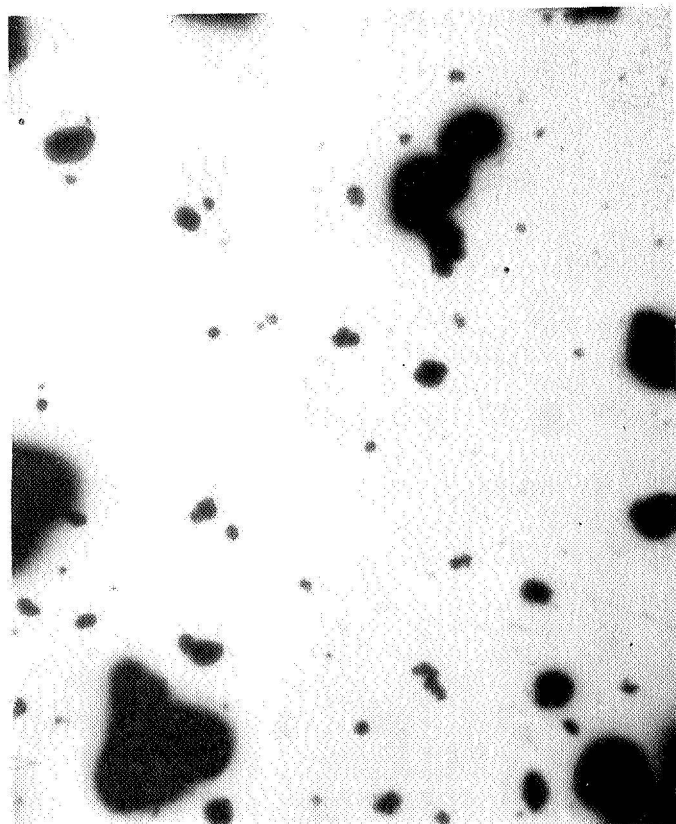
Figure 5 Nickel Powders, as Dusted on Slide at 1000X



a) NRC



b) Sherritt Gordon



c) Vitro Laboratories

Figure 6 Nickel Powders, Dusted and Smeared at 1000X

The powders were studied, using nitrogen as a protective atmosphere during all operations, and the following replication technique was selected for sample preparation to give as representative results as possible.

The powder was dispersed on a glass slide using pure amyl acetate in order to produce very little viscous shear. A carbon film was deposited over the particles and was then removed with a very dilute solution of hydrofluoric acid in distilled water. The dilution was sufficient to avoid attack of the nickel particles.

The carbon film floated off the slide and retained the nickel particles. This was subsequently examined in the electron microscope. Figures 7, 11, and 15 show the three powders at 12,000X, and Figures 8, 9, 10, 12, 13, 14, 16, 17, and 18 show them at 50,000X. The nickel particles appear as silhouettes (black), whereas any foreign particles which are attacked by the dilute hydrofluoric acid solution appear replicated (transparent).

These figures show that the Vitro powder is more highly aggregated and more difficult to disperse than the NRC or SG powders. There is evident in the NRC powder a high population of particles in the range 100 to 200 angstroms (0.010 to 0.020 microns) in diameter.

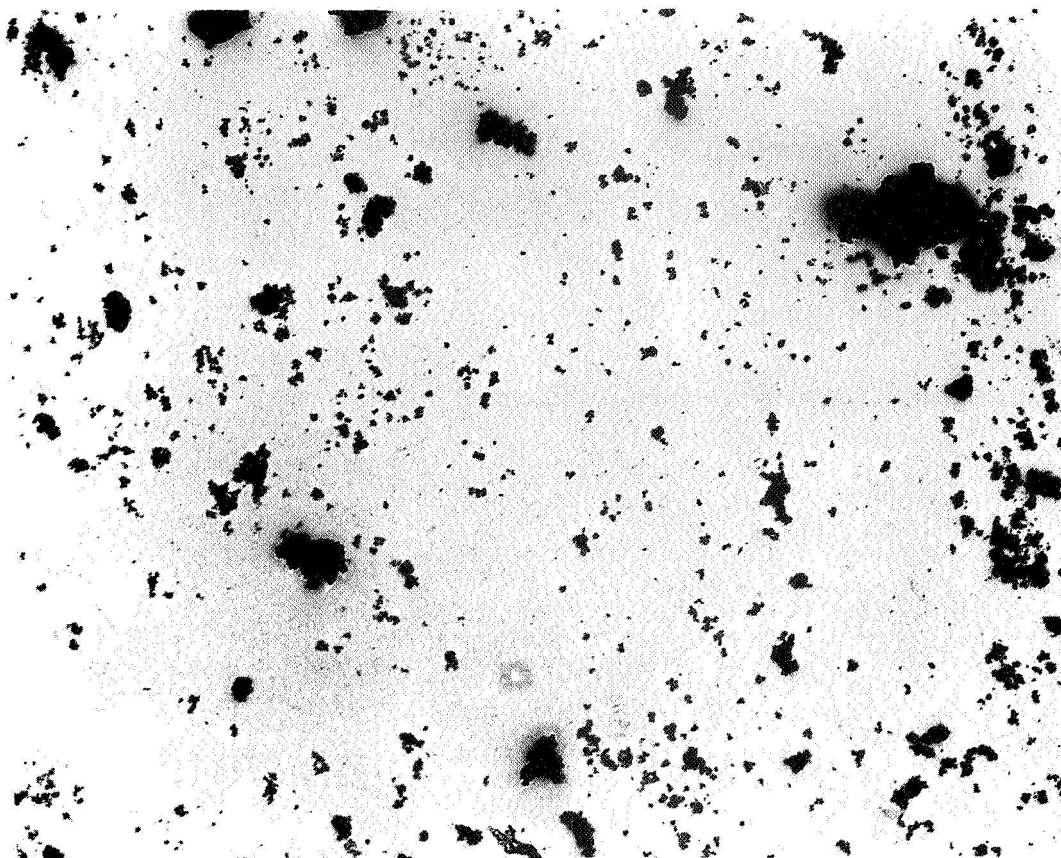


Figure 7 NRC Nickel Powder at 12,000X

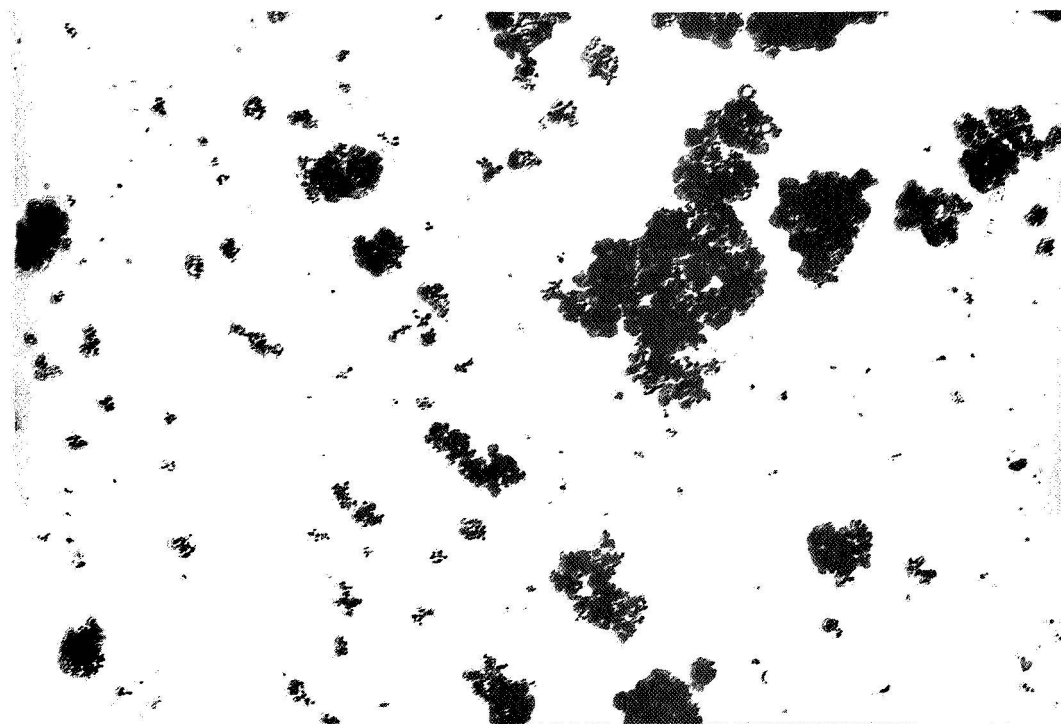


Figure 8 NRC Nickel Powder at 50,000X

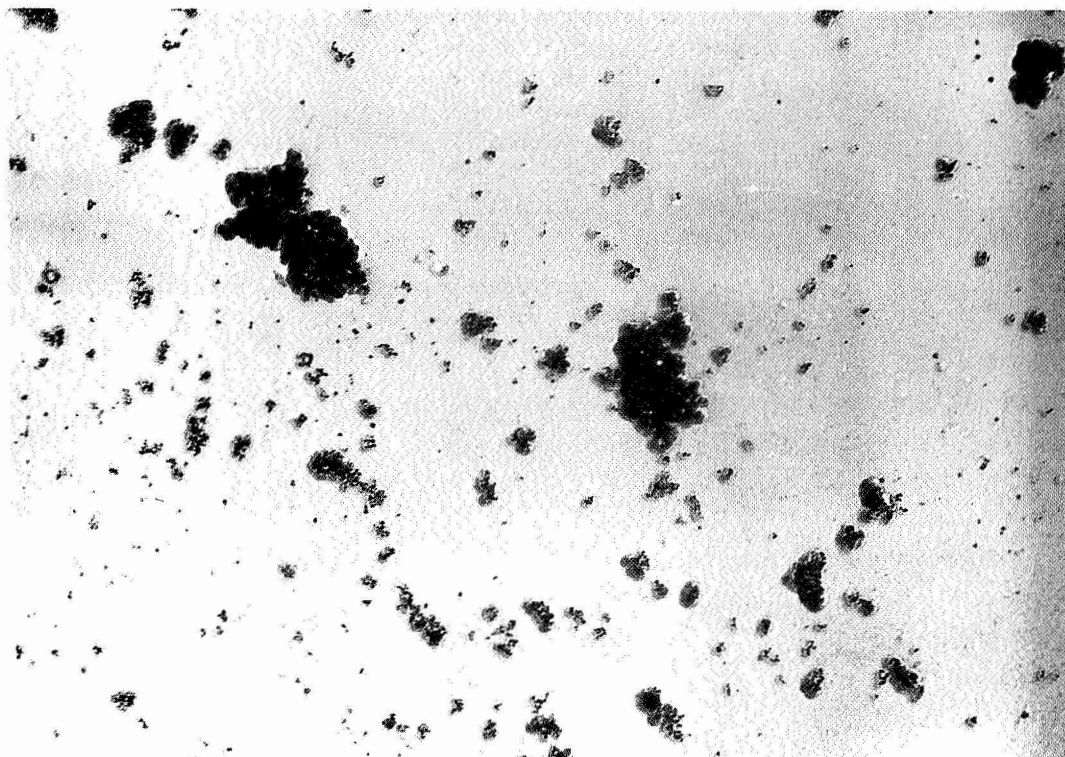


Figure 9 NRC Nickel Powder at 50,000X

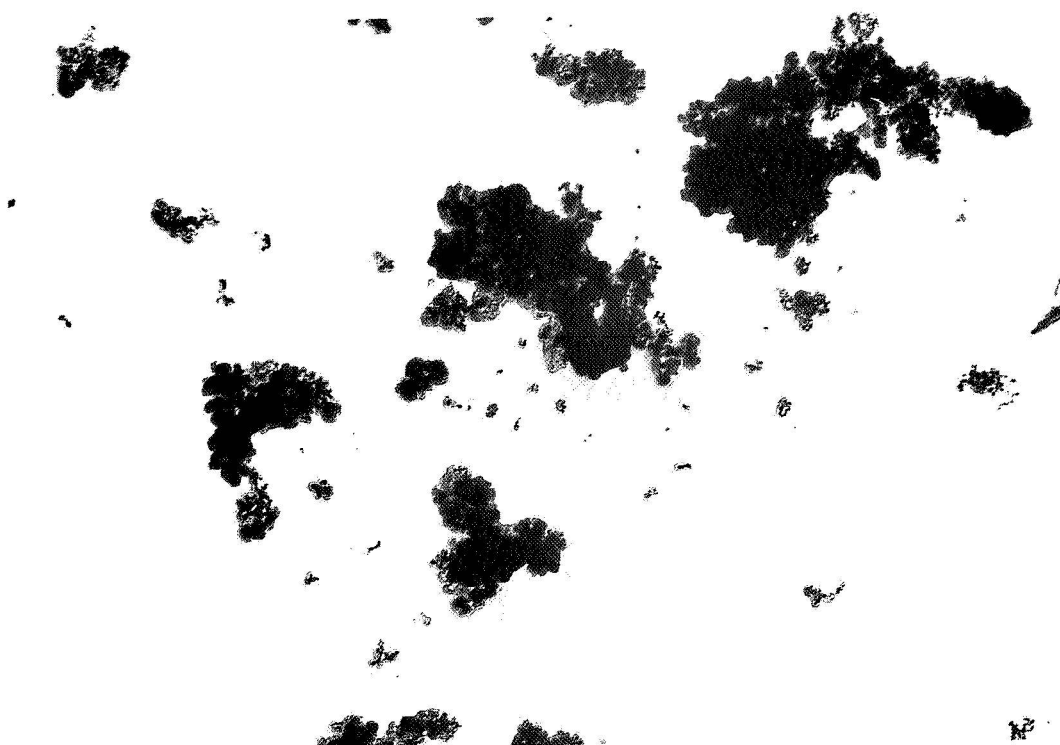
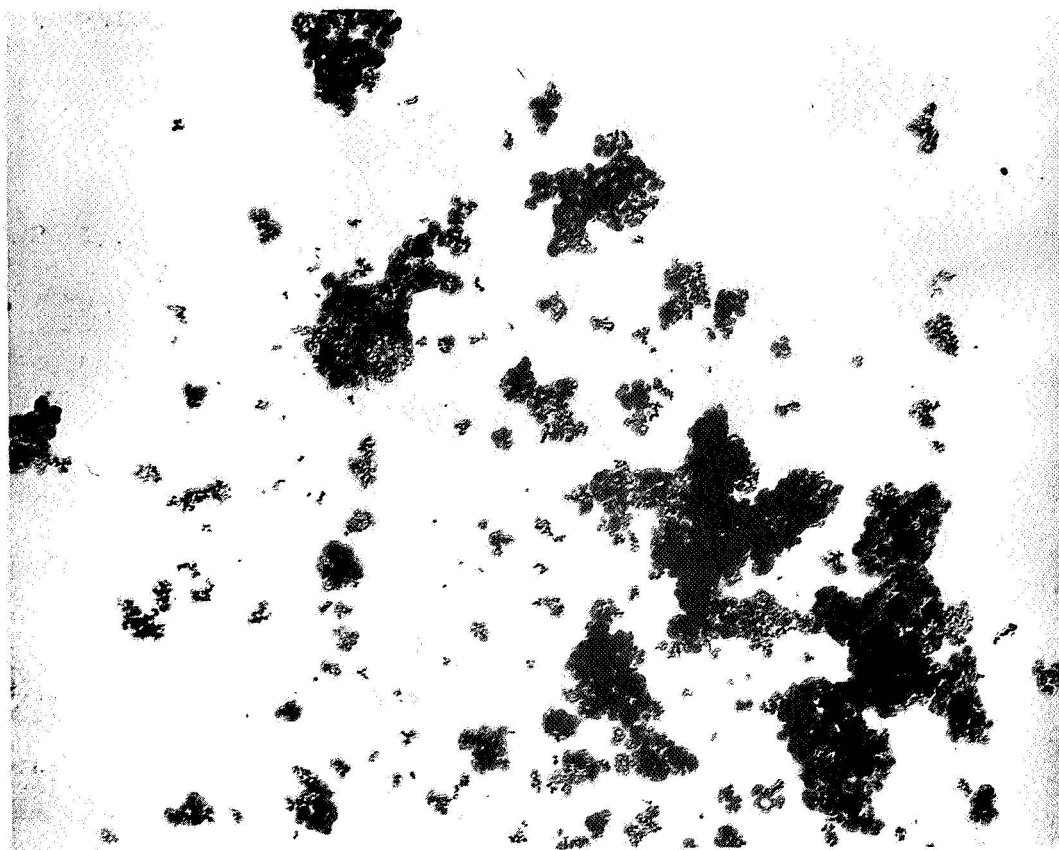


Figure 10 NRC Nickel Powder at 50,000X

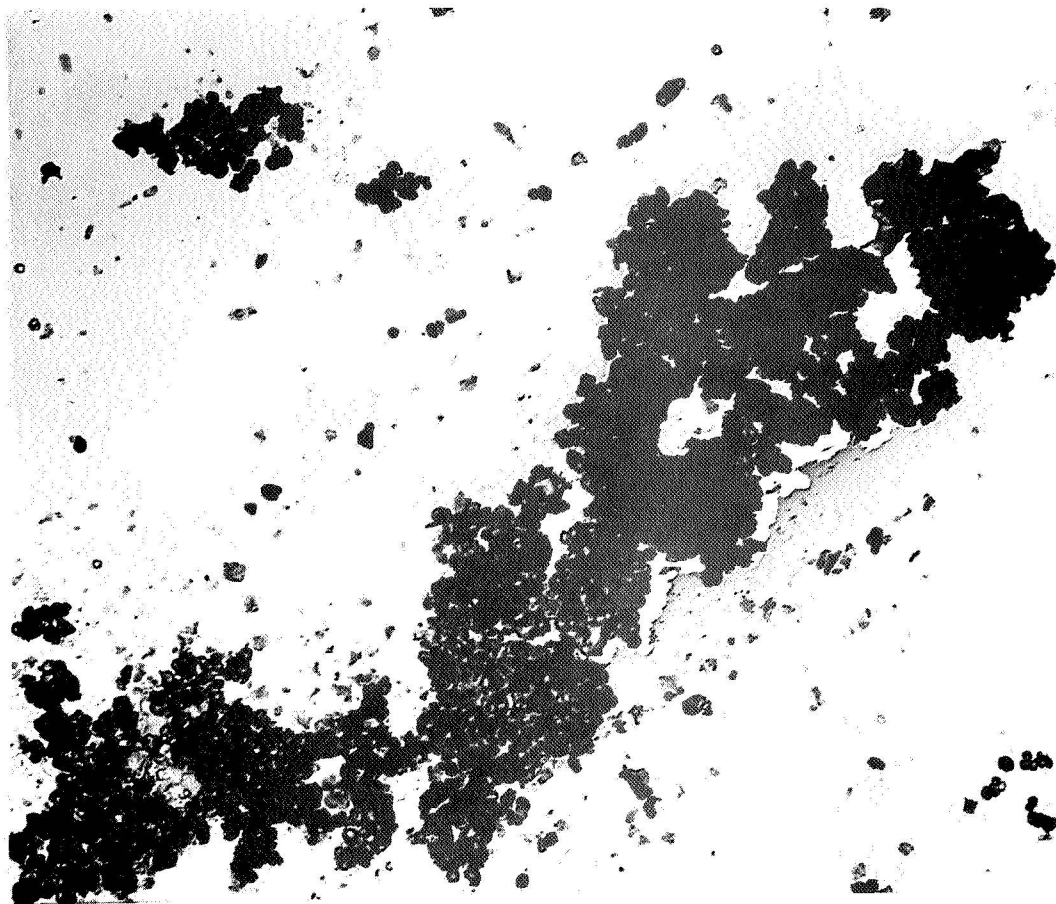


Figure 11 Sherritt Gordon Nickel Powder at 12,000X

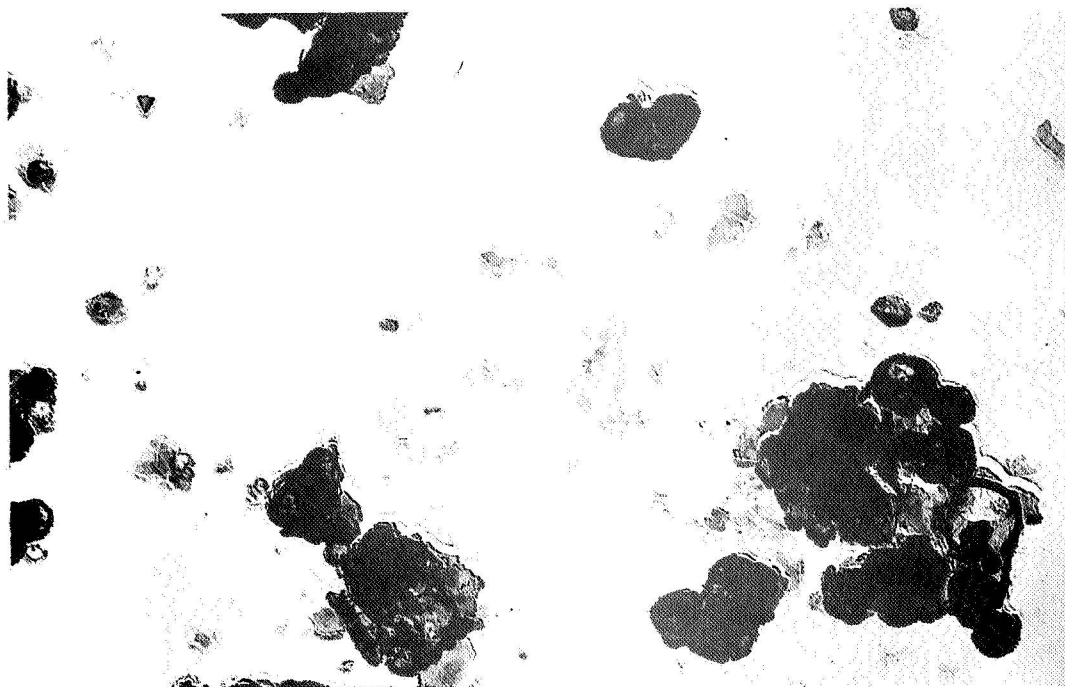


Figure 12 Sherritt Gordon Nickel Powder at 50,000X

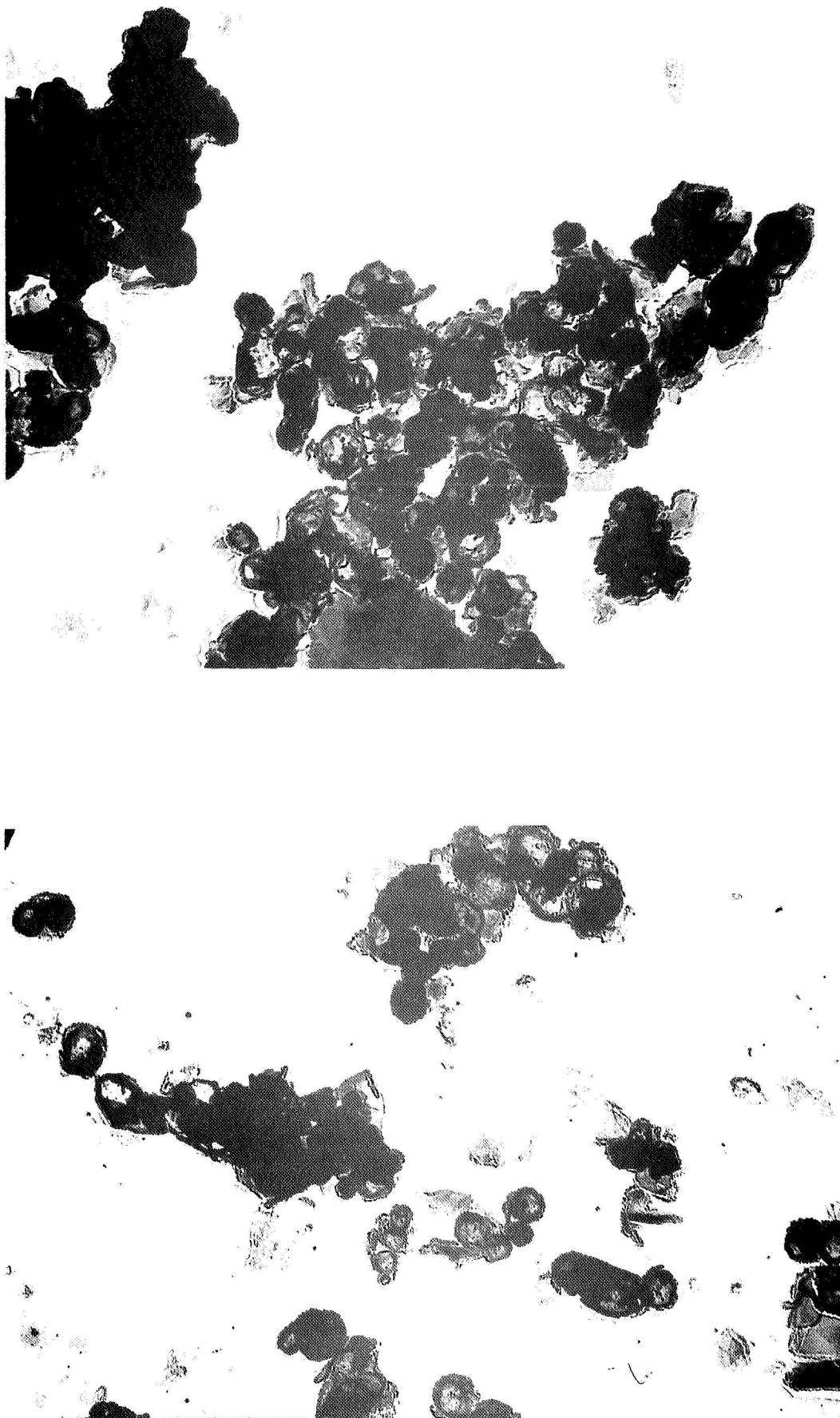


Figure 13 Sherritt Gordon Nickel Powder at 50,000X



Figure 14 Sherritt Gordon Nickel Powder at 50,000X

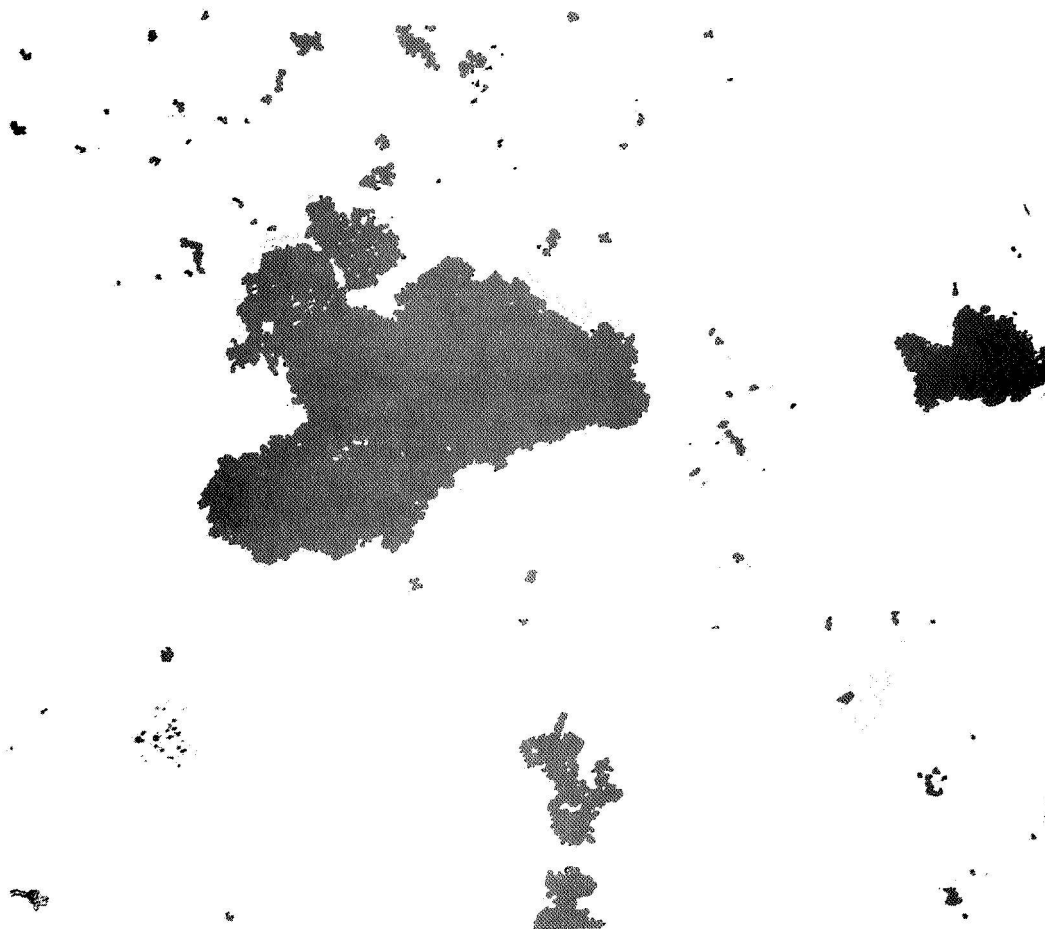


Figure 15 Vitro Laboratories Nickel Powder at 12,000X

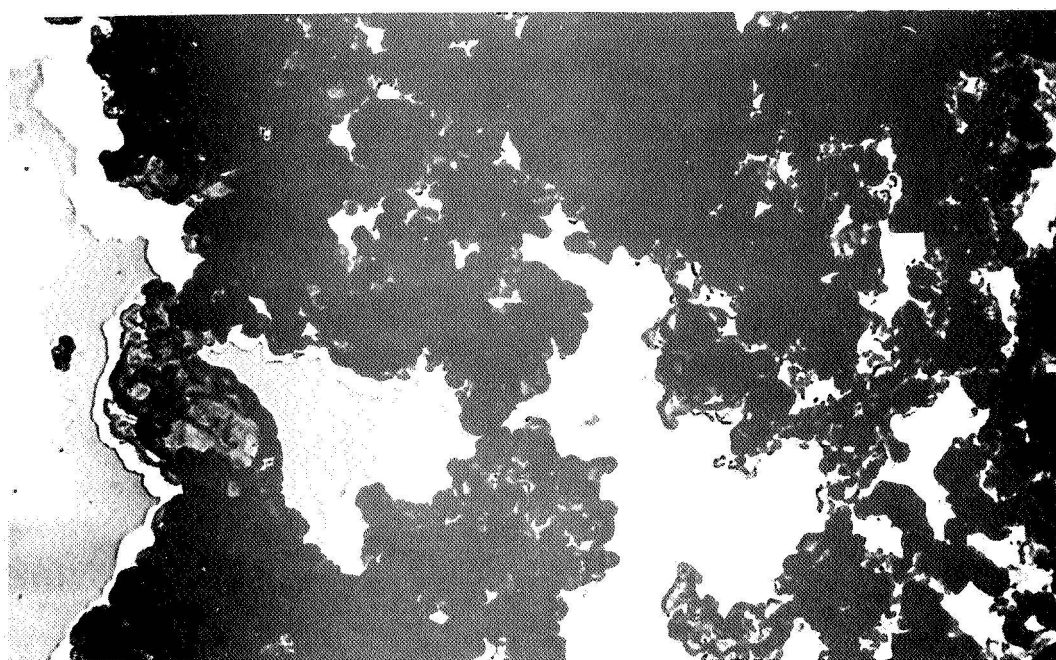


Figure 16 Vitro Laboratories Nickel Powder at 50,000X

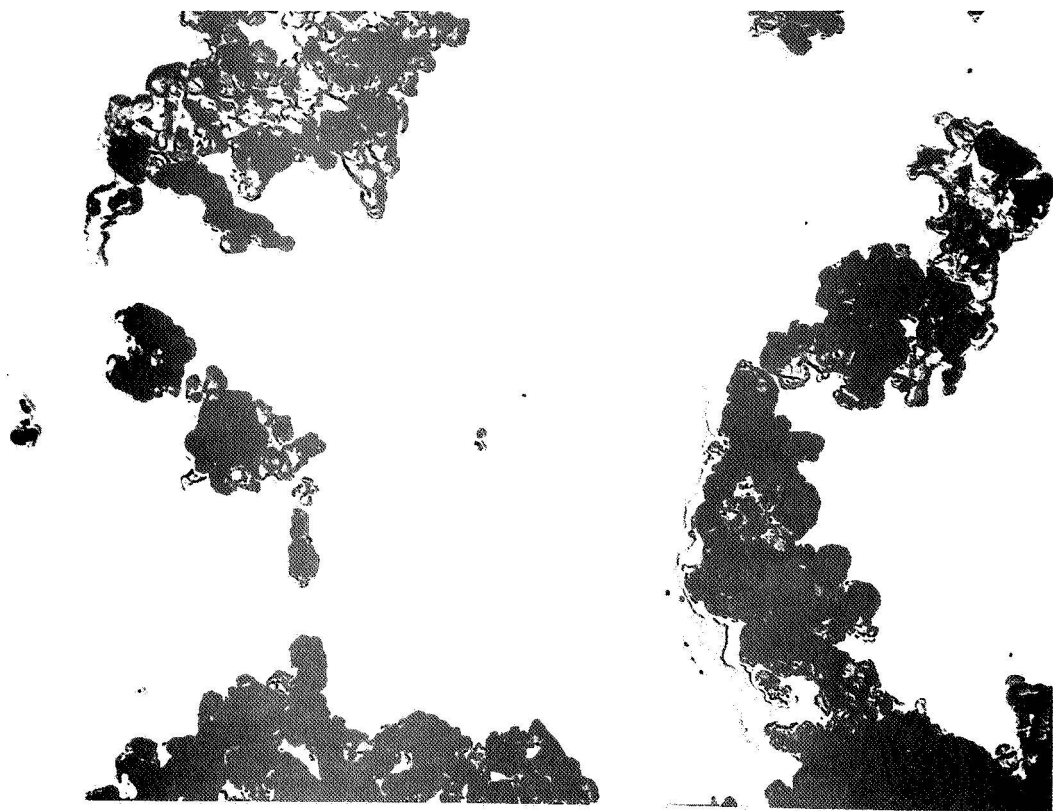
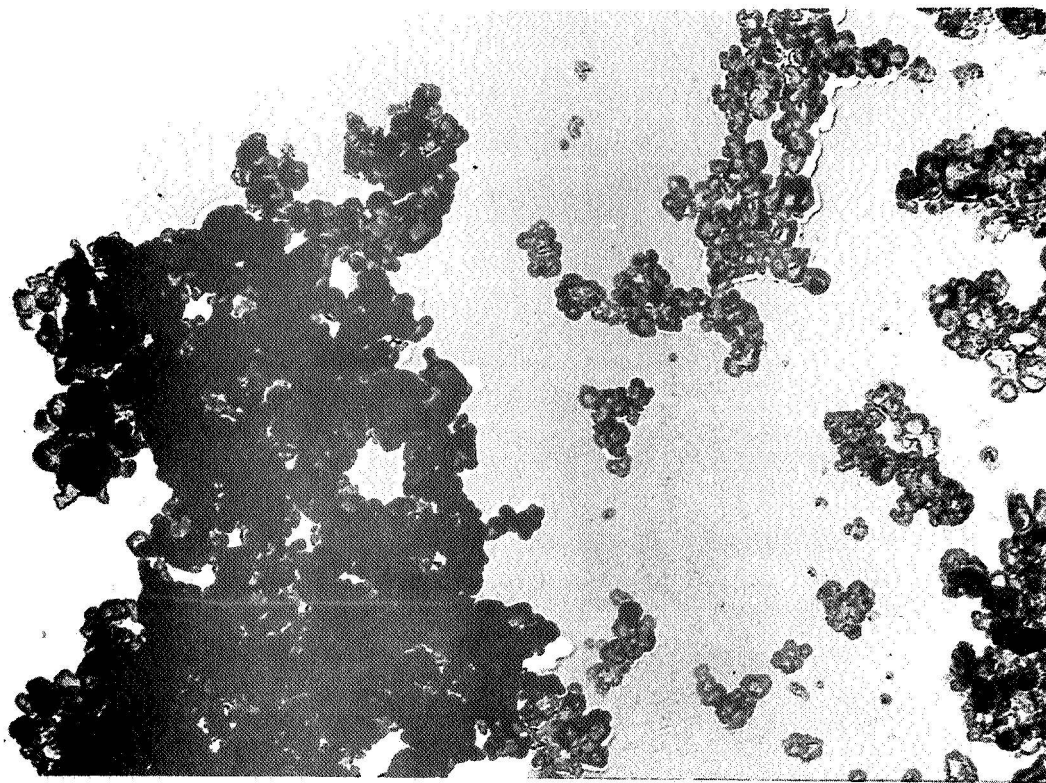


Figure 17 Vitro Laboratories Nickel Powder at 50,000X

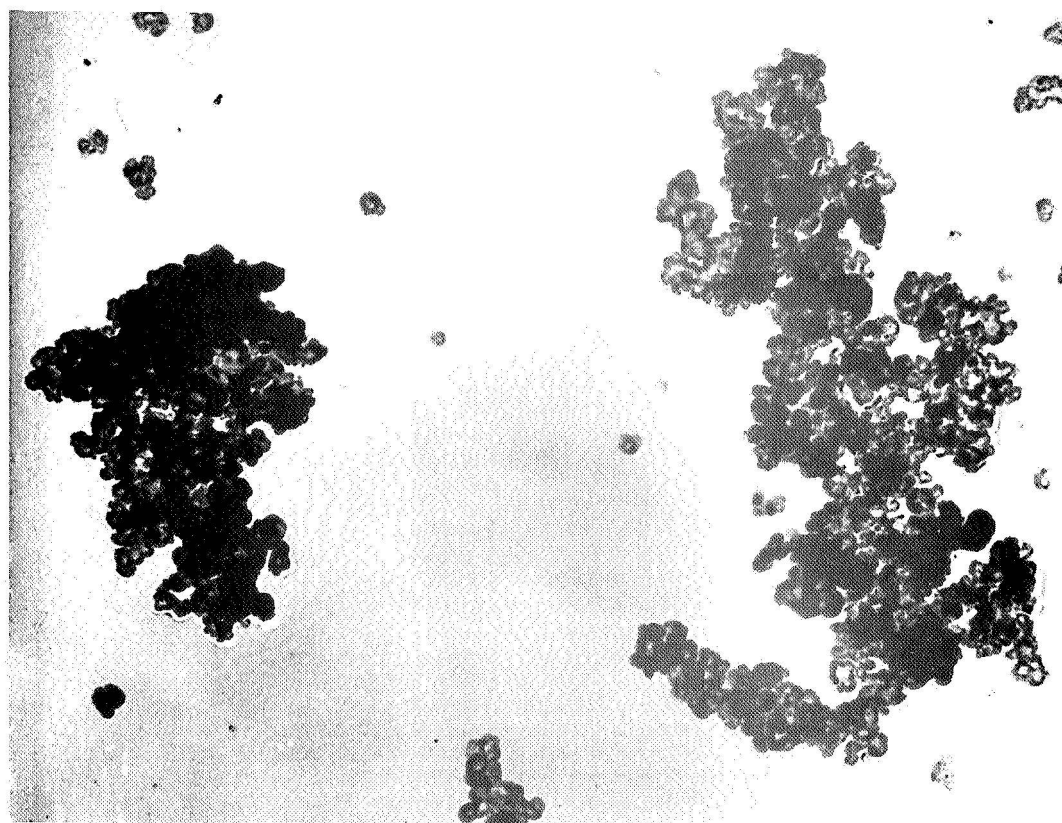
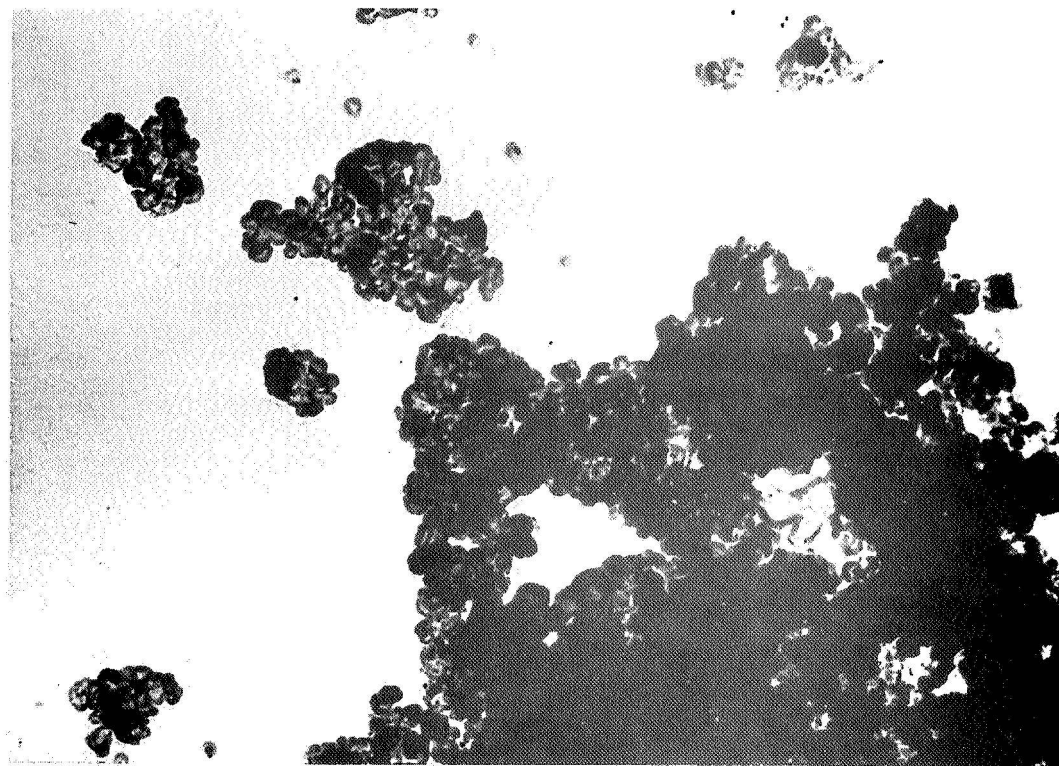


Figure 18 Vitro Laboratories Nickel Powder at 50,000X

The main advantages of the Sherritt Gordon powder over the Vitro powder are low price, low sulfur content, less reactivity in air, higher surface area, better particle-size distribution as indicated by the Micromerograph, and ease of dispersion of the powder agglomerates as indicated by microscopic smears and deagglomerator pressure. The main advantages of the Sherritt Gordon powder over the NRC powder are low price, better spectrographic analyses, and somewhat better (smaller) particle-size distribution as indicated by both high and low pressures in the Micromerograph. The Vitro powder is definitely not a desirable choice, but the NRC is a possibility, based primarily on the electron micrographs at 50,000X. These show the NRC powder to be more readily dispersed into very small particles (under 200 angstroms) than the Sherritt Gordon under the conditions used for preparation of electron micrographs. However, undispersed agglomerates are present in the prepared samples of the NRC as well as the other powders, and may still account for a high-weight fraction of the sample.

Two additional types of measurements were made on the purchased sub-micron nickel powders, as described below.

Nature of the Oxygen Content

Samples of each powder were obtained in the glove box in a good argon atmosphere and submitted to our Analytical Laboratory for a series of measurements.

Each sample was heated in a tube furnace with a nitrogen atmosphere at 375°C for one hour. After the weight loss was determined, the sample was heated again with a hydrogen atmosphere at 925°C for one hour; and the weight loss again was determined. Part of this hydrogen-reduced sample was then analyzed for residual oxygen in the Leco conductometric analyzer. The weight loss in nitrogen was considered to be absorbed gas or moisture, and the weight loss in hydrogen was considered to be oxygen which had been chemically combined with nickel. The sample after these furnace treatments was well sintered so that the pickup of oxygen from the atmosphere would be expected to be negligible. Therefore, the residual oxygen found by the Leco analyzer was considered to consist entirely of oxygen which was chemically combined with those impurity elements present in the original nickel powder and which was not reducible by hydrogen at 925°C. The results obtained are listed in Table 4.

TABLE 4

Successive Analyses of Nickel Powder

Source of Nickel Powder:	<u>SG</u>	<u>NRC</u>	<u>Vitro</u>
% Loss in N ₂ (H ₂ O)	2.70	0.68	0.22
% Loss in H ₂ (O)	3.04	9.14	1.23
% Residual Oxygen	<u>0.0125</u>	<u>0.146</u>	<u>0.139</u>
Total	5.75	9.97	1.59

One point of significance for the residual oxygen results is that the NRC and Vitro powders contain more oxygen that is not removable by hydrogen reduction at 925°C than the maximum allowable oxygen content (0.05%) of the hydrogen-cleaned powder according to the requirements of this contract.

In the Leco analysis, carbon reduces (at 1600°C) oxides which are present as impurities and are not reducible in hydrogen (at 925°C).

Although it may be difficult to say precisely which metals are reduced by carbon under the conditions of this analysis, it may be desirable to consider the amount of impurity metals which would probably not be reduced from their normal oxides by hydrogen.

Table 5 shows a listing of such impurity metals and their oxygen equivalents based on quantitative and qualitative spectrographic analyses of the samples after hydrogen reduction, but before being analyzed for residual oxygen. (The Sherriitt Gordon analysis used is that of the original "as purchased" powder.)

Micromerograph Measurements

The NRC and Sherriitt Gordon powders were run again in the Micromerograph, and the recorder was allowed to run overnight while the particles under one micron in effective size settled onto the detecting pan. A small fraction in this size range was indicated for each powder, as shown in Table 6. The Micromerograph results are considered to be of some significance in this work because they show particle or agglomerate sizes which are effective in determining the powder behavior during settling in a gaseous medium.

TABLE 5
Impurity Metals and Their Oxygen Equivalents
Not Reduced by Hydrogen at 925°C (%)

<u>Metal</u>	<u>Sherritt Gordon</u>		<u>NRC</u>		<u>Vitro</u>	
	<u>Metal</u>	<u>O Equiv.</u>	<u>Metal</u>	<u>O Equiv.</u>	<u>Metal</u>	<u>O Equiv.</u>
Al	0.006	0.005	0.10	0.089	0.005	0.0044
B	N.D.	-	<0.01*	<0.022	N.D.	-
Ca	<0.001*	<0.0004	<0.001*	<0.0004	0.001*	0.0004
Cr	<0.001*	<0.0009	0.01	0.009	0.004	0.004
Mg	<0.001	<0.0007	0.002	0.0013	<0.001	<0.0007
Mn	<0.0001*	-	0.005	0.003	<0.001	<0.0006
Si	0.005	0.006	0.015	0.017	>0.10	>0.114
Ti	N.D.	-	<0.003	<0.002	<0.001*	<0.0007
Zn	N.D.	-	0.05	<u>0.012</u>	N.D.	-

✗ Total O

Equiv.: 0.011/0.013 0.1313/0.1557 >0.1228/>0.1248

N.D. - Not detected by qualitative analysis.

* - Qualitative analyses; all others quantitative.

✗ - Totals: First figure is for total except for items marked <; second figure includes these items.

TABLE 6Overnight Micromerograph Results

Deagglomerator Pressure = 400 psig

Range of Particle Diameters	<u>Percent by Weight</u>	
	<u>NRC</u>	<u>Sherritt Gordon</u>
<u>Microns</u>		
27-9	6.6	0.0
9-1	86.5	97.3
1.0-0.67	4.1	2.7
0.67-0.47	2.8	0.0
0.47-0.30	<u>0.0</u>	<u>0.0</u>
Total	100.0	100.0

RECOMMENDATION

Based on the results reported above for the three purchased sub-micron nickel powders, it was recommended that future work be confined to the Sherritt Gordon powder.

DISPERSING TESTSTABLE OF CONTENTS

	<u>Page No.</u>
INTRODUCTION	34
APPARATUS AND TESTS	37
DESCRIPTION OF APPARATUS	39
Apparatus I	39
Apparatus II	41
Apparatus III	43
RESULTS, VARIABLES AND EFFICIENCY	46
Apparatus III	56
Apparatus I	59
Apparatus II	62
Comparison of Sherritt Gordon and NRC Powders Run in Apparatus II	64
Electron Microscope Examination of Sherritt Gordon and NRC Powders Run in Apparatus II	66
RECOMMENDATION	69

INTRODUCTION

It was necessary to design a laboratory apparatus which would have sufficient flexibility to allow study of many experimental variables. In proposing a design, consideration was given to the following assumptions:

1. The temperature required for reduction would cause the powder particles to grow or sinter together significantly, (so that the surface area would be decreased below the $3 \text{ m}^2/\text{g}$ minimum allowed) if the powder were in a fixed bed or contained in a manner that would allow particles to remain in contact with each other during the heating cycles.
2. Particles of extremely fine powder would have a great tendency to clump together or to agglomerate into much larger masses (agglomerates) of powder which would be held together by relatively weak forces such as surface or electrostatic forces as contrasted with strong interatomic forces such as those present in crystal lattices. This is not to say that such forces would necessarily be easily broken or easily prevented from being effective.
3. Some investigation would be necessary to determine how best to break up agglomerates or to disperse the powder particles before they enter the heated portion of the apparatus.

4. In accordance with Stoke's law, when the powder particles are dispersed successfully as individual particles, their tendency to separate from the reducing gas by gravitational settling will be practically nil because of their extremely small size. This will benefit the reduction step, but will hinder the collection of the reduced powder.
5. A relatively short reduction time may be necessary if agglomerates are broken up, although the possibility exists that the rate of reduction may be limited by the rate of adsorption of hydrogen on, or the rate of desorption of water molecules from, the particles.
6. By achieving a high degree of dispersion of the entering powder particles, it would not be feasible to consider a fluidized-bed type of operation, nor would it be best to consider a centrifugal or cyclone type of collector. These methods become less efficient as the effective particle size is made smaller. However, should a sufficiently high degree of dispersion not be obtainable, or should sufficient residence time not be achieved for some other reason, the fluid-bed approach could be reconsidered.

A conclusion was made to evaluate one or two of the powders by subjecting them to dispersing tests to observe their behavior during passage through a hot zone while dispersed in a gas stream. Most

of the effort involved feeding the Sheritt Gordon powder, although a comparison was made in one setup with the NRC powder. The powders were dispersed in argon or hydrogen, or mixtures of argon and hydrogen. Gas flow rates between 6 and 285 liters per hour and average powder feed rates between 1.2 and 9 grams per hour were used. A hot zone temperature of 700°C was used for all tests except for one at 400°C and for control tests at room temperature. The average residence time of the gas stream in the hot zone was between 1 and 76 seconds. The dispersing tests made use of a high-voltage dispersing technique.

The principle involved in the dispersion is that particles which carry the same electrical charge tend to repel each other, whether physically separated or present in the same agglomerate. The unknown factor in using this technique was whether sufficient electrical charge can be imparted to the particles in each agglomerate to cause them to separate and disperse. It was found necessary to cause physical contact of the powder with a conductive surface which is at a high potential (+ or -) in order to impart an electrical charge. In the case of particles of a non-conductive powder, the amount of charge imparted increases as the time of such contact or the effective area of contact increases and the charge distributes itself over the particle surface. However, in the case of a conductive powder, such as nickel, the maximum charge was acquired in a very short time of contact, according to the principles of contact electrification.

It had been found in other unrelated work with submicron non-conducting powder that dispersing was improved by causing the powder to contact small metallic cones at a high electrical potential placed pointed end up in the downward flowing powder-gas stream.

APPARATUS AND TESTS

Preliminary tests were made to appraise the problem of evaluating the high voltage disperser. Figure 19 shows a photograph of the feeding apparatus, the transparent quartz dispersing chamber, and a conical metal disperser. It was found that the powder collected on the sloping sides of the cone when a low voltage or no voltage was applied to it. A voltage of 12 kilovolts or above caused the powder particles to be repelled from the cone, but a layer could still collect on the sloping surfaces of the quartz chamber.

Powder samples were collected on glass microscope slides which were examined at a magnification of 1,000X. This was inadequate for evaluation of the effects of the high voltage, since the smallest agglomerate which could be seen on a photomicrograph is about one half micron in size. Larger agglomerates were easily visible, but comparisons could not be made to evaluate dispersion efficiency. Therefore, a total of three different setups were constructed for the purposes of obtaining powder dispersions, and of evaluating the effectiveness of the dispersing process. These are illustrated by the sketches shown in Figures 20, 21, 22, and 23. Transparent quartz tubing was used in the construction of each setup.

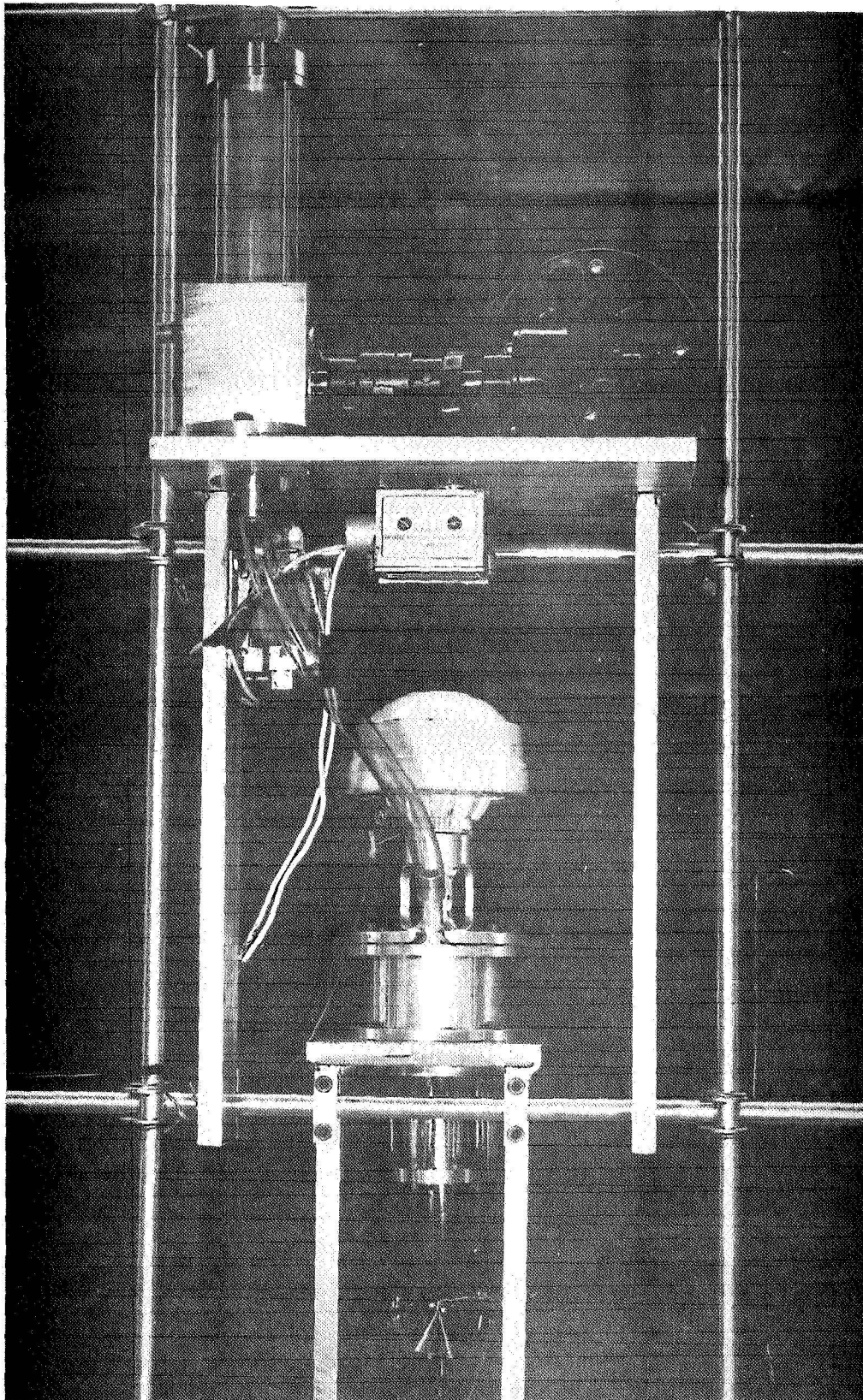


Figure 19 Feeding Apparatus

This was insulated with asbestos tape (placed over it) and the heating was regulated by a temperature controller and thermocouple.

DESCRIPTION OF APPARATUS

Apparatus I

The apparatus shown in Figure 20 provided for contact of the powder with a hollow tantalum or nickel cone (#1 head) or a hollow nickel frustum (#2 head), passage of the powder dispersed in argon through the 12-inch-long hot zone, and collection of the powder by gravitational settling in a flask of large cross-sectional area. The exit gas passed through a bubbler containing vacuum pump oil, which was found to trap the small amount of powder which did not settle out in the collection flask.

Sherritt Gordon powder was fed over a period of time with an argon flow rate between 6 and 30 liters per hours.

For the tests run using this apparatus, the voltage applied to the disperser cone was in the range -2 to -12 kilovolts or in the range +2 to +9 kilovolts. After a reasonable quantity of powder was collected in the flask, the operation was stopped and the flask was disconnected at the Tygon connections and stoppered. The flask was then placed in the glove box. Samples of the powder were placed in sample containers for measurements of the specific surface.

It was observed that occasionally, during the test run, clumps of powder agglomerates were dislodged from the sloping quartz surface

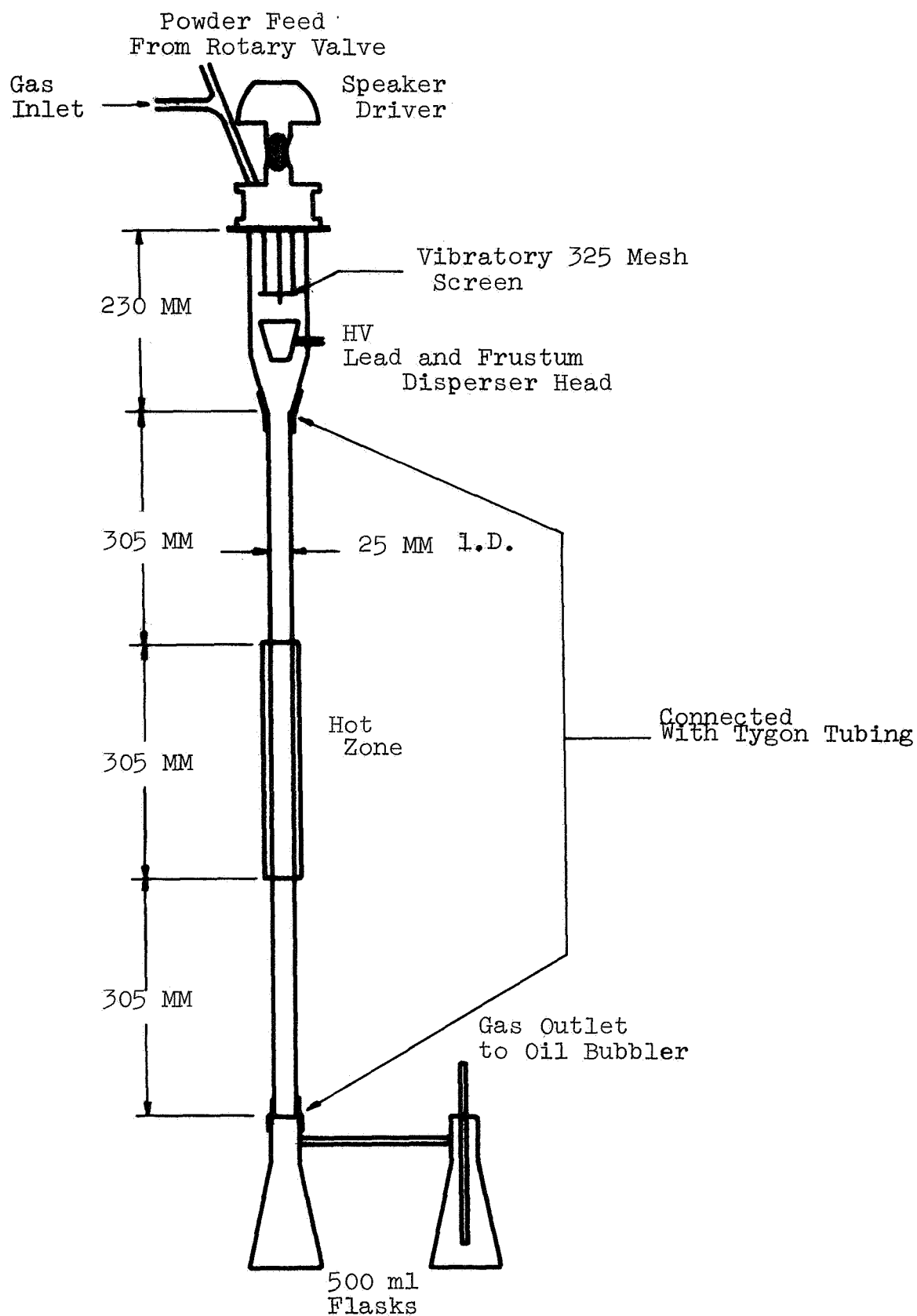


Figure 20 Apparatus I

in the disperser chamber and fell rapidly through the hot zone into the collection flask. When this occurred, the gas flow through the hot zone was disturbed and produced periodic surges which were seen in the discharge gas bubblers.

Apparatus II

The apparatus shown in Figure 21 was designed to prevent undispersed powder falling through the hot zone and being included in the collected powder. Any undispersed powder fell into a separate detachable vessel located directly beneath the feeder and disperser head. The dispersed powder was carried out through the horizontal outlet tube and then through the hot zone and collected separately in a manner similar to that used before. The collection flask could be detached by removing a short section of rubber tubing from the quartz tube which contained the hot zone. The flask was isolated from the atmosphere by first closing the rubber tubing with a squeeze clamp. The flask could then be placed inside the glove box for extraction of the powder in an argon atmosphere. The vertical quartz tube was smaller in I.D. (12 mm) to minimize back flow or eddying in the hot zone. Using this setup, tests were run to evaluate dispersing efficiency in a manner similar to that used before. Argon, hydrogen, or mixtures of these gases were used with flow rates between 72 and 285 liters per hour. Average powder feed rates were between 0.5 and 9.4 grams per hour and potentials applied to the disperser head were between -4 and -15 kilovolts or between +4 and +17 kilovolts, as shown below with the results. All samples were measured for

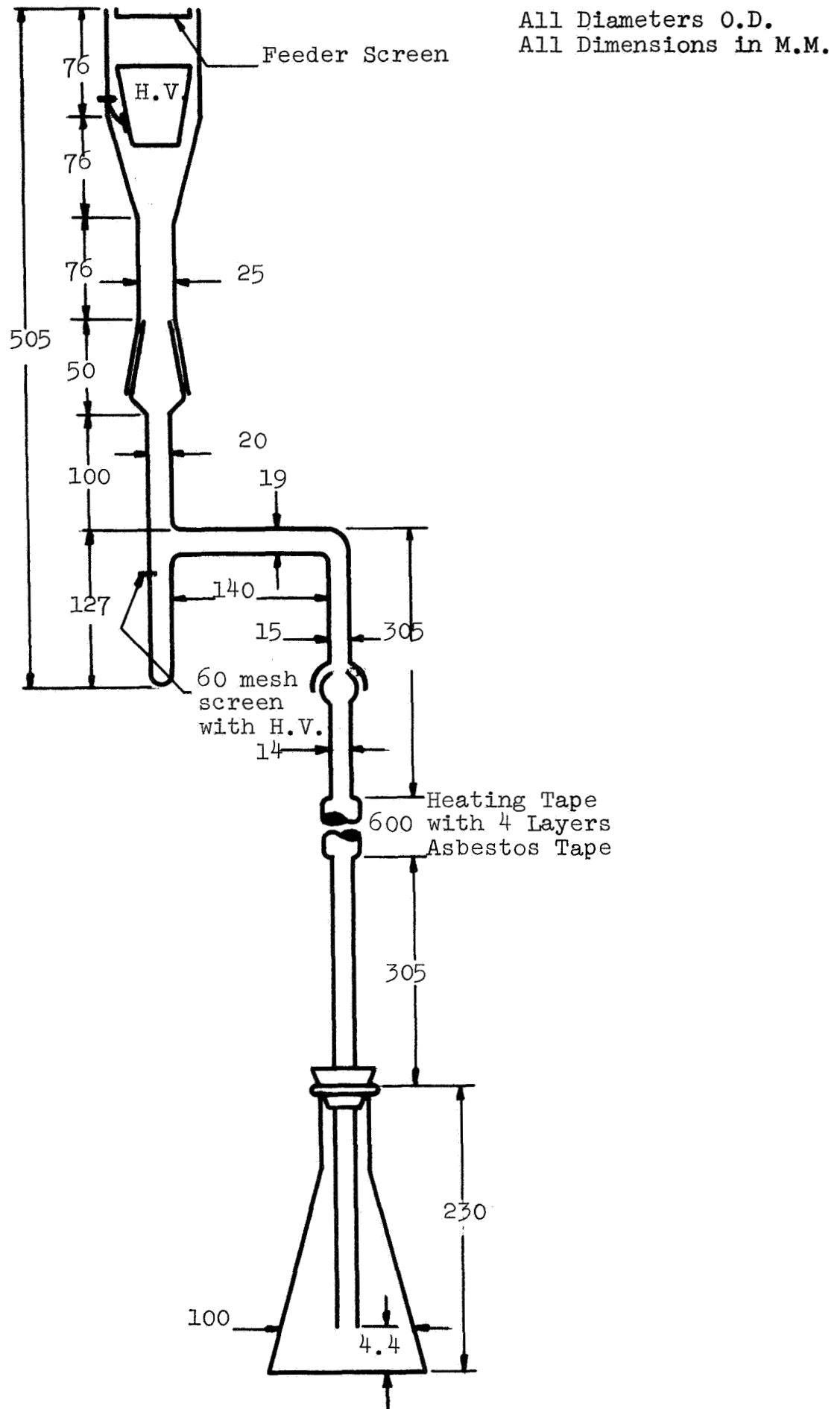


Figure 21 Apparatus II

specific surface if they were large enough, and some samples run in the presence of hydrogen were also analyzed for oxygen content to give a preliminary concept of the ease of oxygen removal.

Apparatus III

The apparatus shown in Figures 22 and 23 was designed to obtain more benefit in dispersing the powder from the inlet flowing gas stream, and provide a greater probability of contact of the undispersed powder, as well as of the powder coming directly from the feeder, with the disperser head. The powder fed from the vibratory screen fell onto either the disperser head, which consisted of a hollow nickel frustum, or the 400-mesh screen through which the inlet gas flowed. Both were connected to the high voltage source and aided in charging the powder particles. The dispersed powder was carried out with the gas through the horizontal outlet tube, vertically upward, and then vertically downward, through the hot zone. The treated powder was separated from the exit gas stream either by settling out or by collection on the inside surface of the electrostatic precipitator (Figure 20). The precipitator was located inside the interchange compartment of the glove box and was surrounded by the inert atmosphere of the glove box. After the test run was complete, the powder was removed, weighed, and sampled in the glove box itself.

Tests were run to evaluate this apparatus with various gas compositions and disperser voltages. The total weight of powder fed was determined and also the weight carried over and collected. Samples

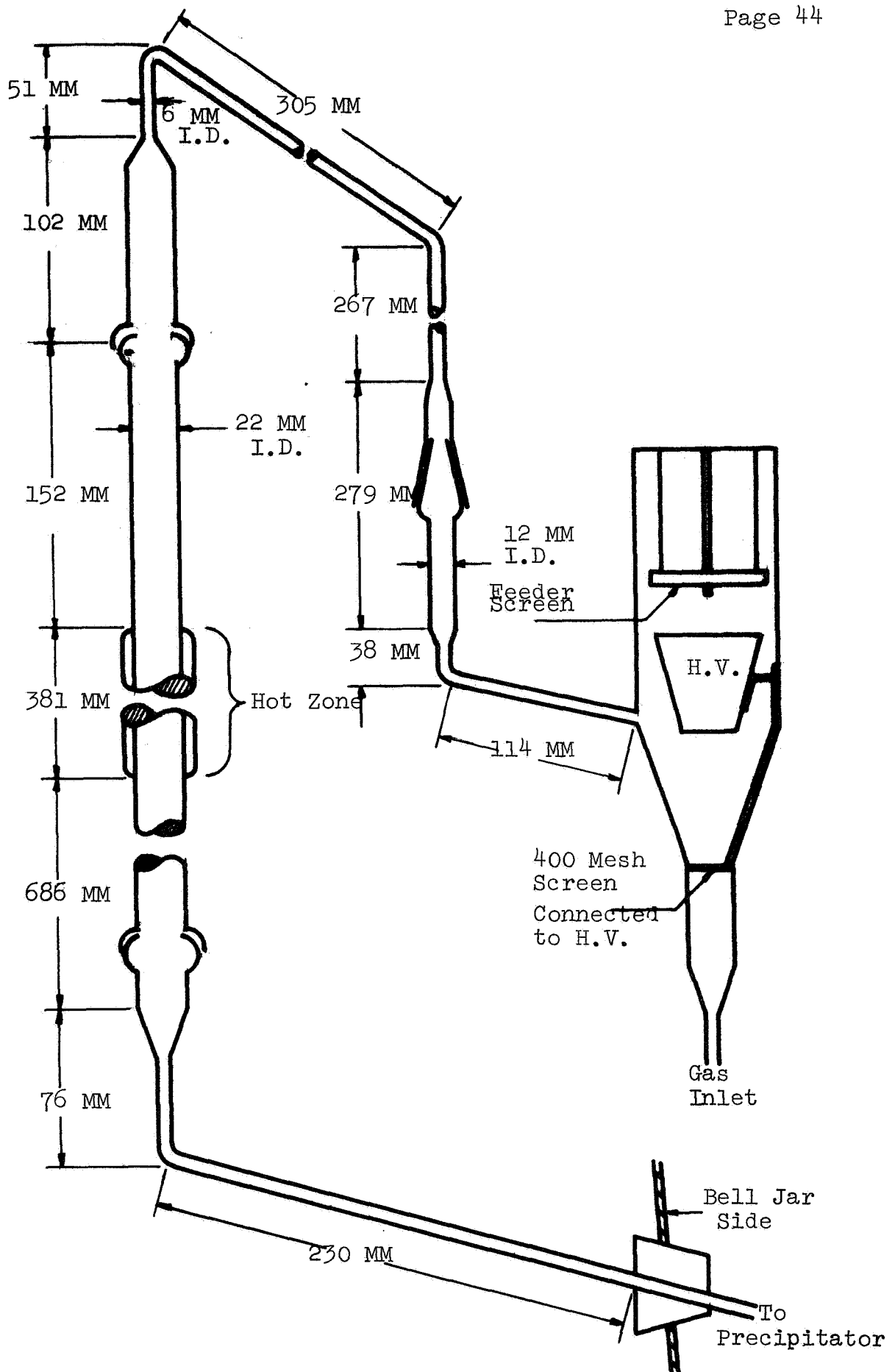


Figure 22 Apparatus III

Main Tube 22 MM I.D.

Arm Tubes 6 MM I.D.

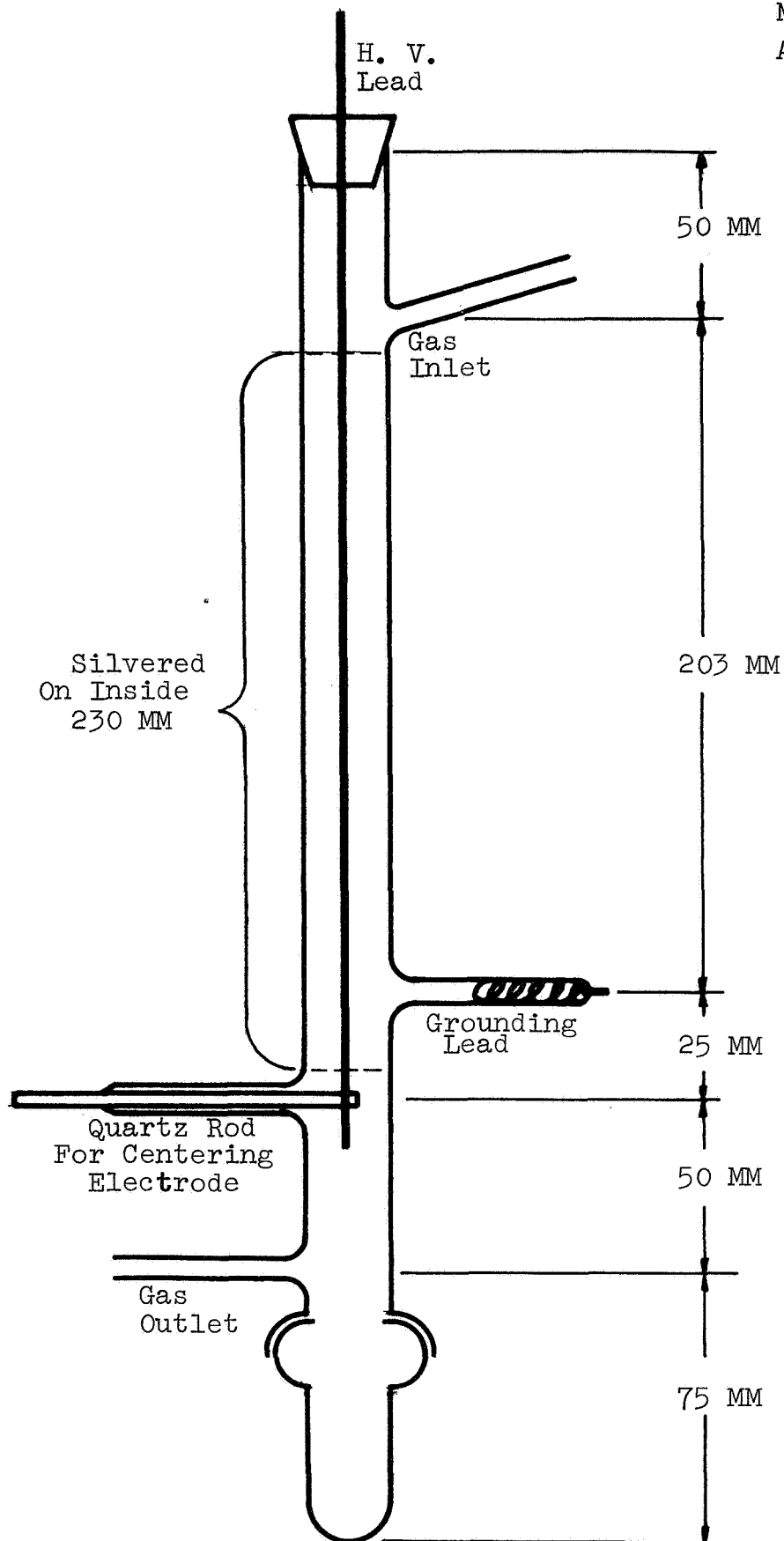


Figure 23 Apparatus III

of treated powders which were large enough were measured for specific surface by the BET method (3). After test 1, the frustum disperser head (A) was removed and a vertical wire was installed which extended from the center of the 400-mesh screen to within 9.5 cm of the feeder screen. This wire which was used for all the remaining tests was, of course, at the same disperser potential as the screen upon which the powder fell (head B).

RESULTS, VARIABLES AND EFFICIENCY

The results of the dispersing tests made in the setups illustrated in Figures 20 and 21 are shown, respectively, in Table 7 and Table 8. These tables show the specific conditions which were changed between tests as well as the measurements made on the resulting powder. Plots of some of the data in Table 7 are shown in Figures 24 and 25. Plots of some data in Table 8 are shown in Figures 26 and 27.

The residence time of the gas stream (containing dispersed powder) in the hot zone as listed in each table was calculated as follows:

$$\theta_H, \text{ Residence Time} = \frac{\text{Volume of Hot Zone}}{\text{Volume Flow/Time}}$$

$$\theta_H = \frac{\pi D^2 \cdot L}{v/\theta} = \frac{\pi \cdot (\text{cm}^2) \cdot \text{cm} \cdot 3600 \text{ sec/hr}}{4.1/\text{hr} \cdot 1000 \text{ cc/l}}$$

$$\theta_H = \frac{2.827 (\text{cm})^2 \cdot \text{cm}}{1/\text{hr}}$$

For Apparatus I, $D = 2.3 \text{ cm}$ and $L = 30.5 \text{ cm}$.

$$\theta_H = \frac{2.827 (2.3)^2 \cdot 30.5}{1/\text{hr}} = \frac{456.1}{1/\text{hr}}$$

TABLE 7

Dispersing Tests I

Using Apparatus Shown in Figure 20

No.	Disperser Head	Argon Flow l/hr	Gas Residence Time Seconds	Temp. °C	Disperser Potential kv	Specific Surface m ² /g	Particle Diameter Microns
1	#1 Ta cone	6	76	400	0	23.3	0.019
2	#1 Ta cone	6	76	700	-12	12.9	0.035
3	#1 Ni cone	15	30	700	+9	12.5	0.036
4	#1 Ni cone	12.9	35	700	+5	8.7	0.052
5	#1 Ni cone	12.9	35	700	+2	7.3	0.062
6	#1 Ni cone	12.9	35	700	-8	21.3	0.021
7	#1 Ni cone	12.9	35	700	-5	7.3	0.062
8	#1 Ni cone	12.9	35	700	-2	16.4	0.027
9	#1 Ni cone	12.9	35	700	-5	10.1	0.044
10	#1 Ni cone	6	76	700	+5	9.5	0.047
11	#1 Ni cone	30	15	700	+5	10.1	0.044
12	#1 Ni cone	12.9	35	700	0	4.5	0.10
13	#1 Ni cone	30	15	700	0	6.6	0.068
14	#2 Ni frustum	12.9	35	700	+7	8.0	0.056
15	#2 Ni frustum	12.9	35	700	-7	11.1	0.041
16	#2 Ni frustum	12.9	35	700	+4	9.3	0.048

TABLE 8

Dispersing Tests II

Using Apparatus Shown in Figure 21

No.	Ar Conc. Vol. %	Gas Rate l/hr	Residence Time Seconds	Powder Rate g/hr	Powder Conc mg/l	Disperser Potential kv	Dispersing Efficiency %	Specific Surface m ² /g	Particle Diameter Microns	Oxygen %
1	100	72	3.4	9	125	+ 8	0.6	23.3	0.019	-
2	0	285	0.9	9	33	+17	3.7	5.6	0.080	0.4
3	0	285	0.9	7	24.6	-15	2.4	14.6	0.031	0.3
4	0	90	2.7	1.2	13.0	+15	0.0	-	-	-
5	14	94	2.6	2.2	23.0	+15	0.0	-	-	-
6	30	150	1.6	1.5	10.0	-10	9.5	7.8	0.058	0.4
7	30	150	1.6	2.7	18.0	-10	15.1	3.6	0.13	0.3
8	50	150	1.6	4.5	30.0	-10	8.7	10.3	0.044	-
9	38	195	1.3	6.6	34.0	+10	2.6	-	-	-
10	0	225	1.1	3	13.0	-15	3.2	-	-	-
11	0	240	1.0	5	21.0	-14	3.6	-	-	-
12	5	240	1.0	7.2	30.0	-10	7.4	10.0	0.045	-
13	10	240	1.0	5.1	21.0	-10	10.0	6.7	0.067	0.35
14	10	240	1.0	5.2	22.0	-10	9.5	4.0	0.11	0.35
15	30	240	1.0	8.7	36.0	-10	14.0	14.6	0.031	-
16	30	240	1.0	5.5	23.0	-10	12.2	10.0	0.045	0.4
17	30	240	1.0	4.4	18.0	-12	17.7	3.6	0.13	0.4
18	30	240	1.0	3.0	12.5	+10	7.1	-	-	0.35

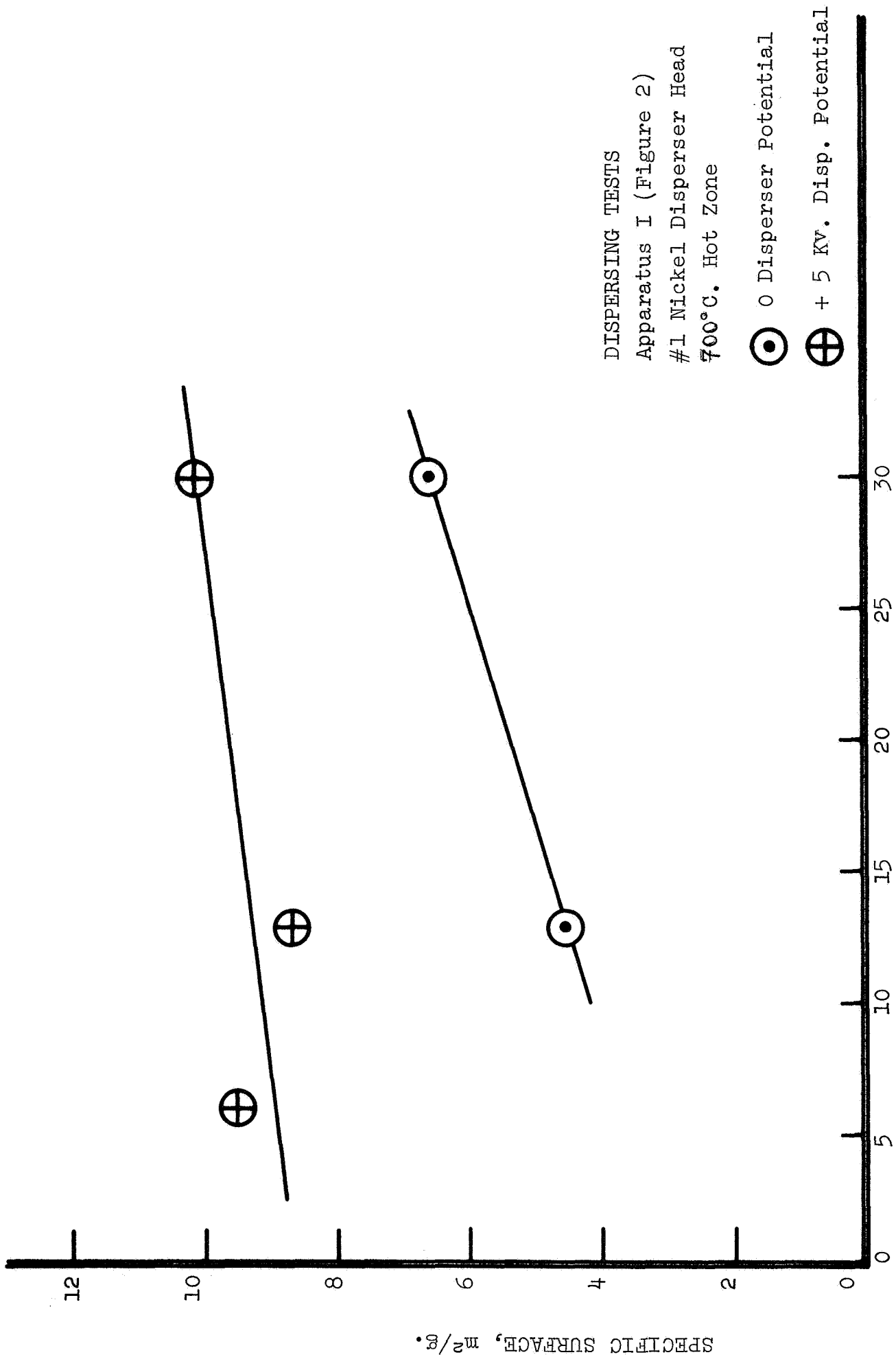


Figure 24 ARGON FLOW RATE, liters/hour

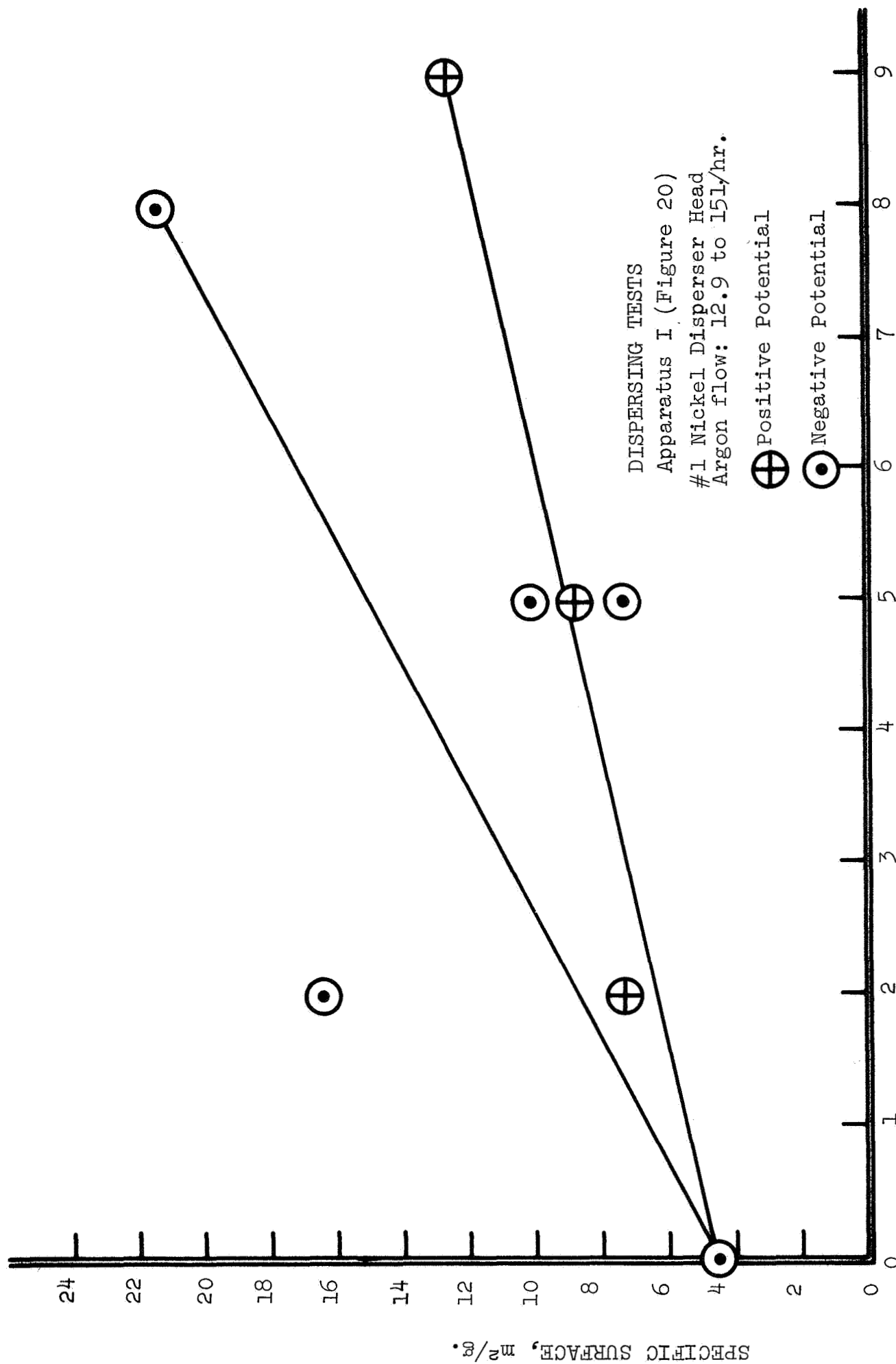


Figure 25 DISPERSER POTENTIAL, Kilovolts

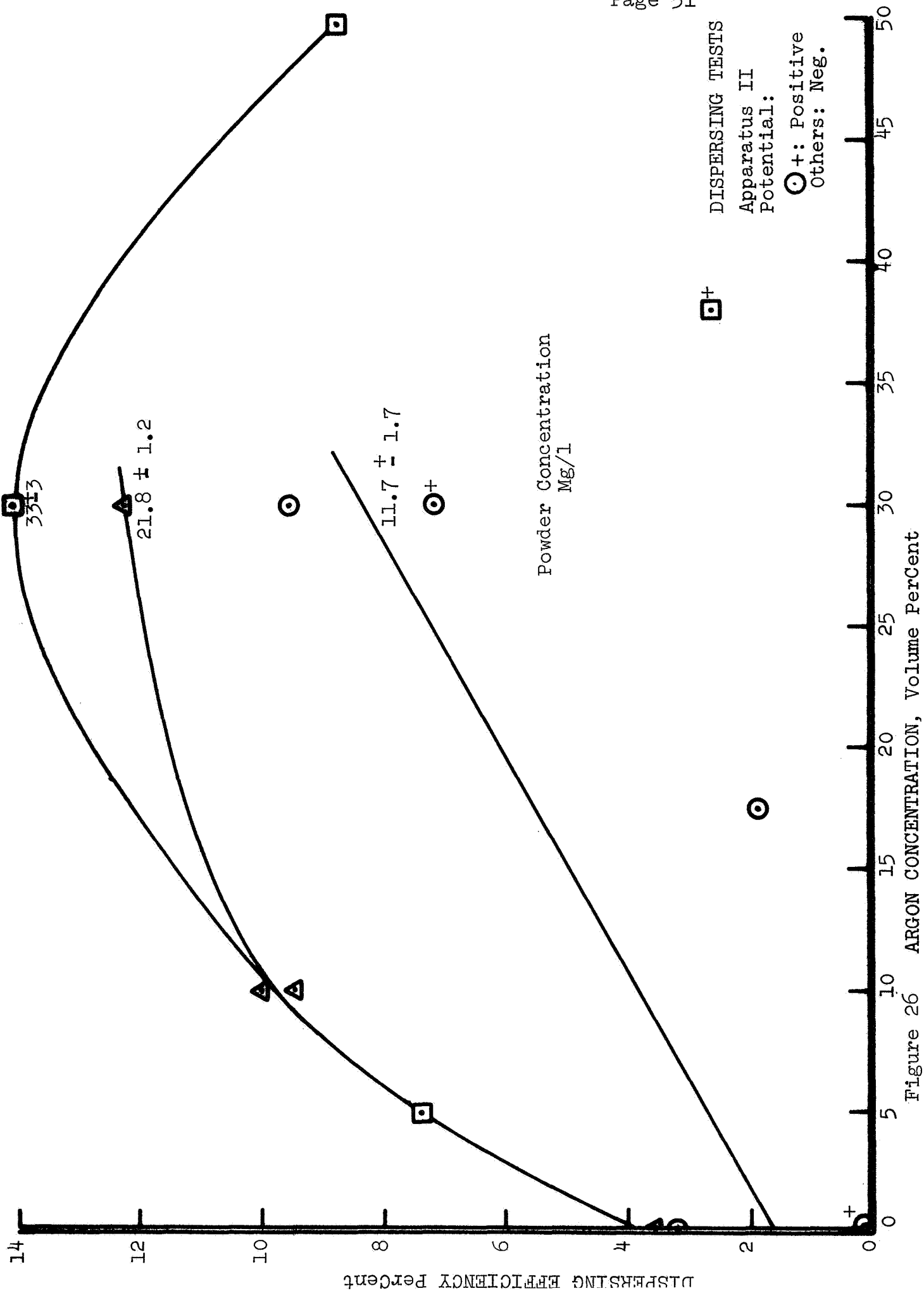


Figure 26

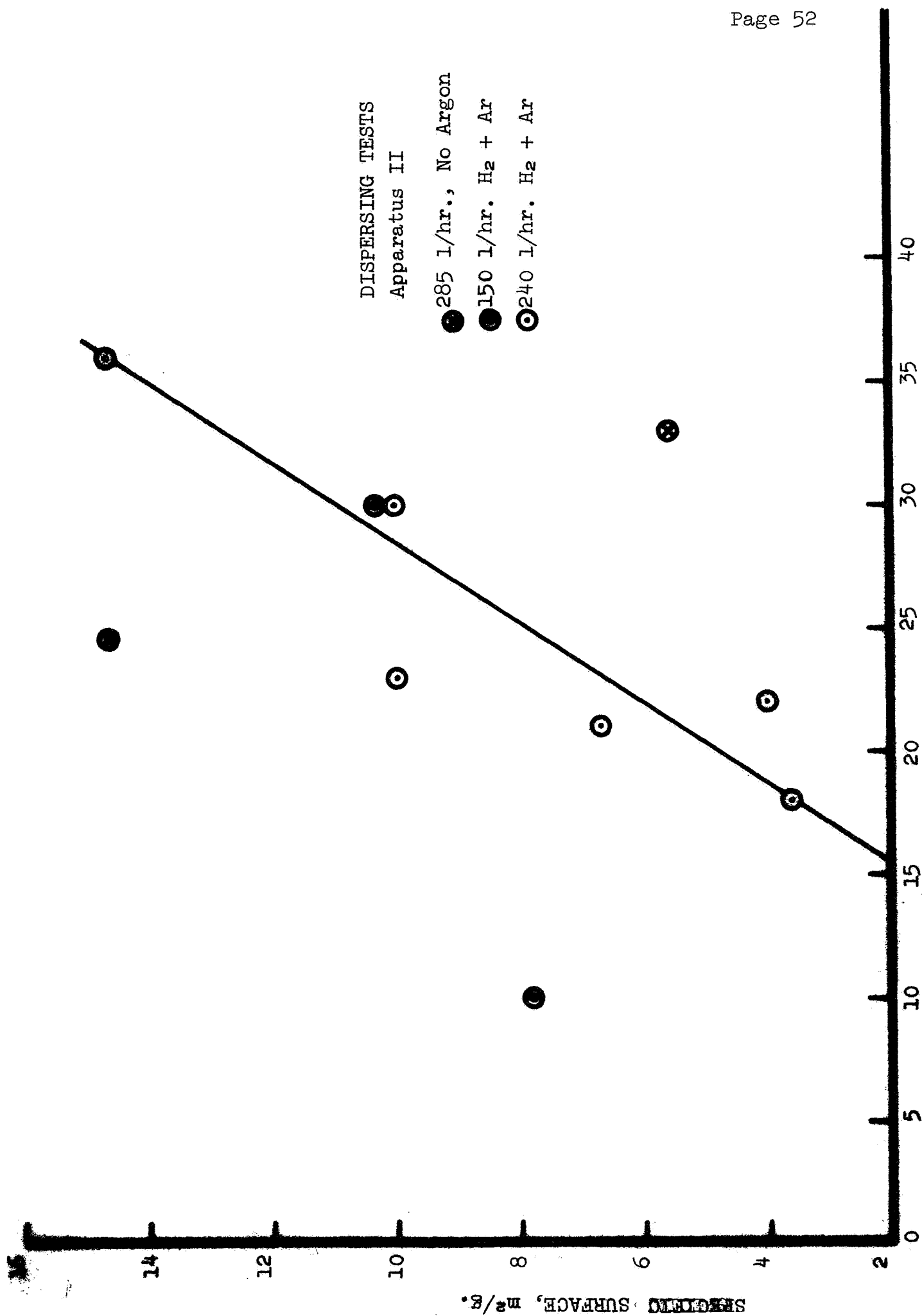


Figure 27 POWDER CONCENTRATION M-%

For Apparatus II, $D = 1.2$ cm and $L = 60$ cm.

$$\theta_H = \frac{2.827(1.2)^2 \cdot 60}{1/\text{hr}} = \frac{244.2}{1/\text{hr}}$$

The residence time of the powder particles could have been less than that for the powder should the powder particles or agglomerates be large enough to fall more rapidly through the hot zone. If the powder were completely dispersed into the ultimate particles whose size would be equivalent to that calculated from the specific surface, the maximum separation rate of particles from gas due to gravity would occur in the case in which the smallest specific surface (largest particle size) was obtained. This specific surface was 3.6 square meters per gram for test numbers 7 and 17 (Table 8). The equivalent particle diameter in all cases was calculated from the specific surface using the following relationship:

$$D_p = \frac{4}{d \cdot S}$$

where D_p = particle diameter, microns

d = absolute density of particle, g/cc

and S = specific surface, m^2/g

The calculated particle diameter in this case is 0.125 microns using the density of nickel as 8.9 g/cc. The terminal settling velocity for a 0.125-micron spherical particle can be calculated from the following equation (4):

$$V_t = \frac{2ga^2(d_1-d_2)}{9n}$$

$$V_t = \frac{2 \times 980.3(6.125 \times 10^{-6})^2(8.9-0.0018)}{9(5 \times 10^{-4})}$$

$$V_t = 1.51 \times 10^{-4} \text{ cm/sec}$$

where V_t is in cm/sec

g is cm/sec^2

a is radius of particle, cm

d_1 is density of sphere, g/cm^3

d_2 is density of medium, g/cm^3

n is viscosity, poises

The distance this particle would settle out of the gas during the residence time of the gas would be:

$$l_s = \theta_H (\text{sec}) \times V_t (\text{cm/sec}) = \text{cm}$$

The decrease in residence time caused by the particle settling this distance is proportional to this distance in relation to the zone length:

$$\Delta\theta_H = \frac{l_s}{L_H} \times \theta_H$$

$$\text{or } \Delta\theta_H = \frac{(\theta_H \times V_t)}{L_H} \times \theta_H = \frac{\theta_H^2 \times V_t}{L_H} (\text{sec})$$

For the 0.125-micron particle (assuming it to be spherical)

$$\Delta\theta_H = \frac{(1.6 \text{ sec})^2 \times 1.51 \times 10^{-4} \text{ cm/sec}}{60 \text{ cm}} = 6.4 \times 10^{-6} \text{ sec} \\ (\text{or } 0.0004\%)$$

A greater change in residence time would occur in those cases for which a relatively high residence time for the gas occurred. For example, using the same procedure, a calculated change in residence time of 0.004 seconds (0.0053%) was found for test no. 10 in Table 7, even though the equivalent particle size was smaller. Such a small change in residence time is, of course, insignificant. However, all the ultimate particles apparently do not become separated from other ultimate particles, but remain somewhat agglomerated, so that a greater change (decrease) in residence time than calculated above could occur. No attempt was made to determine either the extent of agglomeration after dispersing, or the change in residence time. Qualitatively, agglomeration in the fraction of powder passing through the hot zone may be judged by the specific surface measured on the collected powder. The cause for decrease in specific surface from the original ($25 \text{ m}^2/\text{g}$) in the finer fraction which is dispersed must be chiefly the sintering between agglomerated (ultimate) particles which occurs in the hot zone. Therefore, those collected samples which exhibit the lowest specific surface must be those which were the most agglomerated, or the least effectively dispersed.

Another evidence of agglomeration in the finer (dispersed) fraction was the settling of some powder onto the bottom of the horizontal connecting tube which led the powder to the hot-zone tube. This would not be expected to occur if none but completely dispersed ultimate particles, e.g., 0.02-micron particles, were present.

The specific surface values reported were the results of measurement at one point only of the BET isotherm using nitrogen as the adsorbed gas. There is evidence to indicate that a correction factor of approximately 0.76 should be applied to the reported values. Two comparison samples were measured both by the same technique and apparatus as were the nickel samples, and by Lewis Research Center. These measurements differed by the above factor. However, cross-checks on nickel samples have not been made.

Apparatus III

The results of the dispersing tests made in apparatus III are shown in Table 9. This table shows the specific conditions which were changed from test to test as well as the measurements made on the resulting powder. As the table shows, a concentration of 10 volume percent argon was used in the carrier gas for each test except for the last one in which 30 volume percent argon was used. A total gas-flow rate of 240 liters per hour was used for each test, which corresponds to an average residence time of the gas in the hot zone of 2.2 seconds.

The residence time in the hot zone was obtained from the following formula (p.46):

$$\theta_H = \frac{2.827 D^2 \cdot L}{V} \text{ (seconds)}$$

For Apparatus III, $D = 2.2 \text{ cm}$, $L = 38.1 \text{ cm}$

$$\theta_H = \frac{2.827 (2.2)^2 \cdot 38.1}{240} = 2.2 \text{ seconds}$$

TABLE 9

Dispersing Tests III

Using Apparatus Shown in Figure 22
Hydrogen-Argon Mixtures in 700°C Hot Zone

No.	Argon Conc. Vol. %	Gas Rate l/hr	Residence Time Seconds	Dis- perser Head	Disperser Potential Kilovolts	Dispersing Efficiency %	Specific Surface m^2/g	Particle Diameter Microns
1	10	240	2.2	A	-12	9.0	2.4	0.19
2	10	240	2.2	B	+23	1.8	7.6	0.06
3	10	240	2.2	B	+ 4	8.8	2.7*	0.17
4	10	240	2.2	B	+10	1.4	-	-
5	10	240	2.2	B	0	3.2	-	-
6	10	240	2.2	B	+ 4	4.6	9.7	0.05
7	10	240	2.2	B	- 4	6.1	2.2*	0.21
8	10	240	2.2	B	-10	1.1	-	-
9	30	240	2.2	B	- 5	30.2	2.3*	0.20

* These values calculated from multiple-point BET measurement (2).

The dispersing efficiency reported is the percentage of powder fed that was carried through the apparatus dispersed in the gas stream. The specific-surface values reported for tests 1, 2, and 6 were the results of measurement at one point only of the BET isotherm using nitrogen as the adsorbed gas. The values for tests 3, 7, and 9 are the results of determination of the BET isotherm from several points determined with the Numec surface-area apparatus. The equivalent particle diameter in all cases was calculated from the specific surface using the following relationship:

$$D_p = \frac{4}{d \cdot S}$$

where D_p = particle diameter, microns

d = absolute density of particle, g/cc

and S = specific surface, m^2/g

No definite trend of dispersing efficiency or particle size appears as the disperser potential is varied. However, a better efficiency is obtained with 4 kilovolts on disperser B than is obtained with either no voltage, or 10 kilovolts or higher. This was obtained for either positive or negative potentials. A significant increase in efficiency was obtained, however, when the argon concentration was increased from 10% to 30%. Although an efficiency of 30% was obtained (test 9), it is still doubtful that this method of dispersing the powder is practical.

The disperser head A (frustum) was found to allow arcing to occur at voltages much above 12 KV, and powder collected on the internal surfaces of the quartz dispersing chamber. Therefore, this head was replaced by the wire as described above. The new setup permitted a voltage as high as +30 kilovolts to be used on the disperser head without arcing. However, after powder was fed, arcing did occur and the voltage was reduced to 23 kilovolts. Under these conditions the powder was repelled by the vertical wire and some collected on the under side of the feeding screen and holder.

Apparatus I

As mentioned in the previous section, the apparatus (I) shown in Figure 20 was found to have an undesirable operating characteristic. Clumps of powder were observed to fall periodically through the hot zone and were unavoidably included in the sample to be evaluated for degree of dispersion. The validity of the evaluation is based on the assumption that all the powder passing through the hot zone would be dispersed adequately enough so that all fractions would be subjected to the elevated temperature to approximately equal extents.

This operating anomaly, however, voided this basis because the extraneous clumps of powder not only passed through the hot zone much more rapidly than the gas and the better dispersed powder, but its temperature rise is expected to be at a lower rate than the dispersed powder. It would therefore give the same indication, i.e., a high specific surface, as extremely well-dispersed powder, whereas

in fact it was hardly dispersed at all. For this reason, it is somewhat doubtful whether the results obtained with this apparatus are as meaningful as later results. However, they were studied to determine whether any trends were produced by variations in any of the operating conditions. The more definite trends observed are illustrated in Figures 24 and 25, although a trend may not be established in the case of Figure 24. This figure shows the variation of specific surface accompanying a change in the flow rate of argon when the potential applied to the disperser head is the same. A change in flow rate automatically causes an inverse change in the hot-zone residence time, so any real effect shown may be the change in specific surface with time in the hot zone rather than a change in the effectiveness of dispersing with a change in argon flow rate. A more significant factor in dispersing appears to be the potential applied to the disperser head. This is indicated by the higher specific surfaces obtained using a potential of +5 kilovolts than those obtained using zero potential. The lower (or absence of) slope of the 5-kv line also indicated the small effect of a change in hot-zone residence time when a potential is applied. Additional time in the hot zone would not be expected to exert any significant effect on particles which are well dispersed.

Better results were obtained, i.e., higher specific surfaces, when the potential applied to the disperser head was further increased, either in a positive, or in a negative direction, as

illustrated in Figure 25. This figure shows the changes in specific surface obtained when changes in the disperser potential were made while using argon flow rates of either 12.9 or 15.0 liters per hour. A smaller scale than was used in the previous figure for the specific surface was used to accommodate the higher values obtained. The regular increase using a positive potential seems to indicate rather definite benefits to be derived from the use of high voltage in that better dispersing of the powder evidently results. The erratic increase in the case of a negative potential raises a question as to the real cause of the higher values of specific surface obtained in two instances. The problem discussed above could have been more serious in these cases, so that the higher values resulted to a greater degree from the relatively unaffected powder clumps which passed rapidly through the hot zone.

Higher potentials than +9kv or -8kv could not be applied to the #1 nickel cone without producing an arc in the argon-powder mixture. The top of the 2" high cone was located 1 1/4" below the vibratory screen which was kept at ground potential.

The #2 nickel disperser head which was in the shape of a frustum was placed at the same distance from the screen. However, arcing was encountered at only -7.5kv with this head. This shape was tried to determine whether the powder would be more effectively kept away from the quartz walls by directing the powder toward the center instead of toward the walls.

Apparatus II

The apparatus (II) shown in Figure 21 was operated using hydrogen, argon, or mixtures of these gases. Upon discharging from their respective flowmeters, the gases were mixed while flowing through 1/4-inch copper tubing to the dispersing chamber. The composition of the mixed gases expressed in volume percent of argon is listed in Table 8 for each test run. The average powder feed rate during each test is also listed and was used with the total gas flow rate to calculate an average powder concentration which is listed as milligrams per liter.

This apparatus allowed collection of both a dispersed fraction of the powder which passed through the hot zone and an undispersed fraction which fell directly through the dispersing chamber into a detachable collection vessel. Both fractions were weighed after completion of a test run, the total of which was used to calculate the average powder feed rate. The dispersed fraction was also used to calculate a dispersing efficiency as a percent of the total powder fed. This is also listed in Table 8 and was used to help indicate the effectiveness of dispersing along with the specific surface of the dispersed fraction. Both types of data were examined for correlation with operating conditions, the most significant of which appear to be those illustrated graphically in Figures 26 and 27.

The gas composition has a profound effect upon the dispersing efficiency as well as upon the potential which may be applied without arcing. The arcing potential was not always the same,

presumably depending on the nickel powder as well as the gas composition. The gas flow rate seemed to influence this also. This variation caused difficulty in obtaining repeated test runs at the same potential for comparison of other factors.

Figure 26 shows the variation of dispersing efficiency with gas composition for three different levels of powder concentration. This efficiency increases up to 30 volume percent argon, but it is uncertain whether higher argon concentrations would be beneficial or not. Test numbers 1, 8, and 9 in which higher argon concentrations were used, all resulted in lower dispersing efficiency.

The effects of powder concentration in the gas on the specific surface of the heated dispersed fraction may be sought from Figure 27, which shows a plot of these factors with differentiation made for different residence times (gas flow rate) or presence of hydrogen. A trend favoring higher powder concentrations (to give higher specific surfaces) appears to exist, at least for a mixture of hydrogen and argon flowing at 240 liters per hour. The explanation for this trend may involve either the nature of the behavior of charged nickel particles or the mechanism by which the particles lose their charges. However, neither of these factors is well understood now.

The polarity of the applied potential appears to be quite significant in this system. Practically all of the tests run with a

positive potential resulted in very low dispersing efficiencies, whereas all of those with dispersing efficiencies approaching a practical value were run with a negative potential.

The highest dispersing efficiency measured in any of the tests with apparatus II was about 17%. The 83% collected as undispersed powder was not investigated to determine its character or behavior during further treatment. However, even if it had no further value, the extraction of 17% of the original powder which cost \$15 per pound would result in a net cost of this dispersed fraction of

$$\frac{\$15.00}{0.17} = \$90.00 \text{ per pound.}$$

This compares with a price of \$200 to \$350 per pound for other purchased submicron nickel powder, and should be considered as a feasible solution to the dispersing problem should no better solution be reached with a reasonable amount of effort.

Comparison of Sherritt Gordon and NRC Powders Run in Apparatus II

NRC powder was run in apparatus II using the same conditions as were used for a test with Sherritt Gordon powder. The results obtained are shown in Table 10, which includes the specific surface data obtained on the as-purchased powders. Samples of each powder were also run through the apparatus, without the hot zone, as a further comparison. Samples of each powder, both with and without treatment in the hot zone, were submitted for examination by the electron microscope. The electron micrographs obtained both at a

TABLE 10
Dispersing of Sherritt Gordon and NRC
Submicron Nickel Powder

<u>Powder</u>	<u>Powder Rate g/hr</u>	<u>Powder Conc mg/l</u>	<u>Zone Temp °C</u>	<u>Dispersing Efficiency %</u>	<u>Specific Surface m²/g</u>	<u>Particle Diameter Microns</u>
SG	-	-	-	-	25.3	0.018
SG	9.6	40.0	Rm	9.3	26.3	0.017
SG	9.9	41.1	700	13.5	2.7	0.167
NRC	-	-	-	-	39.6	0.012
NRC	4.3	17.9	Rm	5.3	40.5	0.011
NRC	2.97	12.4	700	9.3	3.3	0.136

Argon Concentration: 10%

Gas Flow Rate: 240 l/hr

Potential: -10 kv

magnification of 12,000 and at 50,000 are shown in Figures 28 through 31 for the Sherritt Gordon powder, and in Figures 32 through 35 for the NRC powder.

The NRC powder did not feed as well through the vibratory screen as did the Sherritt Gordon. The dispersing efficiency was also less for the NRC, but this could have been low because of the low powder concentration which resulted from the low feed rate. In any case, the NRC powder did not seem to have enough advantage over the Sherritt Gordon to warrant its consideration for further extensive study.

ELECTRON MICROSCOPE EXAMINATION
OF SHERRITT GORDON AND NRC POWDERS
RUN IN APPARATUS II

All specimens were sealed in metal capsules and placed in glass bottles containing argon when submitted with the descriptions shown in Table 11.

At the beginning of the experimental work, the specimens were surveyed briefly by visible light microscopy. This showed that heating increased aggregate size significantly and to the point where transmission electron microscopy would give, primarily, silhouette images in which elements of aggregate geometry could not be recognized.

These results were in agreement with data obtained by the surface area measurements shown in Table 11.

TABLE 11
Powders Examined by Electron Microscopy

Reference No.	8675-64	8675-65	8675-68	8675-69
	TTC-412	TTC-413	TTC-414	TTC-415
Source	NRC	NRC	SG	SG
*Heated to °C	None	700°C	None	700°C
Specific Surface				
(m ² /gm)	40	3.3	26	2.7

*The dispersed powder was separated from the non-dispersed prior to heat treatment.

For the work in light microscopy, capsules containing the powders were opened in a dry box with nitrogen atmosphere having a dew point lower than -50°C. The powders were dispersed on glass microscope slides in the dry box using amyl acetate and a very low degree of viscous shear. The particles were exposed to air briefly for the microscopical examination.

The work in electron microscopy at 12,200X and 50,000X used the following specimen preparation. The powders were dispersed in the same manner as used for light microscopy. Following dispersion, the slide was placed in a vacuum evaporator and a film of carbon (approximately 100 Å thick) deposited on top of the particles while the slide was rotating slowly below the carbon source. During



Figure 28 SG Nickel Powder, Dispersed and
Collected. 12,200X

deposition, the vacuum was better than 10^{-6} Torr. The method produced a high-resolution, one-stage carbon replica of the surface geometry of the particles. The replicas were removed from the glass slide and from the particles by brief treatment in a solution of 10 drops of hydrofluoric acid (48%) in 50 ml of distilled water; washed briefly in distilled water; and mounted on specimen screens for examination in the electron microscope.

In this preparation method, the replicas were formed before the particles experienced exposure to moisture or air. Some specimen material remained attached to the replicas, was photographed in the electron microscope, and appeared as silhouettes on the micrographs.

Later in the program, typical replicas prepared by the method outlined above were analyzed by selected area electron diffraction to determine if nickel oxide and/or other phases less than 1000 Å in crystal size were produced as artifacts during specimen preparation. The NRC specimen TTC-412 was the only case where NiO was detected. In this specimen, crystallites of both Ni and NiO less than 200 Å in size were identified with NiO being present in substantial concentration. Pattern geometry for the other three specimens indicated that these materials contained primarily crystals larger than about 1000 Å in size. These were too thick to be sampled adequately by electron diffraction methods.

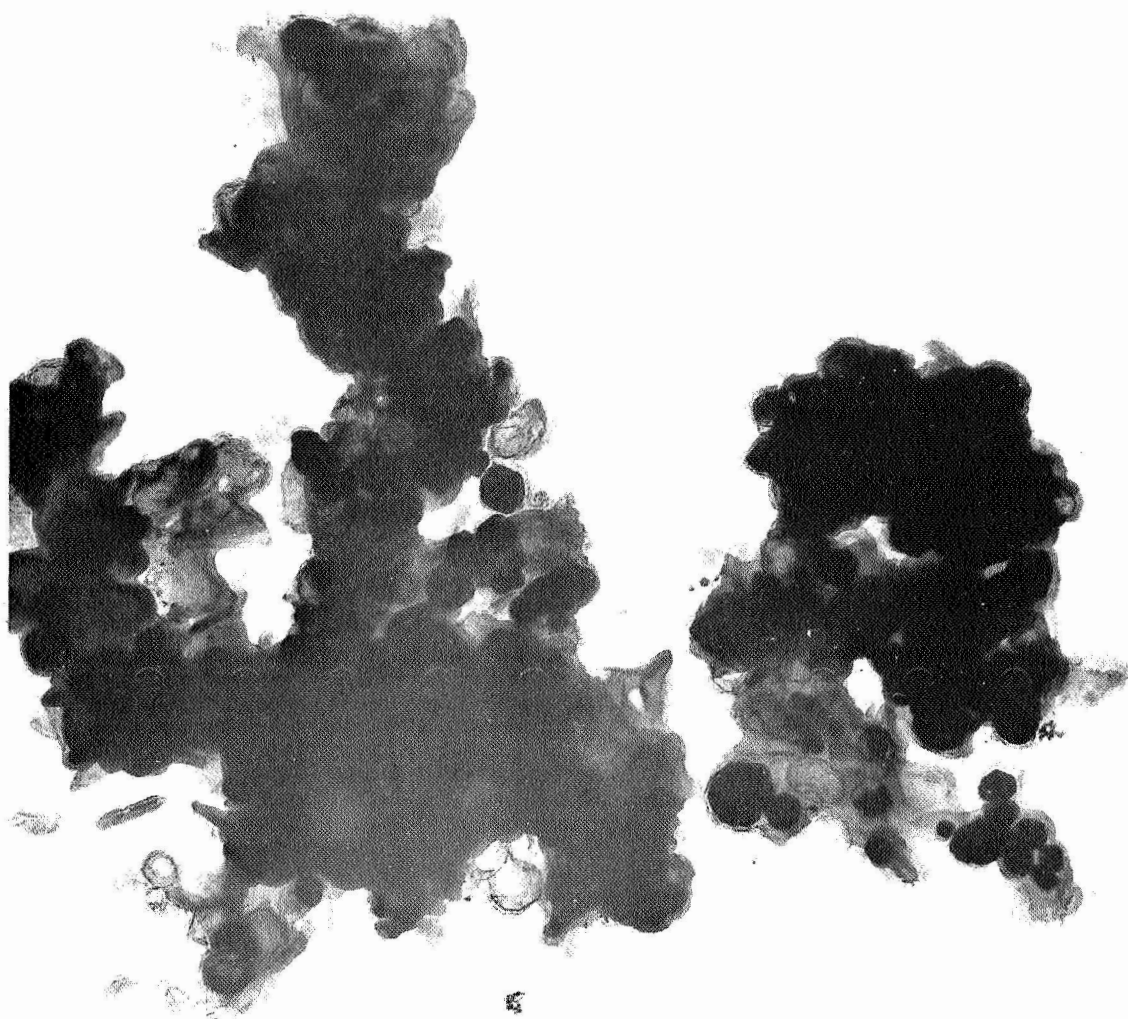


Figure 29 SG Nickel Powder, Dispersed and
Collected. 50,000X

Because of the relatively high NiO content in the TTC-412 specimen, as detected by electron diffraction, it was decided that in the later work, all specimens should be analyzed by X-ray diffraction powder methods. All specimens were mounted in quartz fibers of glass-like structure, while protected by nitrogen atmosphere in the dry box. Results of the analyses showed that TTC-412 contained NiO in significant population of crystals larger than 1000 Å. After heating, the NiO concentration was reduced considerably. The heated specimen contained also an unidentified phase of low population. Only nickel metal was detected in TTC-414 and TTC-415.

Combined results from electron and X-ray diffraction suggest that specimen preparation for electron microscopy did not introduce any substantial crystalline contamination into the specimens.

Because some elements of surface geometry in all specimens and the ultimate crystal size in specimen TTC-412 could not be observed to best advantage at 50,000X, micrographs were prepared during the later work which showed the specimens at 106,400X.

RECOMMENDATION

Based on the powder-dispersing tests reported in Apparatus III, it was recommended that no further dispersing tests be made, at least until the overall feasibility of reaching the oxygen-purity goal was established.

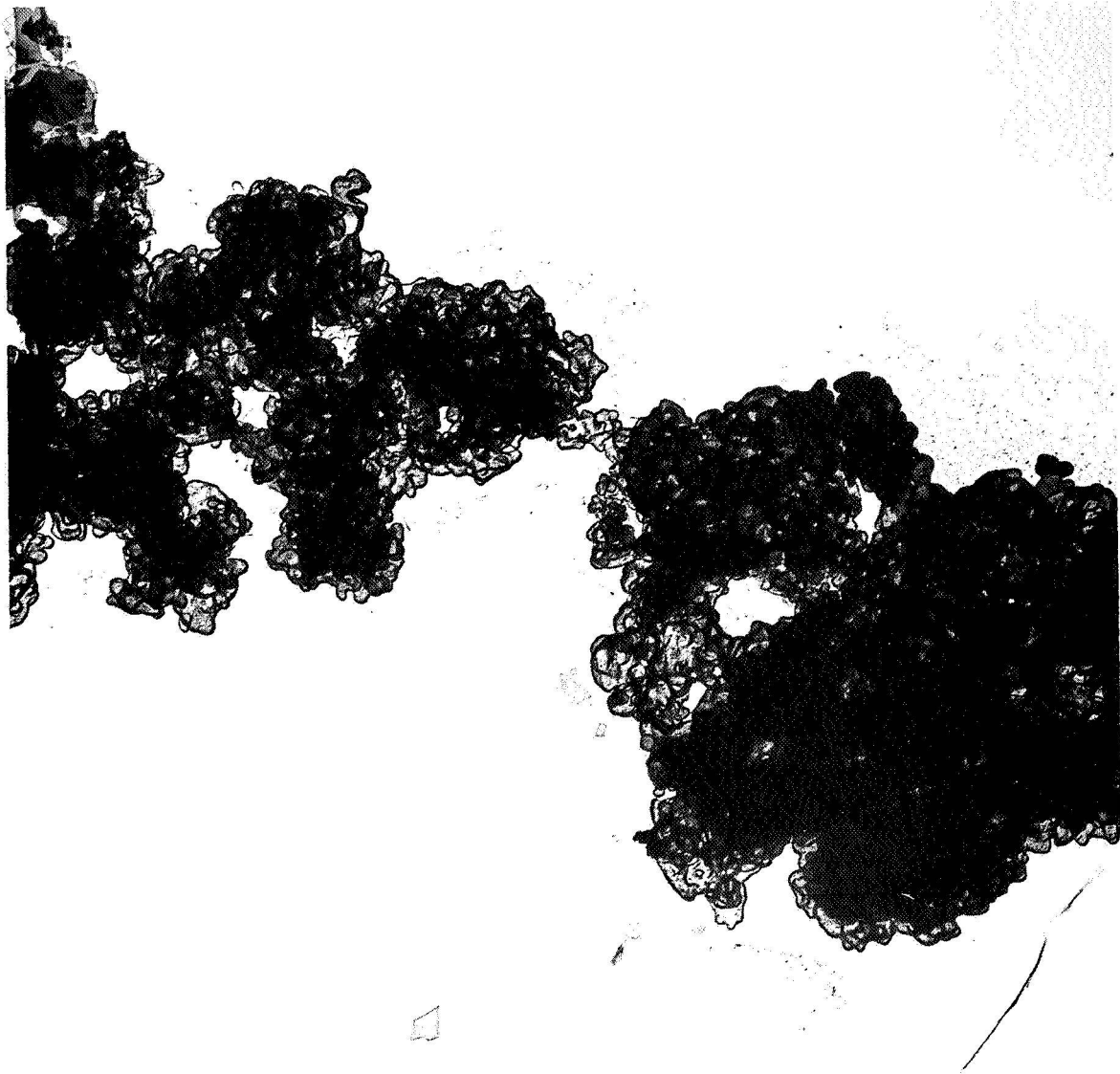


Figure 30 SG Nickel Powder, Dispersed, Heated
to 700°C., and Collected. 12,200X

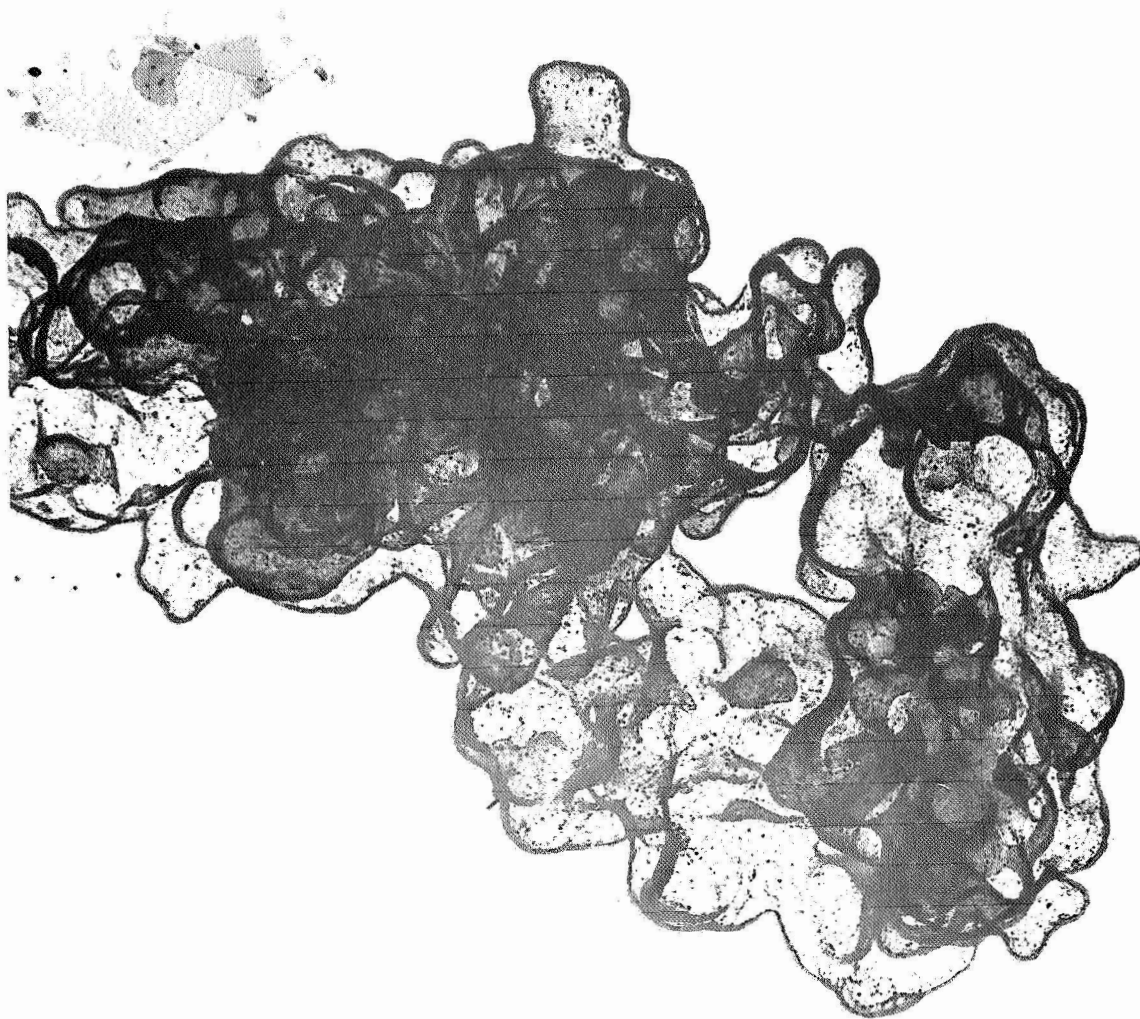


Figure 31 SG Nickel Powder, Dispersed, Heated to 700°C., and Collected. 50,000X



Figure 32 NRC Nickel Powder, Dispersed
and Collected. 12,200X

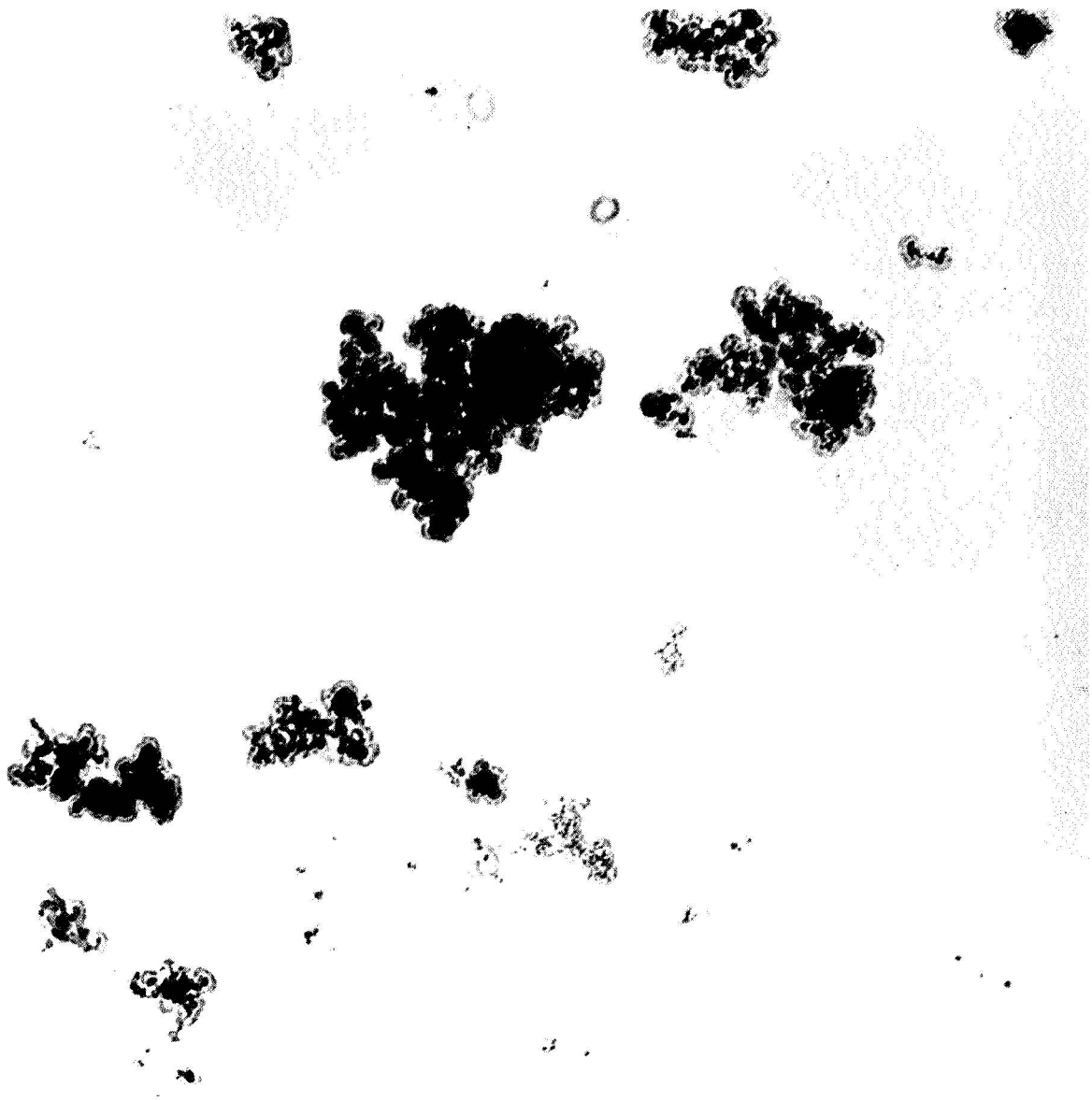


Figure 33 NRC Nickel Powder, Dispersed and Collected. 106,400X



Figure 34 NRC Nickel Powder, Dispersed, Heated to 700°C., and Collected. 12,200X

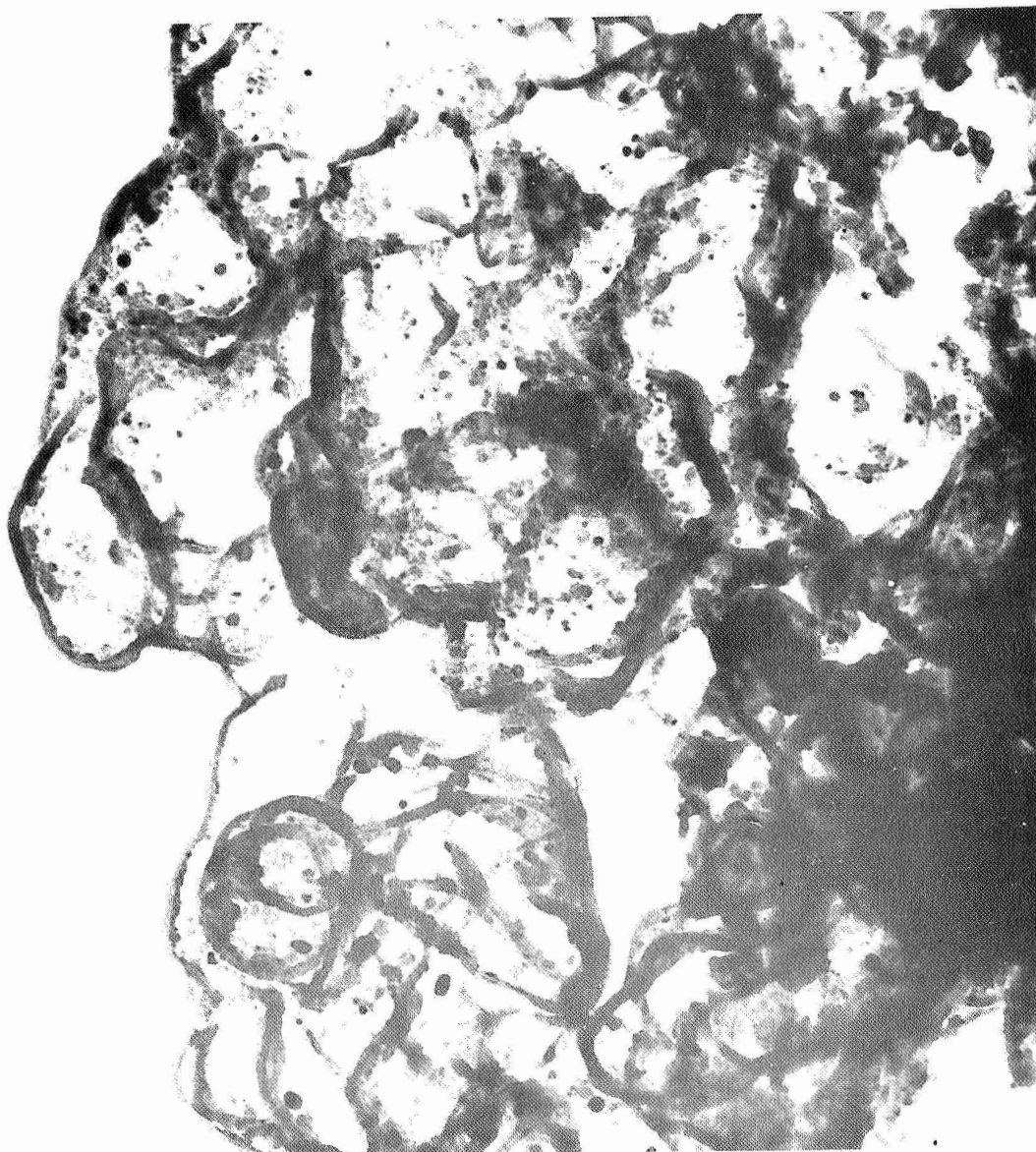


Figure 35 NRC Nickel Powder, Dispersed, Heated to 700°C., and Collected. 106,400X

POWDER PURIFICATION

	<u>Page No.</u>
APPARATUS AND PROCEDURE	76
Loading Assembly	76
Feeding Apparatus	79
Purification	81
Correlation of Gas and Tape Temperatures	82
Collection of Powder	83
Glove-Box System	86
RESULTS OF REDUCTION TESTS	86
RESULTS OF STORAGE TESTS	92
REDUCTION OF NICKEL AND Ni-Cr POWDER	100

APPARATUS AND PROCEDURE

The apparatus was designed and fabricated to allow all the powder handling and processing to be done without any contact with air or oxygen.

The major necessary equipment to accomplish this was the glove box and its auxiliary system, in which argon was circulated and purified with respect to oxygen and water. This is described in detail below.

Figure 36 shows the apparatus as mounted on a rack, and Figure 37 outlines parts of the feeding apparatus including the detachable loading assembly.

LOADING ASSEMBLY

The assembly, mounted at the top of the apparatus (Figure 37) is detachable at a union for loading the powder in the glove box. Also detachable is a glass container which is sealed with a rubber O-ring. When the container is loaded with powder and is sealed in the glove box, no air can reach the contents while the assembly is being transported and fastened with the union to the feeding apparatus. The space between the two ball valves is then purged with a flow of pure gas which enters from below and exits through a small port next to the union to a bubbler which acts as a check valve to prevent air from entering. After the purging, the ball valve is opened to allow the powder to fall into the chamber of

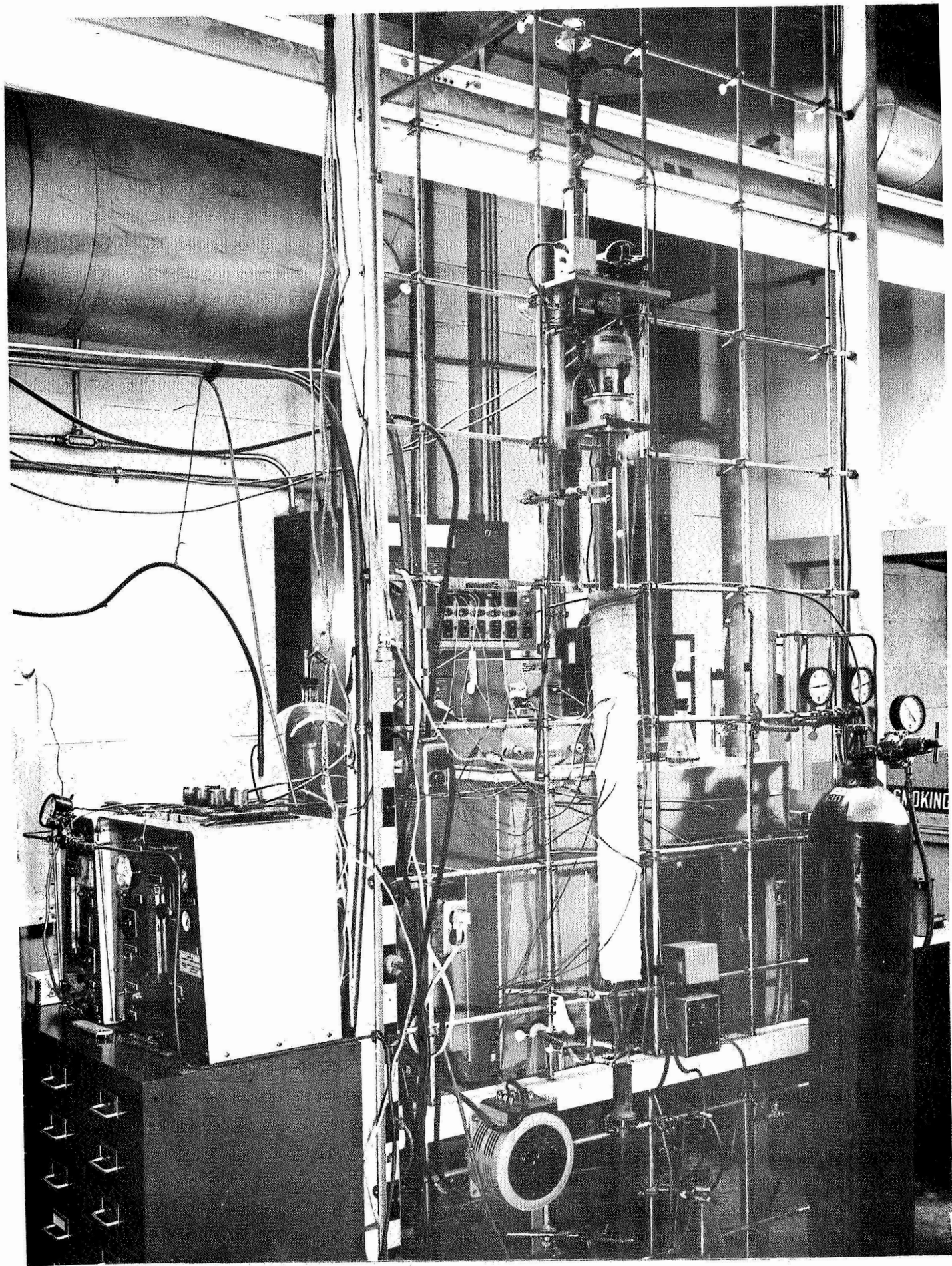


Figure 36 Overall View of Apparatus

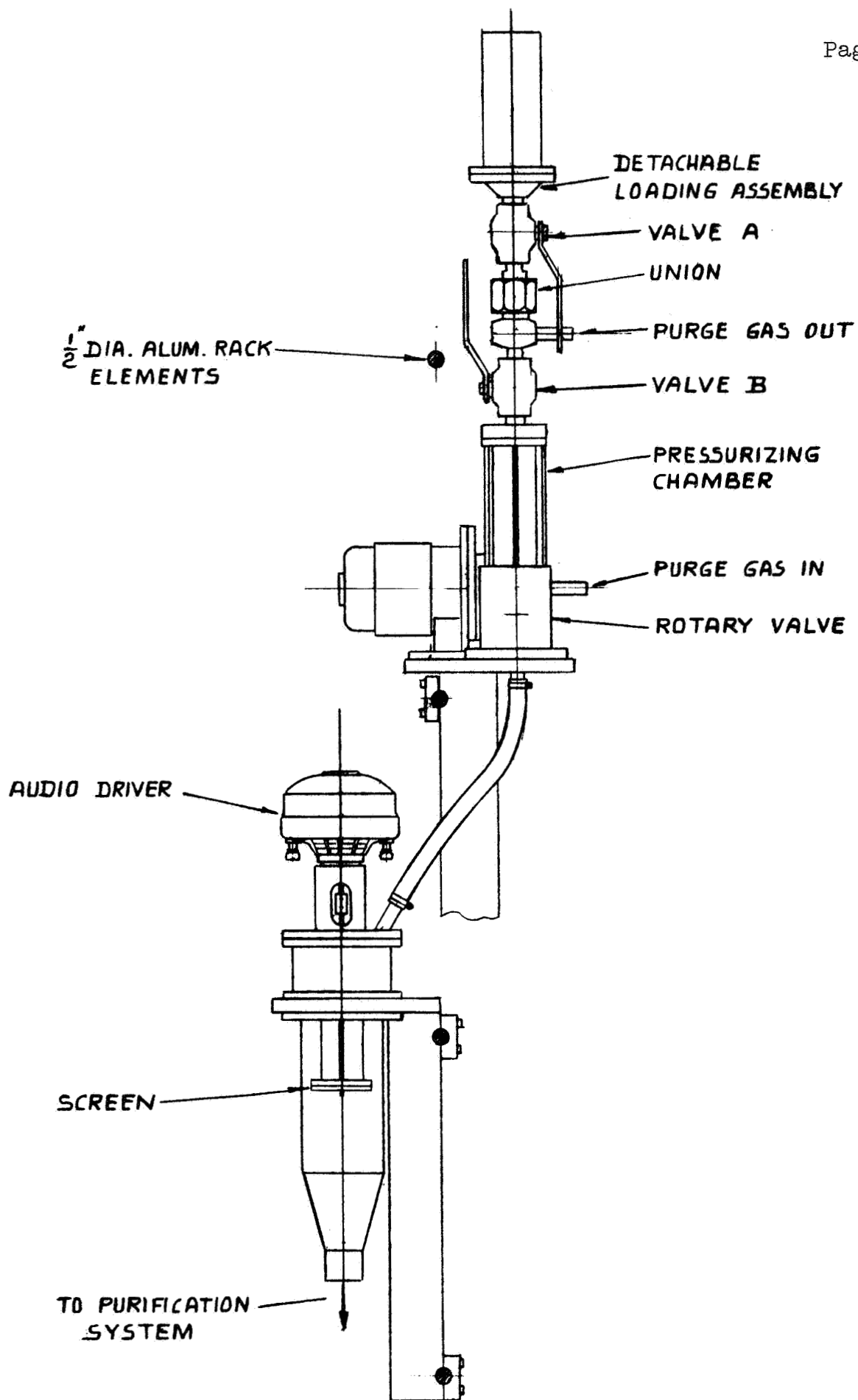


Figure 37 Feeding Apparatus Showing Method of Mounting

the feeding apparatus. This storage chamber can be pressurized, if desired, after the valve at the top is closed. The normal procedure, however, was to leave the powder at atmospheric pressure before and during feeding, as well as during the reduction cleaning.

FEEDING APPARATUS

The apparatus, shown in Figure 38, consists of a rotating valve, a tapping device, and a vibratory screen with its driving equipment. The 325-mesh screen feeds the powder into the quartz chamber in which purification takes place. The rotating valve feeds the powder from the storage chamber onto the screen, upon which it maintains constant depth of powder. The tapping device causes the powder to fill more completely the peripheral cavity in the rotating valve, as well as to empty it more completely each revolution.

The rotating valve consists of a horizontal cylinder fitted tightly in a housing within which it is rotated by an adjustable-speed B&B gearmotor. A cavity in the side of the cylinder is aligned with an entrance port at the top and an exit port at the bottom of the housing through which powder flows by gravity and tapping. The rotating valve assembly is tapped sharply by an electrical solenoid which strikes the under side of the assembly base plate at the time the cavity is in position to receive or discharge powder. The solenoid is timed from a cam mounted on the shaft of the rotating valve and a microswitch activated by it.

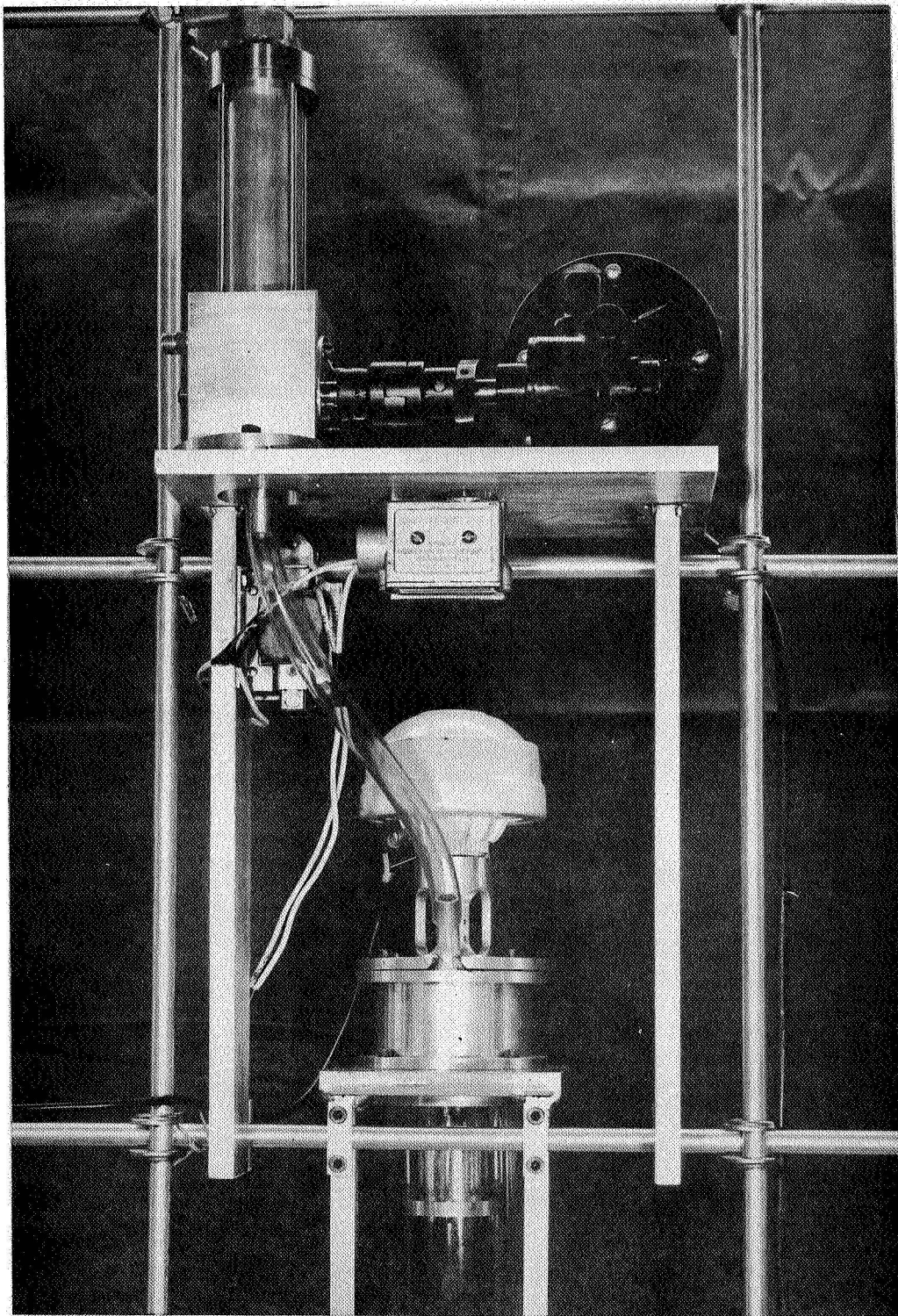


Figure 38. Feeding Apparatus

The screen is driven at any desired vibration frequency and amplitude by a mechanical connection to the diaphragm of an audio driver. This is driven by an amplifier which receives a signal from an audio generator.

PURIFICATION

The reactor section consists of a vertical, transparent fused quartz tube, 70-mm I.D. wrapped with a high-temperature heating tape and Refrasil*insulating tape. The heated zone is 38 cm. long, although a few test runs were made using an 81-cm zone. The temperature is sensed for monitoring and control by a Chromel-Alumel thermocouple inserted between the heating tape and the quartz tube. This tape temperature was compared with the gas temperature measured under various conditions as described below.

The upper end of the quartz reactor tube was sealed with an O-ring to the feeding apparatus. At the bottom it was tapered to a 30-mm I.D. tube and sealed to the metal collector tube with Tygon or rubber tubing and a hose clamp. It was found desirable to eliminate a tapered section of the reactor tube above the hot zone because of the tendency for powder to collect on the quartz wall until a layer formed sufficiently thick to fall off. When this occurred periodically, the powder fell rapidly through the hot zone in an undispersed condition and failed to be properly cleaned.

* Trademark of H. I. Thompson Fiber Glass Co.

Correlation of Gas and Tape Temperatures

A shielded, non-aspirated thermocouple probe was fabricated and installed at the center of the quartz tube chamber at the bottom of the heated zone. The thermocouple was made from 28-gauge Chromel and Alumel wire. Measurements were made for various gas flow rates and heating-tape temperatures for argon and hydrogen. Results are summarized in Table 12.

TABLE 12
Gas-Temperature Measurements

Flow Rate, l/hr.	<u>Hydrogen</u>		<u>Argon</u>	
	<u>60</u>	<u>240</u>	<u>60</u>	<u>240</u>
<u>Temperature of Heating Tape, °C</u>				
300	173°C	200°C	183°C	215°C
450	276	308	288	322
600	393	422	402	434

The temperature profile of the gas as it emerges from the hot zone was measured using the thermocouple probe which was modified for this purpose by making it adjustable in position. Various positions between the outer wall and the center of the quartz tube were each chosen to be midway between imaginary concentric circles which divide the cross-sectional area of the tube into seven (or

four) equal areas. The temperature measurements were averaged arithmetically to give an estimate of the average temperature of the entire gas stream on a volume basis.

The average temperatures measured and the ranges of temperatures found across the diameter of the tube are listed in Table 13, according to the various heating-tape temperatures, gases, and gas flow rates used.

Collection of Powder

An electrostatic collector was chosen because of the extremely small ultimate particle size based on the specific surface of the submicron nickel powder. However, since our dispersing techniques did not produce a dispersion of the ultimate particles, and since it was found difficult to prevent arc-over when some quantity of powder had been collected, another collection method may have been preferable.

An electrostatic precipitator was fabricated from a steel tube, as illustrated in Figure 39. A concentric metal rod which serves as the ionizing electrode is supported by the Neoprene stopper at the bottom. The outer tube is at ground potential to attract the particles, while the gas discharges through the glass outlet tube and subsequently through two bubblers containing vacuum pump oil.

At the end of a running period, a squeeze clamp is tightened evenly on the connecting rubber tubing until the gas flow, as observed in the exit gas bubbler, stops. After turning off the inlet gas flow

TABLE 14

POWDER PURIFICATION

Run No.	Temperature, °C. Tape	Gas	Carrier Gas % H ₂	Rate, l/hr.	Powder Feed Rate, g/hr.	Residence Time, Sec.	Particle Dia. μ	Specific Surf., m ² /g.	Oxygen %	Other Variables
1	275	150	100	15.	0.63	352	0.06	7.76	1.25	
2	275	160	0	15.	2.97	352	0.04	12.5	2.4	
3	700	495	100	240.	1.69	22	0.18	2.51	0.048	
4	700	517	0	240.	0.58	22	0.06	7.41	3.1	
5	700	482	100	120.	1.36	44	0.23	1.95	0.15	
6	700	508	50	240.	4.83	22	0.29	1.55	0.15	
7	700	500	75	240.	6.74	22	0.22	2.04	0.23	
8	700	512	25	240.	1.96	22	0.20	2.27	0.23	
9	600	415	100	240.	1.95	22	0.18	2.48	0.043	
10	600	390	100	15.	2.23	352	0.20	2.27	0.048	
11	700	495	100	240.	0.49	22	0.41	1.10	0.051	
12	500	335	100	240.	0.55	22	0.16	2.80	0.38	
13	700	495	100	240.	1.74	22	0.23	2.00	0.14	
14	500	335	100	240.	0.65	22	0.18	2.51	0.15	
15	700	508	50	240.	1.17	22	0.19	2.34	0.48	
16	500	308	100	15.	0.17	352	0.09	4.83	0.34	
17	600	390	100	15.	1.57	352	0.20	2.24	0.053	
18	550	348	100	15.	3.55	352	0.14	3.25	0.086	
19	500	308	100	15.	1.20	352	0.16	2.81	0.022	
20	550	375	100	240.	1.17	22	0.14	3.29	0.064	
21	500	350	100	360.	1.09	14.7	0.11	4.28	0.087	
22	525	355	100	240.	0.72	22	0.14	3.29	0.054	
23	515	355	50	240.	2.74	22	0.13	3.42	0.059	
24	520	355	75	240.	1.44	22	0.14	3.23	0.093	
25	600	415	100	240.	1.03	22	0.14	3.15	0.107	
26	525	355	100	240.	11.37	22	0.11	4.11	0.027	
27	500	335	100	240.	2.62	22	0.10	4.33	0.024	
28	535	363	100	240.	1.30	22	0.13	3.38	0.038	
29	500	308	100	15.	1.34	352	0.15	3.02	0.041	
30	500	313	100	60.	1.13	88	0.11	4.19	0.060	
31	560	363	100	60.	1.57	88	0.15	3.01	0.054	
32	450	297	100	240.	0.78	22	0.08	5.95	0.044	
33	400	260	100	240.	1.06	22	0.08	5.65	0.062	
34	500	335	100	240.	3.9	22	0.10	4.32	0.034	
35	500	335	100	240.	2.54	22	0.10	4.66	0.036	
36	450	297	100	240.	1.38	22	0.08	5.72	0.062	
37	475	315	100	240.	2.58	22	0.09	4.89	0.042	
38	500	335	100	240.	2.17	47	0.15	3.06	0.048	*81-cm. hot zone
39	450	297	100	240.	1.83	47	0.09	4.88	0.056	
40	500	335	100	240.	3.02	47	0.10	4.32	0.045	
41	500	335	100	240.	3.86	47	0.07	6.19	0.52	-5 kv. Disperser V
42	500	335	100	240.	1.56	47	0.10	4.56	0.061	+5 kv. Disperser V
43	500	335	100	240.	3.32	47	0.10	4.71	0.077	#10 kv Disperser V
44	500	335	100	240.	2.02	47	0.11	3.95	0.060	H ₂ Pre-treatment
45	500	335	100	240.	4.50	47	0.11	3.91	0.038	Powder ran again
46	500	335	100	240.	5.5	47	0.16	2.74	0.046	Processed 2nd time
47	500	335	100	240.	4.6	47	0.15	2.97	0.070	Vacuum Outgas
48	500	335	100	240.	12.1	47	0.10	4.61	0.051	
49	500	335	100	240.	2.25	47	0.17	2.67	0.23	NRC Powder
50	500	335	100	240.	2.83	47	0.15	3.00	0.21	NRC Powder
51	500	335	100	240.	1.71	47	0.06	7.04	0.23	Vitro Powder
52	500	335	100	240.	12.4	22	0.10	4.32	0.049	
53	310	200	100	240.	2.64	22	0.05	9.19	0.245	

*81-cm. hot zone was used for runs 38 through 51.

TABLE 13
Gas Temperature Versus Tape Temperature

Hydrogen

Flow Rate, liters/hr Tape Temp. °C	<u>1.2</u>		<u>60</u>		<u>240</u>	
	<u>Temp.</u>	<u>Range</u>	<u>Temp.</u>	<u>Range</u>	<u>Temp.</u>	<u>Range</u>
300	164	4	168	4	194	10
450	269	6.5	273	7	297	17
600	386	6	396	9	415	17
780	-	-	-	-	570	(Center Temp.)

Argon

	<u>1.2</u>		<u>60</u>		<u>240</u>	
	<u>Temp.</u>	<u>Range</u>	<u>Temp.</u>	<u>Range</u>	<u>Temp.</u>	<u>Range</u>
300	160	1.5	178	6.5	211	11
450	274	5	289	8.5	321	18
600	397	6.5	409	7	438	10

50% H₂-50% Ar Mixture

	<u>120</u>		<u>240</u>	
	<u>Temp.</u>	<u>Range</u>	<u>Temp.</u>	<u>Range</u>
600	-	-	423	10
700	495	8.5	508	11
780	-	-	570	(Center Temp.)

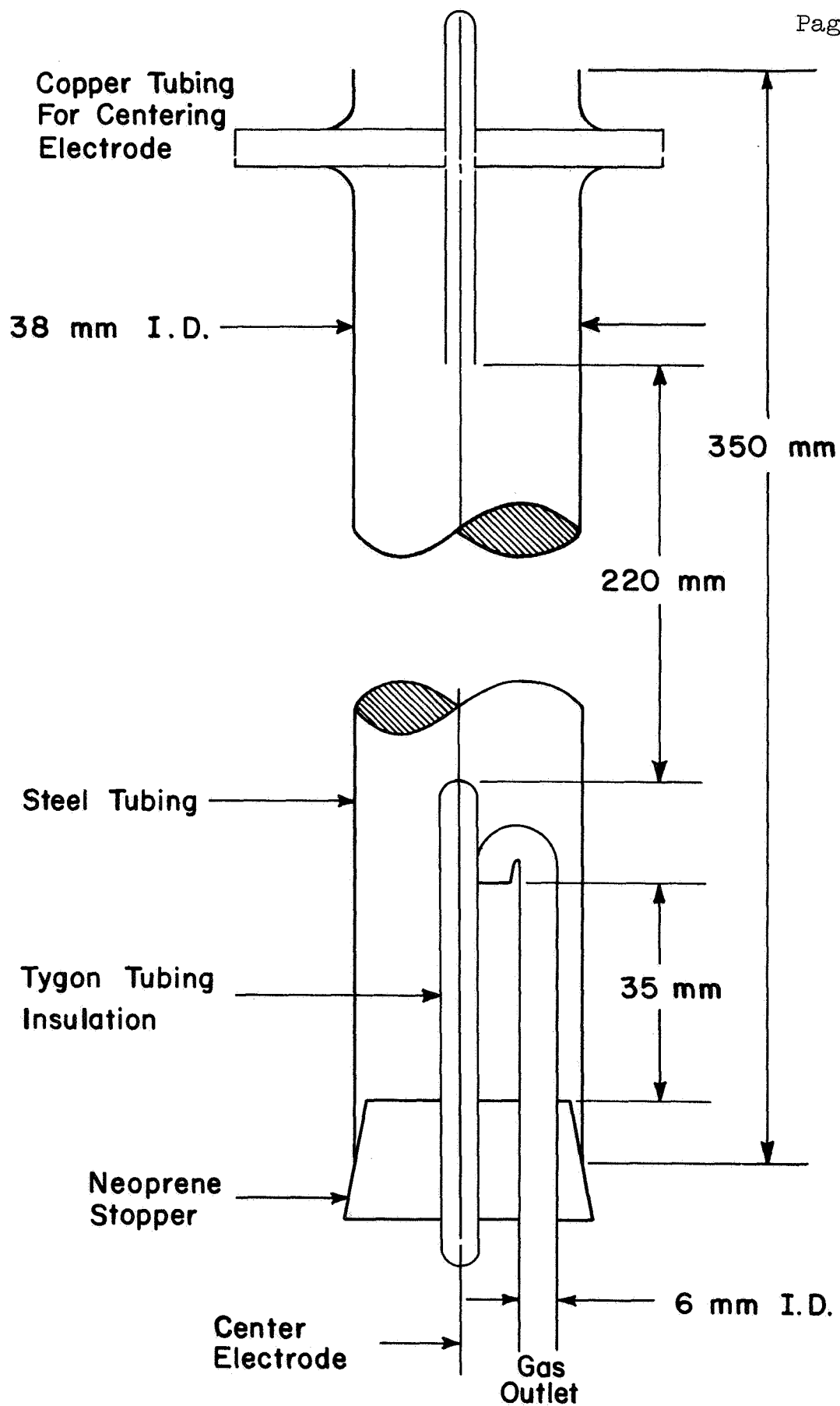


Figure 39 Powder Collector

and clamping the outlet Tygon tubing closed, the collector is disconnected by releasing the rubber tubing from the quartz apparatus and placed in the glove box for extraction of the powder.

Glove Box System

A pure argon atmosphere was maintained in a stainless-steel glove box which was equipped with 0.030" thick butyl gloves and a vacuum interchange. An argon-purification system was used to maintain its purity and to reduce the consumption of makeup argon. This is described schematically in Figure 40, and consists of a hermetically sealed pump, oil separator, De-Oxo catalyst, and molecular sieve drying column.

The glove-box argon was continuously analyzed with Meeco analyzers for O_2 and H_2O during any period in which nickel powder was exposed to it. The glove box was used for charging nickel powder to be cleaned into the detachable loading assembly, for extraction of the cleaned powder from the collectors, and for the loading of analytical samples into tin capsules which were sealed by a controlled crimp. During such use, the indicated O_2 and H_2O contents of the glove-box argon were between 2 and 12, and 1 and 8 ppm, respectively.

RESULTS OF REDUCTION TESTS

Table 14 lists the results of the reduction tests as well as the test conditions used for each test run. The effect of heating-tape

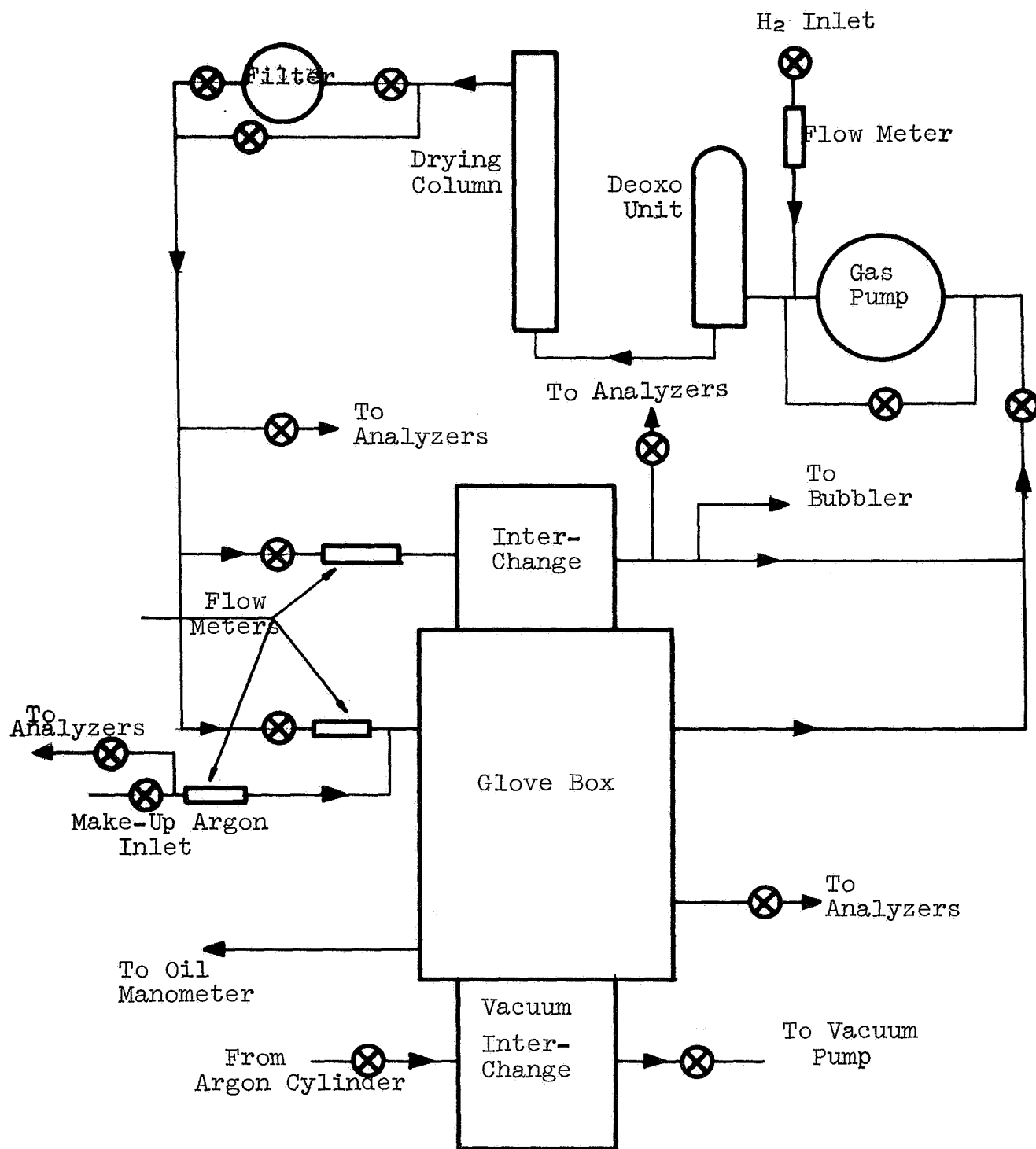


Figure 40 ARGON CIRCUIT

temperature was evaluated using values between 275°C and 700°C, which correspond to gas temperatures estimated to be between 150°C and about 500°C. The effect of gas temperature on oxygen removal from the nickel powder is indicated in the table and illustrated in Figure 41, which is a plot of the data for gas temperature vs. oxygen contents of the cleaned nickel powder obtained when a 15" hot zone was used. The curve drawn through many of the points should indicate the lowest oxygen content one could expect to obtain for any given gas temperature. Since only an error in the analyzed oxygen values on the high side would be expected, the points which are appreciably above the curve may be considered as being probably caused by accidental exposure of the purified powder to traces of oxygen. Later in the program, fewer high oxygen values were obtained, a fact that may be attributable to a gradual improvement in technique to minimize leaks in the tin capsules, or other sources of oxygen contamination. For the same reason, some individual oxygen analyses of cleaned powder were discarded because they differed significantly from the other three or four analyses of the same samples. The maximum deviation allowed in each case was determined by a nonparametric statistical test. (5)

The effect of gas temperature on the specific surface of the cleaned nickel powder is indicated in Table 14 and illustrated graphically in Figure 42, which is a plot of the data for gas

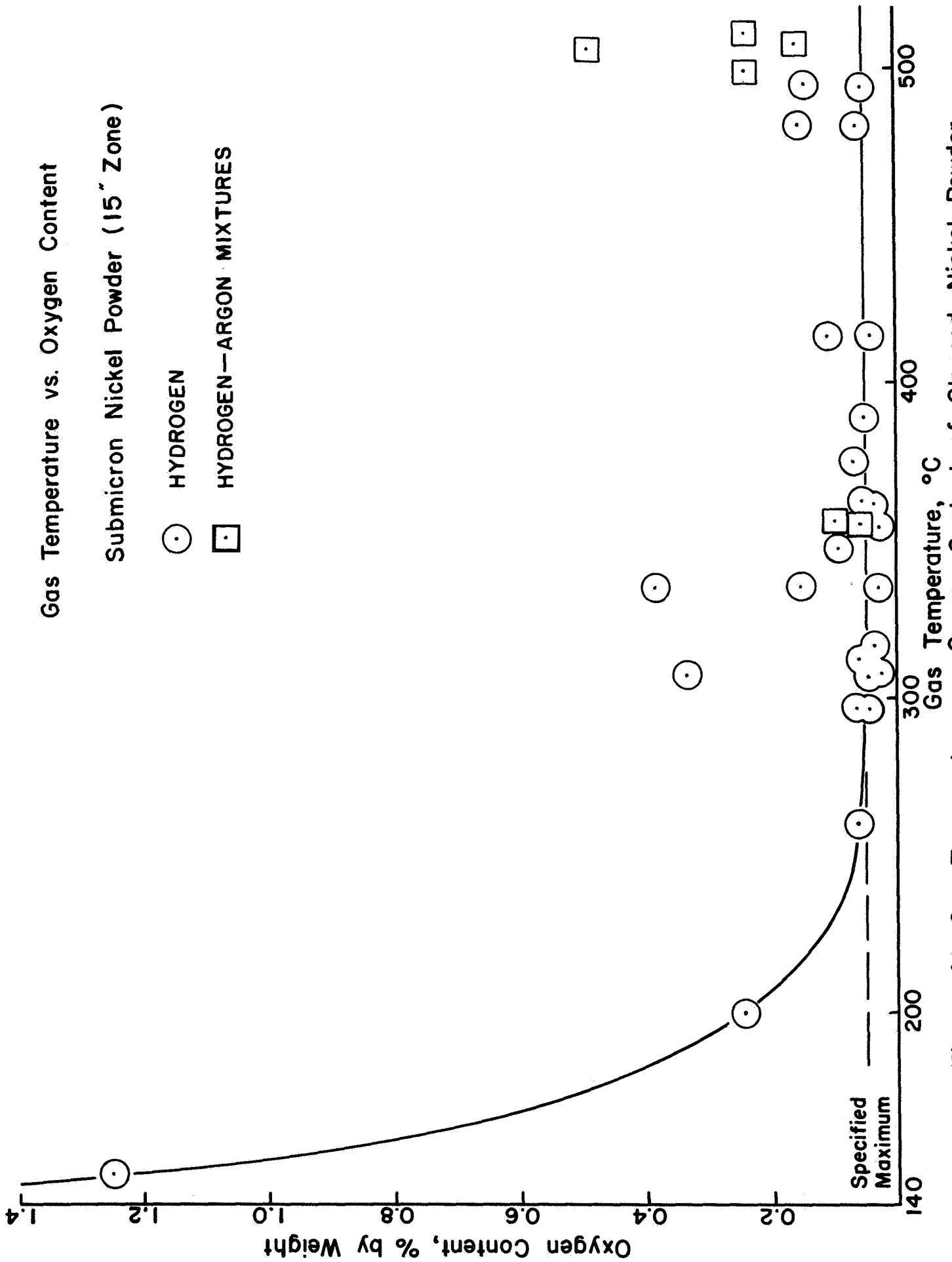


Figure 41 Gas Temperature vs Oxygen Content of Cleaned Nickel Powder

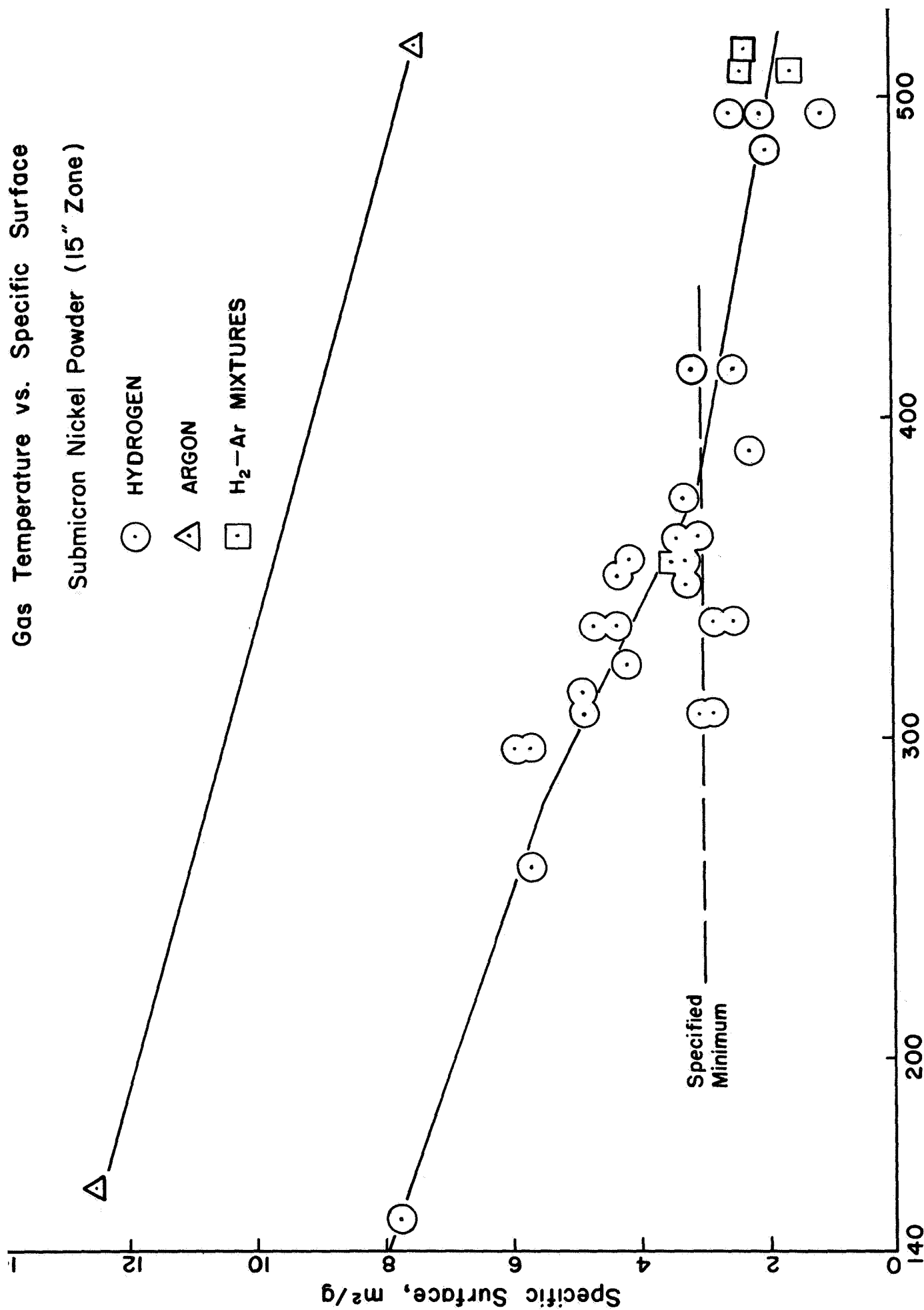


Figure 42. Gas Temperature vs. Specific Surface of Cleaned Nickel Powder

temperature vs. specific surface also obtained when a 15" hot zone was used. The effect of using argon without hydrogen, as the carrier gas, is also indicated in this figure for two extremes of gas temperature. Figure 43 illustrates the effect, when the gas contains hydrogen, of gas-residence time and gas temperature on the average particle diameter of the cleaned powder equivalent to its specific surface.

Figures 44-47 illustrate the structure of the processed nickel powder particles. These are electron micrographs taken from product powder from test run No. 32. Figures 44 and 45 are silhouettes at a magnification of 12,000, and figures 46 and 47 are of direct replicas at magnifications of 12,000 and 19,900, respectively.

RESULTS OF STORAGE TESTS

Table 15 summarizes the results of the storage tests as well as indicating the methods used and the number of tests made by each method. The variability of results obtained in different tests of the same method is indicated by the "minimum" and "maximum" columns which list the lowest and the highest rates of oxygen increase observed for any test of that method. The results of all storage tests are listed in Table 16 with the conditions of storage used for each test. Additional storage tests were conducted using a stainless-steel container having a clamped, gasketed cover. The conditions tested and results of tests of these containers are

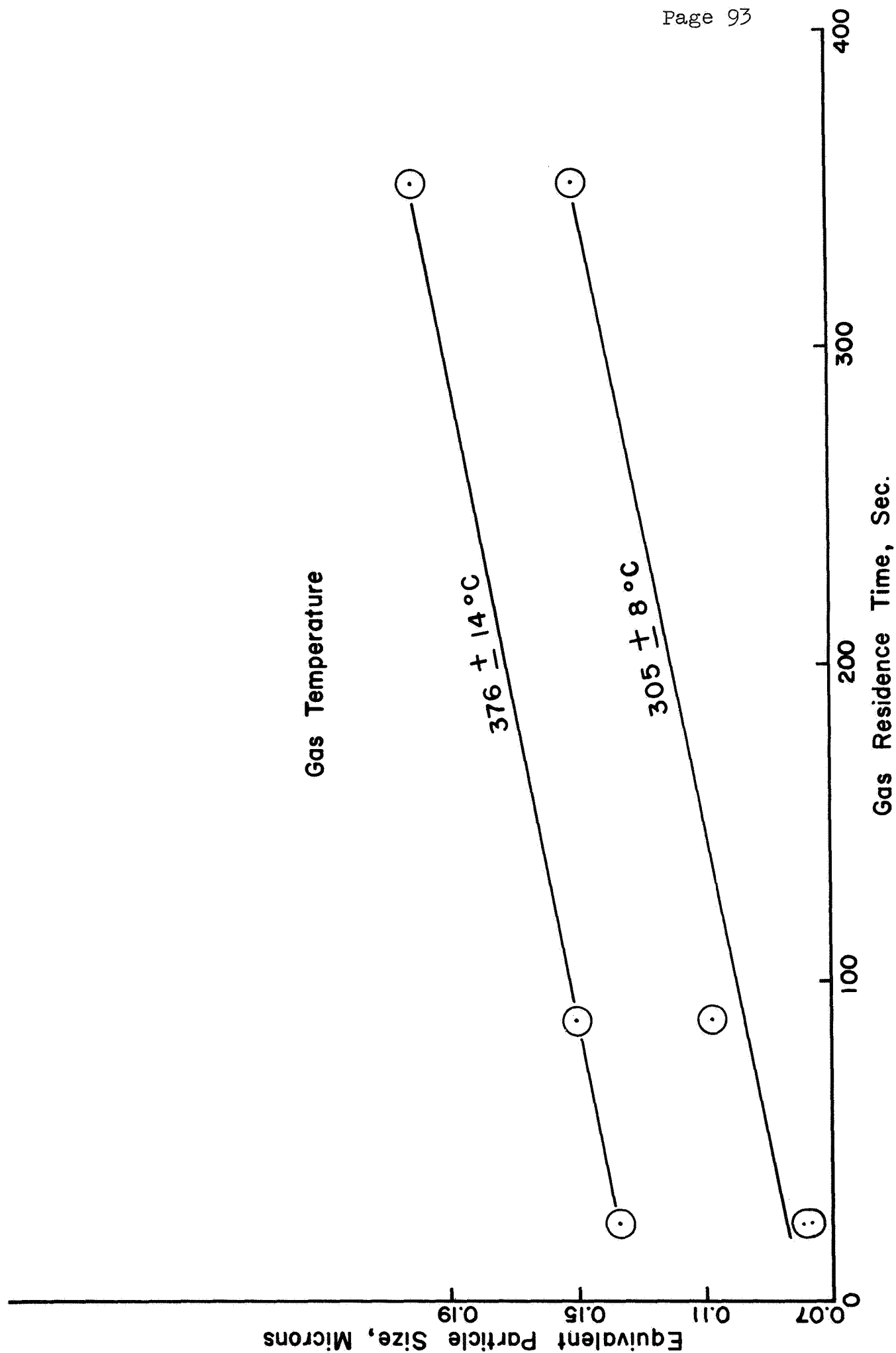


Figure 43. Gas Residence Time vs. Equivalent Particle Size of Cleaned Nickel Powder

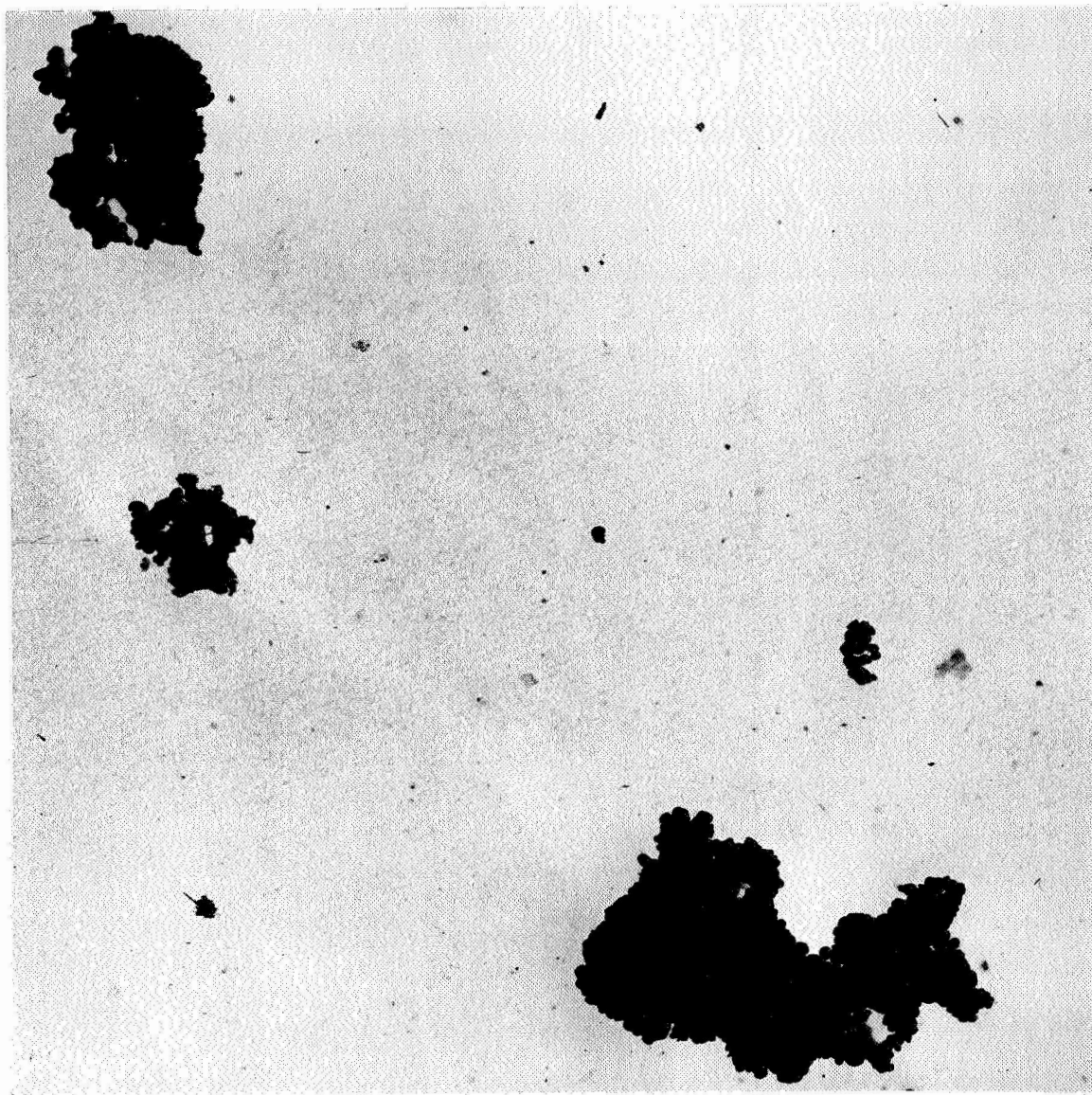


Figure 44. Electron Micrograph Silhouette of Cleaned Nickel Particles at 12,000X.

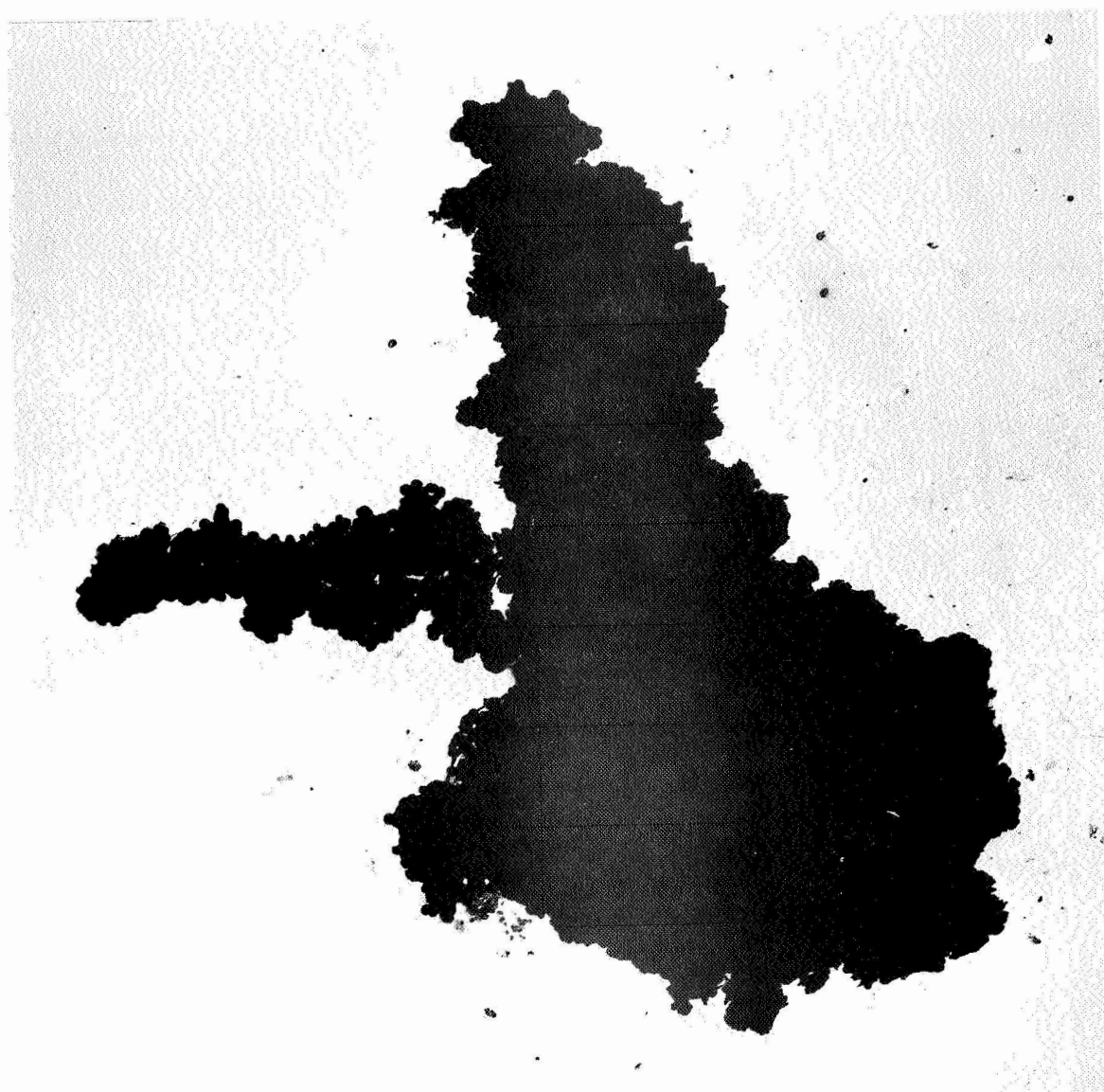


Figure 45. Electron Micrograph Silhouette of Cleaned Nickel Particle at 12,000X.

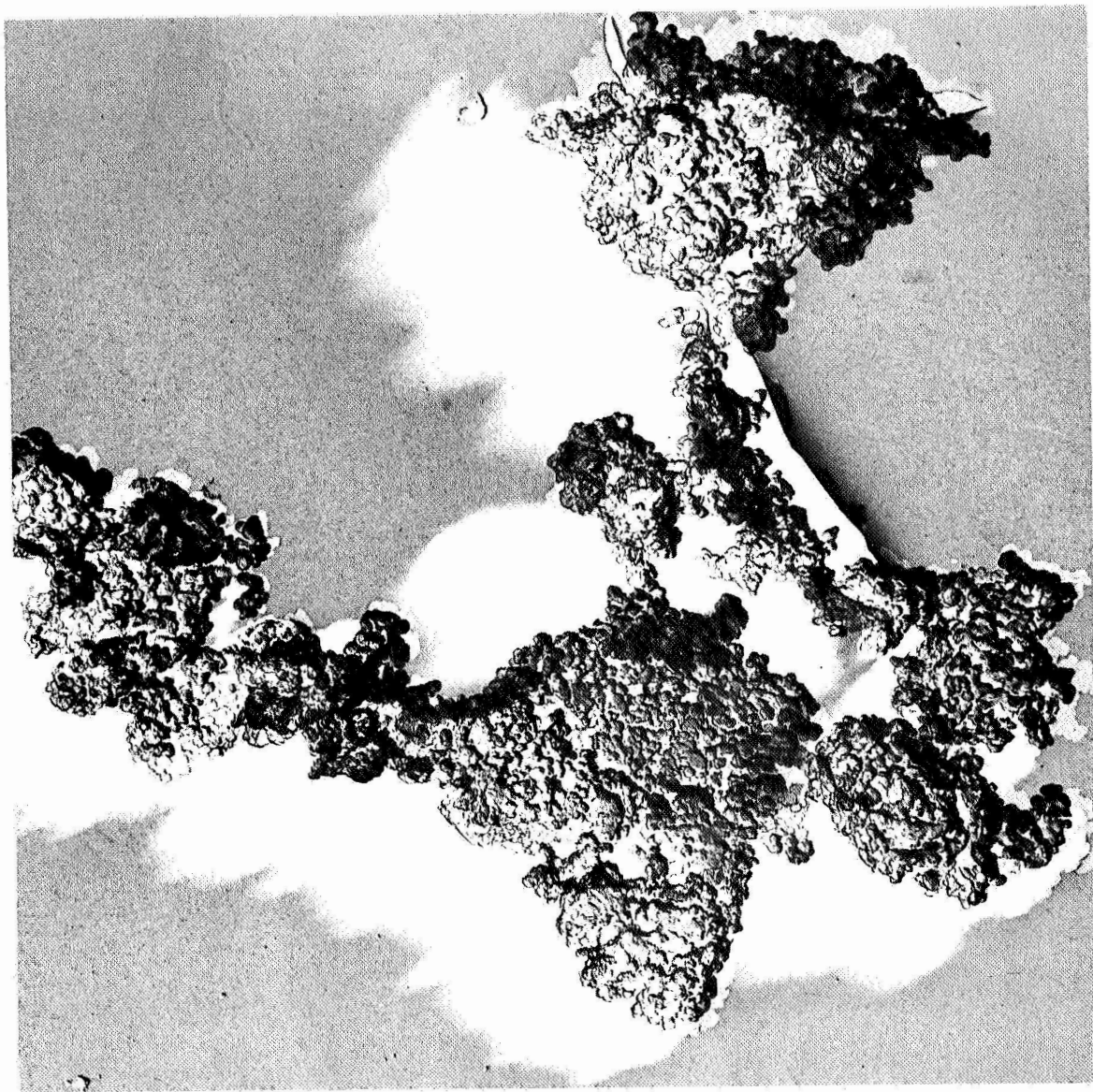


Figure 46. Direct-Replica Electron Micrograph of Cleaned Nickel Particle at 12,000X.

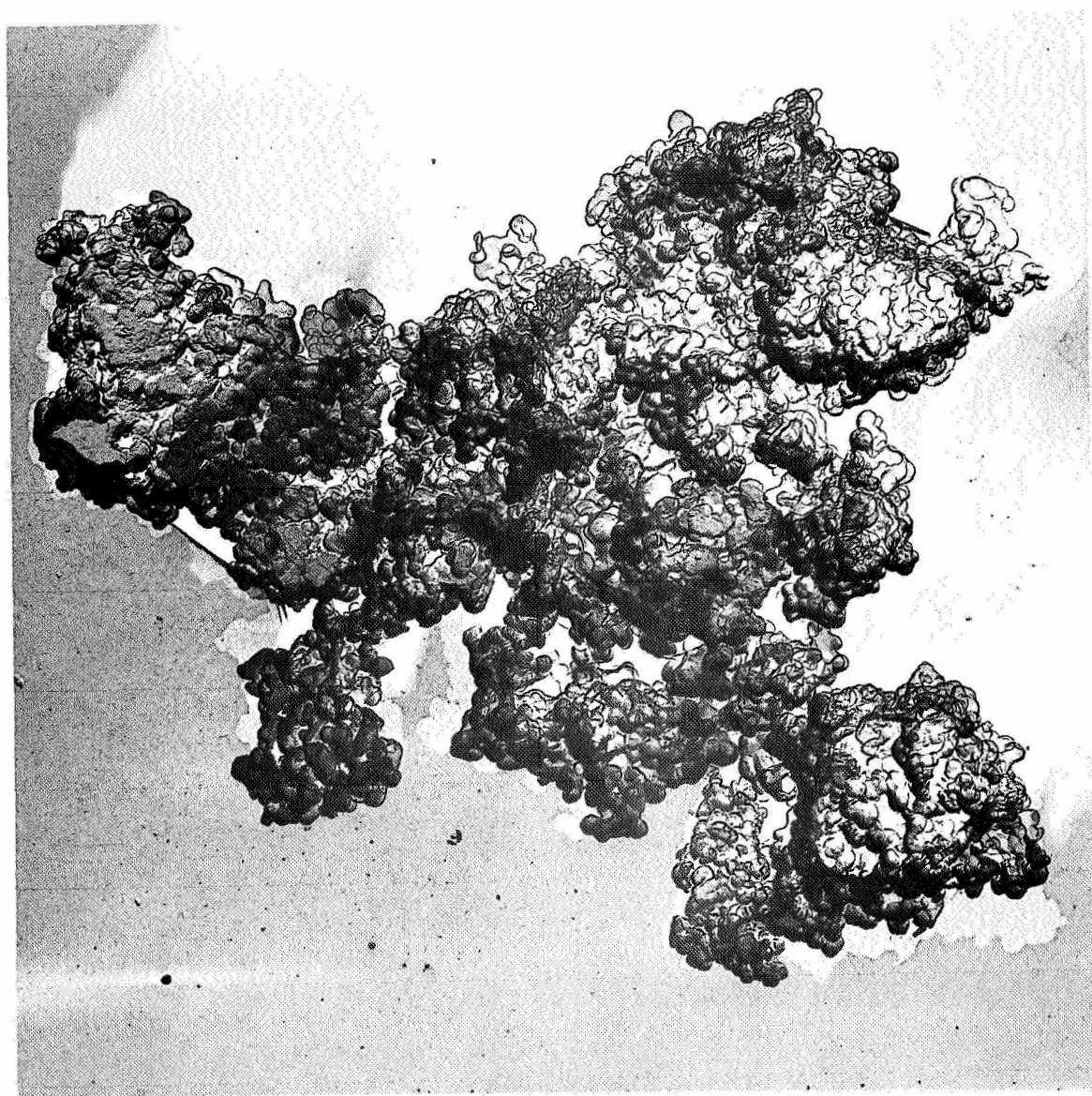


Figure 47. Direct-Replica Electron Micrograph of Cleaned Nickel Particle at 19,900X.

TABLE 15

Summary of Powder Storage Tests

Method	Number of Tests	Oxygen Increase, ppm per day			
		Raw	Average Corrected*	Minimum	Maximum Raw Corrected*
1. Paint can, 1/2-pint	14	141	59	0	1200 130
2. Paint can sealed RTV rubber	10	187	108	21	900 297
3. Paint can sealed Teflon tape	2	89	89	58	120 120
4. Paint can sealed Teflon spray	1	2220	2220	-	- -
5. Glass bottle sealed aluminum foil	3	99	99	52	157 157
6. Glass flask sealed vacuum grease	2	63	63	6	120 120
7. Glass flask evacuated	2	58	58	22	95 95
8. Copper tube pinch- off seal	7	96	11	0	420 28

* Corrected values obtained by eliminating individual data judged to be non-representative on the basis of a statistical test. (3)

TABLE 16

Powder Storage Tests

Run No.	Storage Atmosphere		Time Days	Method*	Opening Atmosphere				Powder Oxygen % by Weight		Oxygen Increase	
	ppm O ₂	ppm H ₂ O			ppm O ₂		ppm H ₂ O		Before	After	Total %	ppm/day
					Before	After	Before	After				
5	14	7.5	28	1	20	74	9	11	0.15	0.17	0.02	7
6	11	11	28	1	13	>30	1	-	0.15	0.14	-0.01	-4
8	17	6.3	23	1	12	38	2.7	2.7	0.23	0.36	0.13	57
9	12	3.7	19	1	12	38	3.0	3.0	0.043	0.25	0.207	110
9	12	3.7	77	1	2.2	85	6.4	6.3	0.048	0.387	0.34	44
17	17	17	31	1	3.3	5.0	31	31	0.053	0.21	0.157	51
17	17	17	34	1	4.5	4.5	43	43	0.053	0.29	0.237	70
17	17	17	62	1	2.5	110	7.0	8.2	0.053	0.325	0.27	43
18	18	17	33	1	4.5	4.5	43	43	0.086	0.50	0.414	125
19	20	9	32	1	7	7	39	41	0.022	0.066	0.044	14
23	3.3	14	25	2	4	20.5	23	26	0.059	0.54	0.481	193
23	3.3	14	25	1	5.5	9	38	39	0.059	0.38	0.321	130
24	4.8	39	19	2	3.9	7.1	42	44	0.093	0.49	0.397	210
25	7	18	22	1	10	30	19	19	0.107	0.28	0.173	79
25	7.5	21	22	2	10	10	19	19	0.107	0.76	0.653	297
25	8.0	24	22	3	4	730	19	19	0.107	0.37	0.263	120
25	8.5	27	22	5	8.4	8.4	20	20	0.107	0.30	0.193	88
25	7	18	48	1	1.6	47	8.0	8.1	0.107	0.297	0.19	40
25	7.5	21	48	3	1.9	46	7.4	7.6	0.107	0.386	0.28	58
25	8	24	48	2	1.9	2.3	6.7	6.7	0.107	0.283	0.18	37
25	8.5	27	48	5	2.0	9.2	6.7	6.7	0.107	0.355	0.25	52
26	4.7	20	46	2	2.7	2.7	10	10	0.027	0.194	0.17	37
30	7.5	180	14	2	-	-	-	-	0.06	0.17	0.110	79
32	3	64	21	2	1.4	1.4	3.5	3.5	0.044	0.43	0.386	184
34	3.8	30	31	2	2.5	2.6	10	10	0.034	0.144	0.11	35
35	3	22	10	2	2.1	8.4	8.7	18	0.049	0.14	0.091	91
37	4	19	8	4	2.1	-	8.7	-	0.042	1.82	1.78	2220
39	1.5	12	2	8	1.6	1.6	6.3	6.3	0.056	0.14	0.084	420
39	(vacuum)		2	7	1.6	1.6	6.3	6.3	0.056	0.075	0.019	95
39	1.5	12	14	8	1.6	1.6	7.1	7.1	0.056	0.096	0.040	28
40	1.8	9	2	6	7.7	7.7	12	12	0.045	0.069	0.024	120
40	1.8	9	2	8	7.7	7.7	12	12	0.045	0.094	0.049	195
40	1.8	9	14	8	2.5	2.5	13	13	0.045	0.053	0.008	6
40	1.8	9	14	6	2.5	2.5	13	13	0.045	0.053	0.008	6
41	1.6	6.3	13	8	2.5	2.5	13	13	0.52	0.475	-0.045	-35
42	1.5	18	12	8	2.5	2.5	13	13	0.061	0.086	0.025	21
42	(vacuum)		12	7	2.5	2.5	13	13	0.061	0.094	0.027	22
43	1.7	11	10	8	1.6	1.6	7.1	7.1	0.077	0.075	-0.002	-2
43	1.7	11	10	1	1.6	46	7.1	8.1	0.077	1.27	1.20	1200
46	3.4	3.0	4	5	2.5	5.6	9	9	0.046	0.68	0.63	157
46	3.4	3.0	4	2	2.5	2.5	8.5	8.5	0.046	0.41	0.36	900
one	1.4	3.5	13	1	2.5	2.5	8.5	14	-	-	-	-

Method: Number refers to numbered method in Table II.

described in the Appendix. Table 16 lists the purity of the argon present in the glove box when the storage samples were sealed, and of the argon when the samples were opened. Since many of the samples, when opened, caused the oxygen and/or water content of the argon to rise, the extent of this rise is also listed. The oxygen analyses of the nickel powder before and after the storage period are listed as well as the increase in oxygen content.

REDUCTION OF NICKEL AND Ni-Cr POWDER

Nickel

A 450-gram lot of Sherritt Gordon powder was received from Lewis Research Center to be purified and returned for further testing.

An initial reduction test was made using 6 grams of this lot to check for satisfactory purification. The result was not good, since it analyzed 0.076% oxygen. Later an 11-gram batch was run, which analyzed 0.046% oxygen, so it was decided to proceed with the remainder of the lot. Each day's run of 15 to 30 grams was analyzed for oxygen before it was added to previously purified batches.

The purification was done using the following conditions which had been found to be optimum:

1. Gas: pure hydrogen at 240 liters/hour.
2. Temperature: heating tape was 500°C, giving an estimated gas temperature of 335°C.
3. Time: residence time in the heated zone was approximately 22 seconds.

Oxygen analyses:

Before processing:

Weight loss in nitrogen: 3.26% (H_2O)Weight loss in hydrogen: 7.24% ($H_2O + O_2$)Net O_2 : 3.98%

After processing:

Average O_2 : 0.033%

The process efficiency was 88.5%. Losses of nickel during processing occurred as follows:

Retained on feed screen:	10 grams	2.4%
Adhered to reduction tube:	23 grams	5.5%
Entrained in exit gas:	<u>15</u> grams	<u>3.6%</u>
Total	48 grams	11.5%

In addition, 9 grams of product was consumed in oxygen analyses and 17 grams of feed powder was used in two preliminary reduction tests.

A total of 369 grams was sealed in two of the stainless steel containers (see Appendix) and returned to Lewis Research Center for further processing.

80 Nickel-20 Chromium

A 20-gram lot of submicron 80Ni-20Cr powder was also received from Lewis Research Center. This was analyzed for oxygen and

processed in the apparatus in two batches using the same conditions as described above for the nickel powder.

Oxygen analyses:

Before processing:	12.9%
--------------------	-------

After processing:	
-------------------	--

Batch no. 1:	3.6%
--------------	------

Batch no. 2:	6.0%
--------------	------

Each batch which weighed 6 grams was sealed in a separate stainless steel container and returned to Lewis Research Center.

CONCLUSIONS

1. The method of fluidization with transport is capable of producing at a rate of 12.5 grams per hour submicron nickel powder having a maximum oxygen content of 0.05% by weight while retaining a minimum specific surface of 3.0 square meters per gram. Operating conditions which have produced these results include a flow of pure hydrogen of 240 liters per hour through a zone 15" long in which it remains for about 22 seconds and reaches an estimated temperature of about 335°C.
2. Oxygen was more easily removed from Sherritt Gordon Type GX-3 nickel powder than it was from either NRC Ultra-fine nickel powder or Vitro Laboratories Submicron nickel powder.
3. Although the specific surface of Sherritt Gordon GX-3 nickel powder after being treated to remove oxygen appears equivalent to an average particle diameter of about 0.1 micron, the powder is actually agglomerated to particles most of which have diameters well distributed over the range 1/2 to 10 microns, even after being subjected to rather severe shear forces.
4. The oxygen content of Sherritt Gordon powder can be reduced to 0.05% by weight or less at gas temperatures of about 300°C or higher.
5. The specific surface of Sherritt Gordon powder can be maintained above 3.0 square meters per gram (equivalent to an average

particle diameter of 0.15 micron) at gas temperatures of about 380°C or lower when dispersed in a gas whose residence time in the hot zone is 80 seconds or less.

6. The equivalent particle diameter increases with increased gas residence time in the hot zone for constant gas temperatures.
7. The powder-residence time increases with gas-residence time, but the exact relationship was not determined.
8. Argon may be substituted for part of the hydrogen with little effect on specific surface up to about 75% by volume. However, 100% argon results in a significantly higher specific surface than is obtained when hydrogen is present.
9. Very little oxygen is removed from submicron nickel powder in pure argon heated to temperatures up to 500°C.
10. The presence of a high potential on a structure located between the feeder screen and the hot zone has a beneficial effect on particle size, but an adverse effect on oxygen removal during heat treatment, both effects being more pronounced when the potential is negative than when it is positive.
11. Storage of low-oxygen submicron nickel still presents a problem which apparently will require more intensive investigation than could be given in this program.

12. The oxygen increase was limited to an average of 4 ppm per day when the powder was stored in a stainless-steel container sealed with a rubber gasket and which had been thoroughly degassed prior to being loaded.
13. No correlation was found between oxygen increase during storage and oxygen or water content of the argon atmosphere in which the powder was sealed up to 20 ppm oxygen or 180 ppm water.

REFERENCES

1. Tammann, I. G., and Nikitin, N. I., J. Russ. Phys. - Chem. Soc. 56, 115-9 (1925) C. A. 19, 3042 (1925).
2. Cremens, W. S., Use of Submicron Metal and Nonmetal Powders for Dispersion-Strengthened Alloys. Ultrafine Particles, W. E. Kuhn, Ed., John Wiley and Sons, Inc. (1963).
3. Brunauer, S., Emmett, P. H., and Teller, E., J. Am. Chem. Soc. 60, 309 (1938).
4. Handbook of Chemistry and Physics, 43rd Edition, p. 3183 (equation for Stokes' law), Chemical Rubber Publishing Co.
5. Volk, W., Applied Statistics for Engineers, McGraw-Hill (1958) pp. 339, 340.

APPENDIXADDITIONAL STORAGE TESTS

Six welded stainless steel containers having clamped, gasketed covers were received from Lewis Research Center for testing as storage devices for purified submicron nickel powder. These were rinsed with methanol and put into the glove box preparatory to being charged with samples. Powder batch 90 (Table 17) was purified Sherritt-Gordon powder also received from Lewis, but the other batches consisted of between 5 and 38 grams of purified Sherritt-Gordon powder from a lot used for previous reduction and storage tests.

Batch 69 was divided and stored in 2 containers which had been exposed to the pure argon atmosphere for one day, and batch 70 was stored in containers exposed for two days. Some of these containers were opened after various lengths of time and samples for oxygen analysis were removed. The container numbers, the length of time in days and the results of these analyses were as listed in Table 17.

Batch 72 was also divided into two containers which had been exposed to pure argon for 6 days prior to loading. Sample A container, however, was, after being loaded, connected to a mechanical vacuum pump and evacuated for 4 days to a pressure less than 5 Torr. It was then returned to the glove box and argon was admitted for the remainder of the storage period.

TABLE 17Results of Storage Tests in Stainless Steel Containers

<u>Test No.</u>	<u>Container No.</u>	<u>Days</u>	<u>Powder Oxygen</u>		<u>Oxygen Increase</u>	
			<u>Before</u>	<u>After</u>	<u>Total</u>	<u>ppm/day</u>
69-A	2	3	0.059%	0.064%	0.005%	17
69-B	2	10	0.059	0.134	0.075	75
69-C	2	13	0.059	0.100	0.041	31
69-D	3	13	0.059	0.089	0.030	23
70-A	4	3	0.032	0.037	0.005	17
70-B	4	16	0.037	0.084	0.047	29
70-C	6	19	0.032	0.084	0.052	27
72-A	1	23	0.050	0.077	0.027	12
72-B	5	23	0.050	0.058	0.008	3.5
79-A	2	33	0.036	0.049	0.013	4
79-B	3	34	0.026	0.041	0.015	4.4
85-A	6	26	0.035	0.067	0.032	12
90-A	5	24	0.076	0.119	0.043	18

Batch 79 was also divided into two containers which had been used for previous storage tests. Sample-B container was outgassed by evacuation for two days before being loaded for test. Sample-A container was evacuated overnight prior to loading in the glove box. After being loaded with sample, it was evacuated to a pressure of 12 Torr. Then it was returned to the glove box, vented with pure argon and removed for storage.

Batch 85 was sealed in a glass jar with an aluminum-lined cap. This was placed in the stainless-steel storage container which was closed for the storage test. Batch 90 was sealed in a similar manner, but nickel powder remaining from Batch 72 storage tests was placed in the stainless steel container along with the glass container to act as a getter for oxygen leaked in.

It was concluded that a thorough outgassing of the container to be used for storage was essential for low oxygen pickup by the nickel powder. For example, a 6-day exposure to pure argon or a vacuum outgassing gave satisfactory results (less than the requested 9 ppm per day for 22 days). Undoubtedly, a larger quantity of powder stored in one of these containers would suffer even less oxygen pickup than the quantities tested.

SYLVANIA
SUBSIDIARY OF
GENERAL TELEPHONE & ELECTRONICS GTE